

A dissertation submitted to the
UNIVERSITÀ DEGLI STUDI DI NAPOLI FEDERICO II
and produced in collaboration with the
SWISS FEDERAL INSTITUTE OF TECHNOLOGY ZURICH



ETH

Eidgenössische Technische Hochschule Zürich
Swiss Federal Institute of Technology Zurich

Oxygenated Fuels to Reduce Exhaust Emissions from Diesel Engines

Presented for the degree of DOCTOR OF TECHNICAL SCIENCES by

Stefano Emanuele Iannuzzi

Master of Science – Mechanical Engineering

Università degli Studi di Napoli Federico II

Born August 12th, 1981

Citizen of Italy

Scuola di dottorato in Ingegneria Industriale
Dottorato di Ricerca in Ingegneria dei Sistemi Meccanici XXVIII Ciclo

Supervisors:

Dr. Gerardo Valentino
Dr. Christophe Barro

Coordinator of the PhD school:

Prof. Dr. Fabio Bozza

2016

To my beloved wife and daughters

Acknowledgment

The present study has been carried out at the Istituto Motori, Italian National Research Council (this PhD thesis is accepted by the University of Naples “Federico II”) and the Aerothermochemistry and Combustion Systems Laboratory within the Institute for Energy Technology at the ETH Zurich.

I felt particularly proud and lucky for having the possibility of working in these two important institutions. I would like to thank several people, really important for me during this activity: dr. Gerardo Valentino, research manager at Istituto Motori, with whom I had the opportunity of collaborating for long time after my master thesis and even before the beginning of the PhD who helped me in increasing my knowledge on diesel engine research and offered me the opportunity to spend one and a half years of my PhD studies abroad; professor Fabio Bozza, coordinator of the PhD school, for his academic guidance, his scientific input and support during the activity; professor Konstantinos Boulouchos who gave me the possibility of joining the Aerothermochemistry and Combustion Systems Laboratory and working in an excellent university with bright colleagues. I would like to offer my gratitude to all my colleagues, both from Istituto Motori and Aerothermochemistry and Combustion Systems Laboratory for their support and the really good time together. I will never forget them and hope to stay in contact with them in the future. In particular I would like to thank dr. Christophe Barro who supervised all my work at the ETH constantly bringing his scientific support and being helpful and friendly till the end of this dissertation. My thanks also go to the technicians both from Istituto Motori and LAV and secretary staff who made my life in Zürich much easier. Finally I would like to thank my parents for having supported this experience accepting me away from them and my wife for having followed me even though our two daughters (the sunshine of my life!) were so young. This choice brought many more difficulties in her life and she did a really excellent job; nothing would have been possible without her help.

Contents

Abstract	VI
1 Introduction	1
1.1 The diesel engine in the last decades	1
<i>Conventional diesel combustion</i>	<i>2</i>
1.2 Exhaust emissions from diesel engines	2
<i>Carbon monoxide CO.....</i>	<i>4</i>
<i>Unburned Hydrocarbons HC.....</i>	<i>5</i>
<i>Nitrogen Oxides NO_x.....</i>	<i>6</i>
<i>Particulate Matter</i>	<i>8</i>
1.3 In-cylinder emission reduction techniques	10
<i>Low Temperature Combustion</i>	<i>14</i>
1.4 After-treatment systems	18
<i>Diesel Oxidation Catalyst (DOC).....</i>	<i>18</i>
<i>Diesel Particulate Filter (DPF)</i>	<i>20</i>
<i>FAP.....</i>	<i>21</i>
<i>Lean NO_x Trap (LNT)</i>	<i>22</i>
<i>Selective Catalyst Reduction (SCR)</i>	<i>23</i>
<i>Diesel Particulate-NO_x Reduction system (DPNR)</i>	<i>24</i>

1.5 Alternative fuels.....	25
<i>Biodiesel</i>	25
<i>n-Butanol</i>	29
<i>Poly(oxymethylene)dimethylethers (POMDME)</i>	31
1.6 Structure and Objective of the activity.....	34
2 Experimental Procedure.....	36
2.1 Automotive GM diesel engine	36
<i>Engine set-up</i>	37
<i>Investigated fuels</i>	38
<i>Operating conditions</i>	40
2.2 Constant volume cell set-up	40
<i>Cylindrical constant volume chamber set-up</i>	40
<i>Investigated fuels</i>	41
<i>Operating conditions</i>	42
<i>Optical set-up</i>	43
<i>kL factor</i>	46
2.3 MTU-396 Single Cylinder Diesel Engine	52
<i>Engine set-up</i>	52
<i>Investigated fuels</i>	57

<i>Operating conditions</i>	58
3 Experimental Results	59
3.1 Automotive Diesel Engine results	59
<i>Rate of heat release analysis</i>	59
<i>Exhaust emission and performance results</i>	62
3.2 Cylindrical constant volume chamber results	70
<i>Optical results</i>	70
<i>Exhaust results</i>	80
3.3 MTU single cylinder engine results	84
<i>Exhaust emission and performance results</i>	84
4 Conclusions and Outlook	94
<i>Experimental observations</i>	94
<i>Outlook</i>	97
Appendix A	98
Nomenclature	98
List of Tables	100
List of Figures	101
Bibliography	105
Curriculum Vitae	117

Abstract

The present dissertation aims at bringing a further scientific contribution to the knowledge on oxygenated fuels properties and their ability of reducing mainly soot emissions in diesel engine combustion. The activity comprises two different phases. The first phase has been conducted at Istituto Motori, Italian National Research Council in Naples and focused on comparing performance and engine out emissions from conventional diesel and alternative fuels. The second part of this study has been, instead, carried on at the Aerothermochemistry and Combustion Systems Laboratory, ETH Zurich, Switzerland. Different oxygenated fuels have been investigated in a constant volume chamber with large optical access. In particular Poly(oxyethylene) dimethyl ethers (POMDME) with a $\text{CH}_3\text{-O-(CH}_2\text{-O)}_n\text{-CH}_3$ general molecular structure have been studied both in the constant volume chamber and a single cylinder “heavy duty” diesel engine.

The use of oxygenated fuels or biodiesel from renewable sources in diesel engines is of particular interest because of the low environmental impact that can be achieved. The experimental investigation performed at Istituto Motori has provided results from a light duty diesel engine fueled with biodiesel, gasoline and butanol mixed, at different volume fractions, with mineral diesel. The investigation has been performed on a turbocharged DI four cylinder diesel engine for automotive applications equipped with a common rail injection system. Engine tests have been carried out at 2500 rpm, 0.8 MPa of brake mean effective pressure selecting a single injection strategy and performing a parametric analysis on the effect of combustion phasing and oxygen concentration at intake on engine performance and exhaust emissions. The experiments demonstrated that the fuel properties have a strong impact on soot emissions. Blends composed of diesel-gasoline or diesel-butanol determined the maximum reduction in smoke emissions compared to the diesel fuel. No significant difference for NO_x emissions was found between the investigated fuels highlighting that oxygen availability within the fuel may not produce an increase in NO_x formation under late premixed combustion.

Moreover, oxygenated fuels produced from methane-based products have been investigated at the ETH, Zurich. The different oxygenated fuels were investigated in a constant volume chamber with large optical accesses. In order to study the combustion evolution and soot formation and oxidation processes, optical techniques such as OH chemiluminescence and two dimensional two colour pyrometry (2D2CP) have been applied. Moreover, a fast particle spectrometer has been used at the chamber exhaust in order to analyse the soot emissions from the different investigated fuels. The investigation included the calculation of the kL factor, demonstrating a reduction of the soot

formation dominated phase when increasing the oxygenated fraction in the blend. Moreover, fuel jet images show a reduction of the soot formation area when increasing the oxygen content in the blend. The activity even focused on the analysis of soot emissions acquired by means of the fast particle spectrometer and results highlighted nearly smokeless combustion for pure oxygenated fuels and a non-linear soot emission reduction with increasing O₂ content in the blend. In order to achieve a complete overview of the impact of oxygenated fuels on engine performance and exhaust emissions, a second investigation on a single cylinder “heavy duty” direct injection diesel engine has been performed. The comparison between the POMDME-diesel blends and conventional diesel has shown a significant reduction in soot emissions, up to almost 35% reduction with the 10% POMDME in diesel blend. Moreover no significant increase in NO_x emissions was found when fueling the engine with the blends, highlighting as molecular oxygen is not crucial (at least in the percentages investigated in the present dissertation) for NO_x increase even in a premixed plus diffusive combustion mode.

The first introductory chapter of this thesis contains an overview of the problems connected to exhaust emissions from diesel engines, describes the most promising in-cylinder emission reduction techniques and illustrates the after-treatment systems that are nowadays necessary to fulfill the increasingly stricter emission regulations. The second chapter, instead, focuses on the different adopted experimental set-up and describes the applied optical techniques while results of the different activities are presented in chapter three. Finally, conclusion and outlook are reported in chapter four.

Chapter 1

Introduction

1.1 The diesel engine in the last decades

The diesel engine technology has strongly developed in the last two decades allowing an increase of the efficiency and “fun to drive” through the adoption of new technologies. In particular, the adoption of the common rail injection system allowed an increase of injection pressure with benefits on spray atomization and fuel-air mixing and gave the possibility of an independent injection process with respect to engine speed and crank shaft position; moreover the introduction of multiple injections per cycle, coupled with the use of exhaust gas recirculation (EGR) allowed to significantly reduce exhaust emissions. As a result a continuous increasing trend of diesel penetration in the EU15 (European Union) + EFTA (European Free Trade Association) passenger car market has been registered over the last 25 years, as shown in figure 1.1.

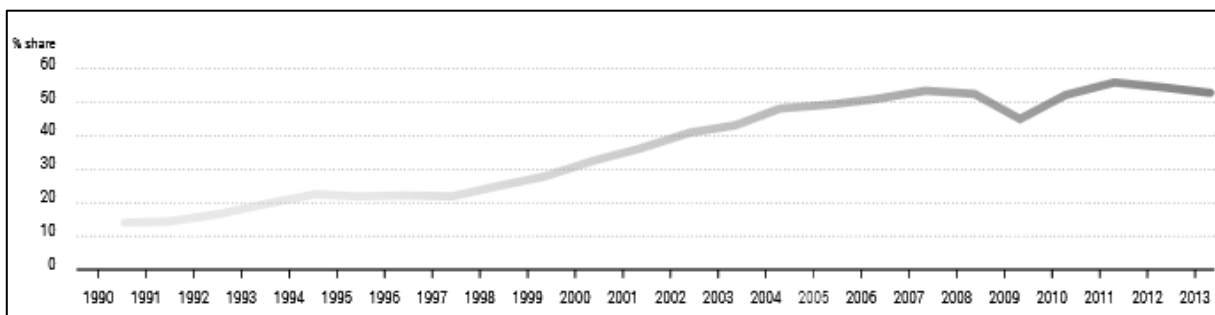


Figure 1.1: Diesel penetration in the EU15+EFTA as percentage of registered new cars [1]

The share of new passenger cars by fuel type is, instead, reported in figure 1.2 with reference to the period 2011-2014. The diesel engine covers almost 54% of the entire market (data averaged over the four years) while petrol and alternative fuels (including pure electric, liquefied petroleum gas engines, natural gas vehicles, ethanol, biodiesel and plug-in hybrid vehicles) less than 44% and 2.2% respectively. The possibility of achieving a 30% increase in fuel economy with respect to gasoline engines and the lower greenhouse emissions rendered the diesel engine more and more popular in the European community.

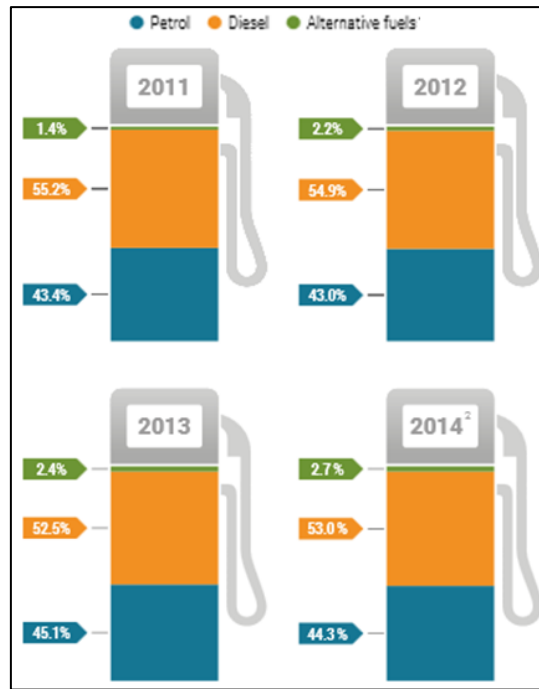


Figure 1.2: New passenger cars share in the EU over the years 2011-2014 [1]

Conventional diesel combustion

Diesel conventional combustion is characterized by a first premixed phase in which the fuel injected during the interval start of injection - start of combustion (this temporal range is the ignition delay) suddenly auto ignites producing a fast increase of in-cylinder pressure and temperature. The following diffusive phase is characterized by injected fuel “instantaneously” evaporating and auto igniting because of the extremely high temperatures at which the charge is by now arrived. During this phase, combustion speed is regulated by fuel evaporation and mixing with air and exhaust gas temperatures, because of the fuel that continues to be delivered and burnt till end of injection, continue to increase up to a maximum value. Finally, in a last phase, temperatures start to decrease and the last combustion reactions are completed. Conventional diesel combustion thus determines high in-cylinder temperatures (over 2000K) and, as a consequence, high production of NO_x . Moreover, because of the diffusion combustion in which air to fuel local ratios range from very lean to very rich, relatively high values of soot emission, coming from the locally rich regions, are achieved.

1.2 Exhaust emissions from diesel engines

Internal combustion engines are one of the main sources of environmental pollution together with industries and home heating. Environmental pollution refers to the ensemble of the chemical, physical and biological agents which determine a modification of atmospheric natural

characteristics. The introduction of harmful substances in the atmosphere through the combustion process and exhaust emissions of internal combustion engines is therefore limited by environmental regulations. Table I.I shows the European Union emission standards for both diesel and gasoline passenger cars. From the introduction of Euro 1 in 1992 the regulations have become increasingly stricter and, with the introduction of Euro 6 in September 2014, more than 95% reduction is imposed with respect to Euro 1 limit with respect to soot emissions. In addition, starting from Euro 5b, a limitation on particles number has been introduced in order to limit particles characterized by very small dimensions which do not significantly contribute to the total detected soot mass but are the most dangerous for human health being able to reach the innermost zone of the respiratory system [2]. The limitation expects a maximum number of non-volatiles particles (where non-volatile particles are defined as ones having a diameter between 23 nm and 2.5 μm and sufficiently low volatility to survive a residence time of 0.2 s at 300°C) of 6.0×10^{11} per kilometer. These particles are counted using the particle number counter (PNC) which has a counting efficiency of $50\% \pm 12\%$ (cut-off size, $d_{50\%}$) for particles of 23 nm and more than 90% for 41 nm [3].

Stage	Date	CO	HC	HC+NOx	NOx	PM	PN
		g/km					
Compression Ignition (Diesel)							
Euro 1 †	1992.07	2.72 (3.16)	-	0.97 (1.13)	-	0.14 (0.18)	-
Euro 2, IDI	1996.01	1.0	-	0.7	-	0.08	-
Euro 2, DI	1996.01 ^a	1.0	-	0.9	-	0.10	-
Euro 3	2000.01	0.64	-	0.56	0.50	0.05	-
Euro 4	2005.01	0.50	-	0.30	0.25	0.025	-
Euro 5a	2009.09 ^b	0.50	-	0.23	0.18	0.005 ^f	-
Euro 5b	2011.09 ^c	0.50	-	0.23	0.18	0.005 ^f	6.0×10^{11}
Euro 6	2014.09	0.50	-	0.17	0.08	0.005 ^f	6.0×10^{11}
Positive Ignition (Gasoline)							
Euro 1 †	1992.07	2.72 (3.16)	-	0.97 (1.13)	-	-	-
Euro 2	1996.01	2.2	-	0.5	-	-	-
Euro 3	2000.01	2.30	0.20	-	0.15	-	-
Euro 4	2005.01	1.0	0.10	-	0.08	-	-
Euro 5	2009.09 ^b	1.0	0.10 ^d	-	0.06	0.005 ^{e,f}	-
Euro 6	2014.09	1.0	0.10 ^d	-	0.06	0.005 ^{e,f}	6.0×10^{11} e,g
* At the Euro 1..4 stages, passenger vehicles > 2,500 kg were type approved as Category N ₁ vehicles † Values in brackets are conformity of production (COP) limits a. until 1999.09.30 (after that date DI engines must meet the IDI limits) b. 2011.01 for all models c. 2013.01 for all models d. and NMHC = 0.068 g/km e. applicable only to vehicles using DI engines f. 0.0045 g/km using the PMP measurement procedure g. 6.0×10^{12} 1/km within first three years from Euro 6 effective dates							

Table I.I: European Union emission standards for passenger cars [4]

If the environmental regulations require a continuous improvement of both combustion process and after treatment systems on one hand, the increasing market demand for more fuel-efficient cars, shown in figure 1.3, force the optimization of combustion process on the other hand.

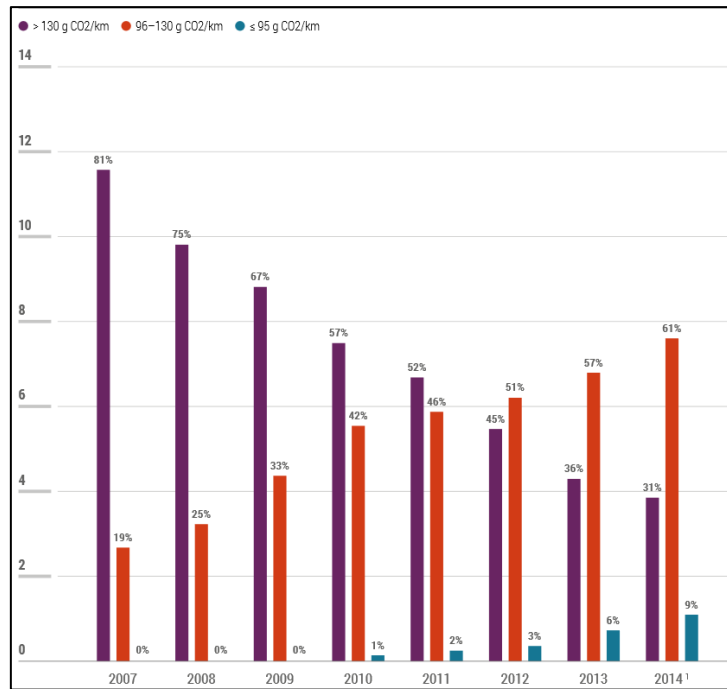


Figure 1.3: New passenger cars (in million units) in the EU by emission classes [1]

In the following an overview of pollutants produced from diesel combustion, namely carbon monoxide CO, unburned or partially burned hydrocarbons, nitrogen oxides NO_x, sulphur oxides SO_x and particulate matter is presented. Carbon dioxide CO₂, oxygen O₂, water H₂O and nitrogen N₂ are found in the exhaust gases as well but are not classified as pollutants being natural components of the atmosphere.

Carbon Monoxide CO

Carbon monoxide is an extremely dangerous gas being odorless, tasteless and colorless. It is not present in nature because it reacts with oxygen to form carbon dioxide. Its production is related to the generic combustion reaction of a CH_y hydrocarbon:



where



are the reactions involved in carbon combustion.

The first reaction is much faster than the second and takes place during the intermediate combustion stages. If oxygen availability is enough, the second reaction completes the process with

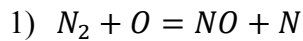
carbon dioxide formation. The factors that influence CO production, in addition to oxygen availability, are temperature and residence time [5]. This generally results in a higher CO production at low loads because of lower combustion temperatures.

Unburned hydrocarbons HC

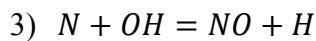
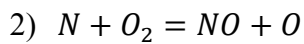
Unburned hydrocarbons are consequence of incomplete combustion of fuel. They can be divided in two main groups: methanic and non-methanic (aromatics, alkanes, alkenes, alkynes). The air – fuel mixture in a diesel engine is known to be heterogeneous: this determines the formation of rich and lean regions. In locally rich regions fuel droplets may not be properly surrounded by oxygen to fully oxidize (over-rich mixture) while in lean regions the air to fuel ratio could be too high to ignite or ensure a complete combustion process (locally over-lean mixture). This over-mixed fuel could then be emitted as exhaust hydrocarbon emission if it does not burn during combustion and expansion [6]. Locally over-rich mixtures can be induced, for instance, by low fuel velocity or inadequate swirl penalizing the air-fuel mixing. They can result in incomplete combustion process as well as pyrolysis products (organic compound decomposition due to in-cylinder temperature) or unburned fuel moving through the valves in the exhaust. Due to pyrolysis, organic compounds not present in the fuel are found in the exhaust. Hydrocarbon emission are strongly dependent on engine load; idle and low loads, for instance, are known to be critical for the formation of hydrocarbons with respect to high loads where the increased temperatures enhance oxidation rate. Under-mixing is the mechanism characterizing the “sac volume”, fuel remaining trapped in the injector tip at the end of the injection process. It is characterized by a very slow evaporation and thus has a great chance to escape the combustion process. Thus the “sac volume” is considered to be another cause of high HC emissions. Hydrocarbon emission is even dependent on wall temperatures because of possible quenching of the flame and engine instability (induced, for instance, because of too late fuel injection) determining partial burning [7]. In addition, a minor source of HC emission is related to the thin film of lube oil on the cylinder wall which can absorb fuel hydrocarbons. These particles will be trapped in this film and may escape the combustion process. Finally, the influence of fuel composition on nature and quantity of hydrocarbon emissions has been studied to be a non-negligible factor. For instance, methyl ester of soybean oil (biodiesel) has been investigated to reduce HC emissions [8]. Hydrocarbon emission is strictly correlated to combustion efficiency being it a fraction of fuel not undergoing to combustion and thus not contributing to generating work on the piston.

Nitrogen oxides NO_x

Nitrogen oxides are composed of nitric oxide (NO), predominant in the engine cylinder plus nitrogen dioxide (NO₂) and nitrous oxide (N₂O). The main source of nitrogen oxides is oxidation of atmospheric nitrogen; however if the fuel contains high amounts of nitrogen, even its oxidation becomes non-negligible. Since diesel engines are always working lean, the NO_x production is higher than that from gasoline engines. NO_x formation from atmospheric nitrogen (*Thermal NO_x*), according to the extended Zeldovic mechanism, can be described with the following equations:



Because of the triple chemical bond of N₂ (N≡N), the reaction requires high activation energy ($E \approx 316 \frac{\text{kJ}}{\text{mol}}$) thus high temperatures, above 2000K.



Significantly lower activation energy is required for reaction 2 and 3, taking place for temperatures over 300K.

Thermal NO_x are strongly influenced by combustion temperature, residence time and atomic oxygen concentration (figure 1.4). The critical time period for NO_x formation is when burned gases reach their maximum temperatures. The gas fraction, burning in an early stage of combustion, is further compressed to higher temperatures while cylinder pressure increases, determining an increase in NO formation rate. Afterwards, as the burned gases expand during the expansion stroke, their temperature starts to decrease and the NO chemistry freezes [9].

To reduce thermal NO_x in internal combustion engines, the most common techniques are EGR (combustion temperature is decreased by means of exhaust gas recirculation), stream reduction (in heavy duty marine engines; reduction of combustion temperature is achieved by injecting water in the combustion chamber which, evaporating, subtracts heat from the system) and air dilution (very lean combustion, $\lambda > 1.5$, while the peak of NO emission is achieved with slightly lean combustion, λ around 1.1).

NO_x formation from fuel nitrogen (Fuel NO_x) refers to the conversion of fuel bound nitrogen during combustion of certain coals and oils. The mechanism of Fuel NO_x is not completely understood but it is assumed that during combustion certain compounds (such as pyridine and quinolone) undergo to thermal decomposition prior to entering the combustion zone. Ammonia (NH₃), hydrocyanic acid (HCN) and cyanide radicals (C-N) are the precursors to NO formation.

Fuel NO are sensitive to air/fuel ratio but weakly dependent on temperature in contrast to the strong temperature dependence of NO formed from atmospheric nitrogen [9]. Fuel NO is formed more readily (occurring on a time scale comparable to that of combustion reactions) than thermal NO because the N-H and N-C bonds, which are very common in fuel-bound nitrogen, are much weaker than the triple bond in molecular nitrogen which must be broken for thermal NO formation [10].

Prompt NO_x are formed by the reaction of atmospheric nitrogen with hydrocarbon radicals in fuel-rich regions of flames, which is subsequently oxidized to form NO_x. Since the prompt NO_x mechanism requires an hydrocarbon to initiate the reaction with nitrogen, it is much more prevalent in fuel-rich than in fuel-lean hydrocarbon flames [11]. Since the CH-N reaction requires a lower activation energy, with respect to the dissociation of molecular nitrogen, the prompt NO_x formation mechanism results to be more significant at low temperatures.

NO_x are dangerous for human health. NO acts on hemoglobin while NO₂ is responsible for breathing apparatus pathologies which may lead to death. Moreover, together with non-methanic hydrocarbons (NMHC), NO_x are the main precursor of the ground level ozone (troposphere ozone) formation through complex and non-linear photochemical reactions in sunlight.

As of the full phase-in of Euro 6 standard in the European Union (September 2015), all newly registered diesel passenger cars will have to meet a NO_x emission limit of 80 mg/km over the European light-duty vehicle emission certification cycle (New European Driving Cycle, NEDC). While all diesel car manufacturers have managed to meet this requirement during the regulated laboratory test, it is widely accepted that the “real-world” NO_x emissions of diesel passenger cars are substantially higher than the certified limit [12]. This has been one of the main drivers behind the recent amendment of the Euro 6 standard to require an on-road, real-driving emissions (RDE) test using portable emission measurement systems (PEMS). Once RDE testing will be legally enforced in 2017, passenger cars will have to demonstrate reasonably low emissions under real-world use conditions (although some aspects, such as cold-start emissions and the effects of high-load driving, will not be fully captured). In the short run, this should lead to more robust implementations of existing NO_x control technologies especially in terms of engine after treatment calibration approaches but in some cases it could also have a significant impact upon the diesel car manufacturers hardware choices. In the long term, RDE should also deliver substantial improvements in urban air quality in Europe as fleet turnover makes pre-RDE diesel cars less prevalent [13].

Particulate Matter

Particulate emissions are one of the main issues of DI diesel engines and are intensely studied by researchers because of their dangerousness for human health (considered to be carcinogen), as reported by the international agency for research on cancer. The Environmental Protection Agency describes the process of soot harming the human body: “Microscopic particles can penetrate deep into the lungs and have been linked to a wide range of serious health effects, including premature death, heart attacks, and strokes, as well as acute bronchitis and aggravated asthma among children” [14].

Particulate matter are separated in a soluble and an insoluble fraction is the combination of soot, a solid substance made almost entirely of carbon (insoluble fraction), and other materials in solid or liquid phase (e.g. evaporated engine lubricating oil [15]). Under ideal conditions, the combustion of hydrocarbons generates only carbon dioxide and water. These conditions are achieved if the oxygen content of the mixture is locally enough to completely convert the fuel; in this case a maximum in both heat release and chemical energy available for mechanical work are achieved [16]. In real combustion conditions, because of a local lack of oxygen, other products of incomplete combustion, such as hydrocarbons and soot are formed. Thus the process of soot formation takes place at high temperatures ($>1600\text{K}$) and in locally fuel-rich regions from unburned fuel which nucleates from vapor to solid phase. The transition from vapor or liquid phase hydrocarbons to solid soot particles comprises five consecutive processes, namely pyrolysis, nucleation, coalescence, surface growth and agglomeration plus oxidation which occurs concurrent to the others [17]. The general features of the processes involved in soot formation are schematically shown in figure 1.4 and explained in the following.

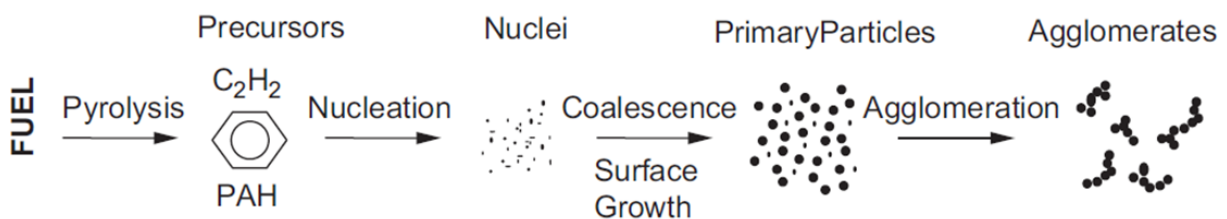


Fig.1.4: soot formation process from gas phase to solid agglomerated particles [17]

Fuel pyrolysis is the process through which an organic compound, altering its molecular structure at high temperatures, turns into unsaturated hydrocarbons (soot precursors), polyacetylenes, polycyclic aromatic hydrocarbons (PAH) and acetylene (C_2H_2). Nucleation, instead, is the formation of particles from gas-phase reactants. These particles act as cores on which other mass will be added during the surface growth process (with the so called HACA process), characterized by gas-phase hydrocarbons absorption on the nucleated soot particles. The surface growth phase

determines, in this way, an increase of soot mass but not of particles number. Since the major fraction of soot mass is build up during this phase, the surface growth residence time strongly influences the total soot mass. The two processes affecting the number of particles are coalescence and agglomeration. Coalescence consists of particle collision, meaning that two particles combine to form a bigger one characterized by a spherical shape and the same mass of the two original particles. On the other hand agglomeration takes place when spherical primary particles agglomerate to form large groups of particles generally in long chain-like structures. Most primary particles are in the range 20-70 nm but after combustion the chain-like structures typically range from 100 nm to 2 μ m [17]. The major fraction of formed soot, though, is not found in the engine exhaust as well, because of being oxidized by OH under fuel-rich and stoichiometric conditions and OH and O₂ under lean conditions [18]. Oxidation takes place during the whole soot formation process and transforms carbon or hydrocarbons into combustion products. Once carbon is transformed into CO it will not have the possibility to evolve in a soot particle again. The oxidation process proceeds at the beginning of the expansion stroke until temperature drops below 1300K [19] and removes more than 90% of the total formed soot. Therefore the soot measured at the exhaust of an engine is given by the difference soot formation – soot oxidation.

The principal physical parameters affecting soot formation and oxidation are temperature, pressure, fuel composition, fuel structure and air/fuel ratio. Reaction rates in both soot formation and oxidation are all enhanced by increasing temperature; thus it may be considered as the most important parameter affecting soot [17]. Maximum soot formation occurs for temperatures around 2000K and local equivalence ratios above 2 as reported in figure 1.5. Since locally rich regions are responsible for soot formation, the addition of oxygen through fuel composition or mixing of fuel and air determines, at a fixed temperature, a reduction of this pollutant. Though, since oxygen is strictly correlated to temperature which has an exponential effect on both soot formation and oxidation processes, it is not trivial to evaluate whether the soot reduction is due to the direct effect of an oxygen increase or an increase in temperature due to increased oxygen. The present dissertation will deal with both premixed combustion and oxygenated fuels to reduce soot emissions in diesel engines. Composition and structure of the fuel are other important factors affecting soot because of the correlation between carbon in the fuel molecule and its tendency to soot. Both higher carbon percentages and C-C bonds enhance this tendency while hydrogen concentration, even though its effect is of minor importance (compared to oxygen), reduces soot formation and the aromatic content. Other parameters affecting soot formation are the combustion chamber geometry because of its impact on swirl and liquid fuel impingement, injection timing determining the

temperature at start of combustion and intake pressure affecting the amount of charge air entrained into the jet.

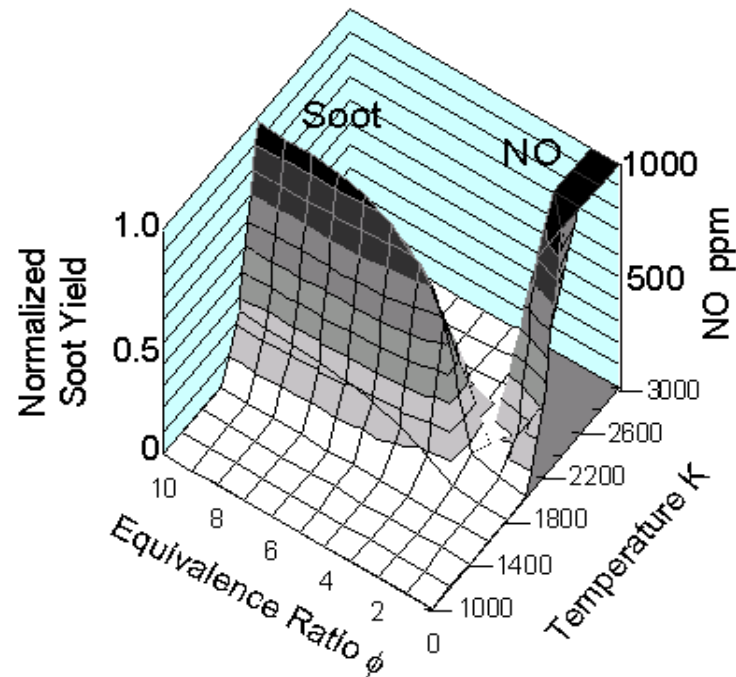


Figure 1.5: ϕ -T map for diesel combustion [20]

1.3 In-cylinder emission reduction techniques

In the following a brief description of the influence of engine actuators on emissions are reported. The importance of in-cylinder combustion optimization, on the emission side, is correlated to the attempt of a maximum reduction of pollutants reaching the after-treatment systems in order to reduce their stress.

Being the NO formation strongly temperature dependent, the correlation between local flame temperature and resulting NO_x emissions has been widely studied [21]–[24] and several technologies which aim to reduce the this temperature have been introduced:

- Exhaust gas recirculation system (EGR) which consists in re-introducing a fraction of exhaust gases in the intake in order to reduce the adiabatic flame temperature. Moreover oxygen availability is reduced as well and the specific heat of the reactants is increased [25]–[27]; EGR percentage is usually measured through the following equation:

$$EGR = \frac{CO_{2Intake} - CO_{2Environment}}{CO_{2Exhaust} - CO_{2Environment}} * 100 [\%]$$

- Flame cooling through water evaporation (e.g. fuel water emulsion);
- Miller Valve Timing [28] which allows a reduction of the reactant temperature

- Variable Valve Timing (VVT).

The Miller valve timing process is characterized by an early closure of the inlet valve in order to expand the charge air before it is compressed (with a loss in efficiency of about 1.5% due to the loss of positive work, assuming positive scavenge pressure). In this way lower temperatures at end of compression are achieved [29]. In addition since the average cycle temperature is reduced, heat losses are decreased with the consequence of improved efficiency (up to 5%, which compensates the loss of efficiency from the earlier inlet valve closure [30]). On the other side a higher boost pressure is required to achieve the same power output (an early closure of the inlet valves reduces the volumetric efficiency) and ignition problems are encountered at low loads. Therefore the Variable Valve Timing technology represents a further improved solution because it allows to work at conventional intake valve timing at low loads and switch to Miller timing at high loads (though it results in an increase in complexity and cost with respect to Miller). This technology, characterized by a hydraulic system coupled to the cam shaft or an electromagnetic engine valve actuator, gives the possibility to control the inlet and exhaust valves events independently of crank shaft rotation, by changing the cam profile. As a result up to 15% fuel consumption reduction (and CO₂ emission) and increase in torque output in a wide range of engine speed may be achieved [31].

In addition the introduction of the common rail injection system for diesel engines has given the possibility of independently control the injection process with respect to the engine speed leading to a simultaneous reduction of soot and NO_x. In fact diesel engines are usually characterized by presenting a trade - off NO_x - soot, meaning that the decrease of the first (e.g. because of an increase in EGR) is followed by an increase of the second and vice versa, as shown in figure 1.6. The simultaneous adoption of EGR and enhanced air-fuel mixing, though, can lead to a denial of the mentioned trade-off trend. In fact the use of EGR permits a reduction in NO_x while enhanced air-fuel mixing promotes oxidation and thus decreases soot formation.

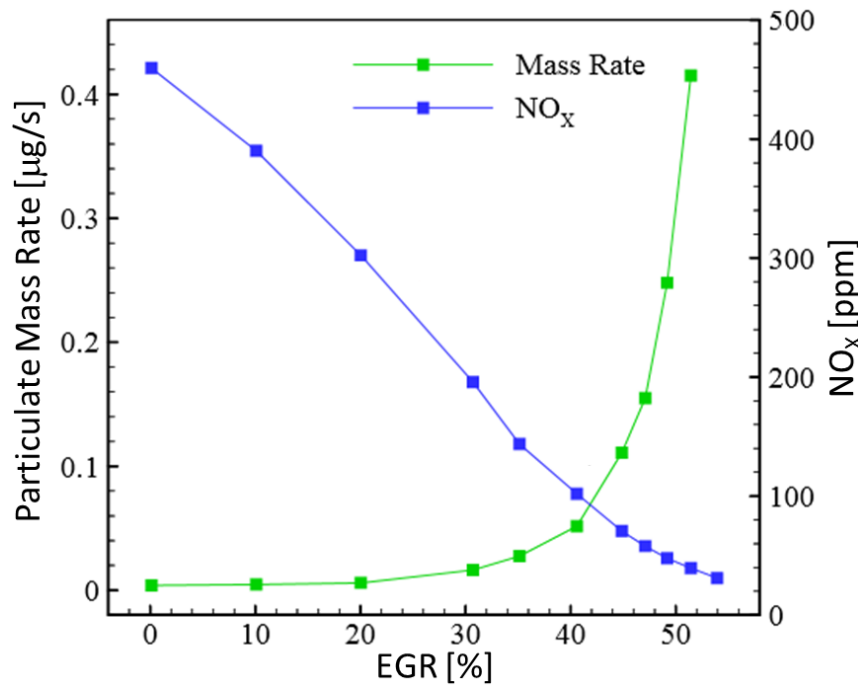


Figure 1.6: NO_x – Soot trade-off in conventional diesel combustion [32]

The common rail injection system permits both an increase of engine performance and a reduction of exhaust emissions through the management of number of injections, injection timing and injection pressure.

The increase in injection pressure (up to 2000 bar in modern injection systems) enhances the air-fuel mixing because of the increased injected fuel velocity determining a higher air entrainment. On the other side, in order to avoid impingement of liquid fuel on cold surfaces (increases unburned hydrocarbons emissions) high injection pressures must be correlated with a suitable combustion chamber geometry, swirl flow and injection timing (determining the combustion phasing and thus the temperature at start of injection which affects the injected fuel evaporation).

Modern electronic control units (ECU) are capable of managing several injections per cycle. The possibility of adopting multiple injection strategies allows improvements on emissions, fuel consumption and combustion noise. In addition, a better fuel distribution is achieved leading to a more efficient use of the charge air; thus the possibility to reduce soot emissions at medium engine loads allowing higher EGR rates [33]. Figure 1.7 shows a sketch of the different injections, namely:

- Pilot
- Pre
- Main (usually one or two injection events, split main)
- After
- Post (from one to three injection events)

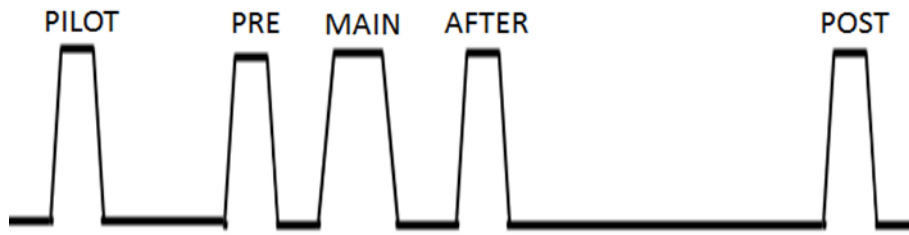


Figure 1.7: Sketch of the different injections

The fuel being injected during the Pilot injection typically burns in a premixed way. In fact in-cylinder temperatures are still low when the injection is activated thus a high ignition delay is detected. Pilot and Pre injections are generally used in cold start and low load conditions in order to increase the temperature at start of Main injection and promote its ignition. In addition these injections are very effective to reduce combustion noise. In fact they shorten the ignition delay of the fuel being injected during the Main event and thus its premixed combustion phase is reduced; as a consequence the rapid in-cylinder pressure rise, characteristic of the premixed combustion mode and directly correlated to combustion noise [34], is decreased as well. Pilot and Pre injections may also be effective in reducing NO_x emissions because of the lower in-cylinder peak temperatures associated to the decrease of the Main injection premixed fraction; this circumstance, though, determines, an increase in soot emissions. The Main injection, with which the requested engine power output is achieved, can be activated as a unique event or splitted in two injections in order to enhance the air entrainment. In this case fuel efficiency results to be increased and engine out particulate and CO emissions are lowered while an increase in NO_x emissions is noticed [35]. Furthermore, splitting the Main injection and changing the dwell time between the pulses gives the chance of modifying the shape of heat release rate and the combustion duration. In particular a splitted Main injection permits to keep the rate of heat release at a higher level for a longer time but with a lower peak value. As a result a more distributed heat release, which is believed to decrease soot emissions and increase fuel efficiency and NO_x , is shown [35]. The After injection has the main role of reducing soot emissions because it allows a temperature rise after the Main combustion enhancing the oxidation process of formed soot. A further reason of the enhanced oxidation process is related to the additional turbulence induced by the After injection. Its capability in reducing engine out soot emissions is, though, strongly depending on injected mass, dwell time and local conditions of the charge [36]–[38] but may be of particular interest in conditions where EGR is requested. Finally, the Post injection which occurs late in the expansion stroke is usually activated in one to three injection events and its objective is an increase in temperature beneficial for the DPF (diesel particulate filter) regeneration. The injected fuel evaporates but does not burn because of the low temperature conditions near to bottom dead center, reaching the exhaust in vapor phase. The

vaporized fuel provides high hydrocarbon levels to the DOC (diesel oxidation catalyst) in which exothermic reaction occur permitting a heavy increase of temperature. The achieved high temperatures allow the soot particles within the DPF to be burned. Both DOC and DPF systems will be illustrated in the after-treatment systems section. A major concern when using Post-injection is that the fuel can impinge on the cylinder walls leading to dilution of the lubricating oil [39]. The oil dilution determines a decrease in viscosity with the risk of operating conditions conducive to wear and engine damage. In order to overcome this problem, different techniques such as the implementation of an HC vaporizer directly in the exhaust of the engine are currently under investigation [40], [41]. The HC vaporizer is proposed to replace the Post-injections by delivering the fuel directly in the exhaust. Its main concern, though, is related to the difficulties of fuel evaporation at low loads because of the cold environment in the exhaust prior to the DOC.

Low temperature combustion

Low temperature combustion (LTC) mechanisms aim to reduce NO_x emissions by reducing in-cylinder temperatures through the removal of the diffusive combustion phase [42]. The basic idea of LTC aims to achieve a unique combustion phase characterized by a global lean mixture and a low temperature (no flame) reaction in order to simultaneously reduce NO_x and soot emissions. Charge dilution, through EGR activation, influences the local equivalence ratio prior to ignition due to lower O_2 concentrations and flame temperature due to the insertion of inert gases (replacing a fraction of the reactant) with increased heat capacity. Affecting both ϕ and T , charge dilution impacts the path representing the progress of combustion in the ϕ - T diagram (figure 1.8) and offers the chance to avoid both soot and NO_x . However, as dilution is increased to the limits, HC and CO can significantly increase [43]. Figure 1.8 shows the local equivalence ratio versus temperature diagram in which the main combustion mechanisms capable of avoiding the main NO_x and soot formation areas, HCCI and PCCI, are reported.

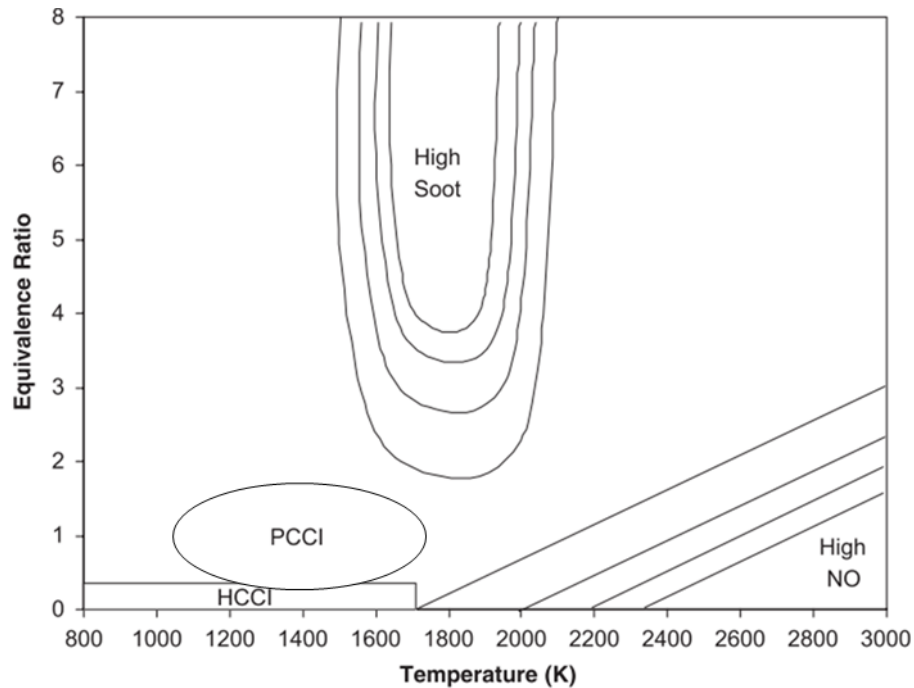


Figure 1.8: ϕ -T diagram with contours of different combustion mechanisms [17]

There are mainly two possibilities of achieving a low temperature combustion mechanism [17]. The first one is related to an injection event taking place very early in the compression stroke where temperature is still too low for fuel auto ignition; as a consequence, achieving high ignition delays, charge air and fuel should have enough time to form a homogeneous mixture. This mechanism, known as Homogeneous Charge Compression Ignition (HCCI), has been widely studied (e.g. [44]–[55]) and is primarily controlled by chemical kinetics. It allows a simultaneous reduction in NO_x (decreasing in-cylinder temperatures with high EGR rates) and soot emissions by premixing the fuel with air to overall lean conditions (in order to avoid locally rich regions where soot is formed). HCCI combustion is flameless and spontaneously occurs at the entire cylinder volume. The homogeneously mixed charge in the combustion chamber is auto ignited during the compressing stroke as soon as the auto ignition temperature is reached. In fact a mixture of fuel and air only ignites if fuel concentration is within the ignition limits and the reactants temperature is sufficiently high. The ignition timing of HCCI combustion strongly depends on the initial conditions of the cylinder charge such as temperature, pressure, and composition [56] and is difficult to control. This means that the combustion mechanism is very sensitive to ambient conditions as well. A further crucial element for HCCI operation in diesel engines is related to wall impingement. In fact, since the injection event takes place in a low temperature environment, the injected low volatile diesel fuel could not evaporate fast enough to avoid wall wetting with a consequent increase in HC emissions and break specific fuel consumption [57]. If on one hand a simultaneous reduction of NO_x and soot can be achieved, on the other hand, once the mixture ignites, combustion occurs very

fast yielding high in-cylinder pressure rise and, consequently, high noise and vibration emissions. The limitations in allowable pressure rise to avoid engine damage set a threshold for the equivalence ratio of about 0.3. Therefore HCCI can be typically operated lean making high-load conditions difficult to achieve.

The second possibility, premixed charge compression ignition (PCCI), is to inject late (around TDC) in the cycle in order to increase ignition delay because of lower temperatures during the evaporation of injected fuel. The increased ignition delay results in the possibility of injecting the whole amount of fuel prior to start of combustion. In this way an enhanced mixing of the spray and the charge air is achieved thus reducing the locally rich regions responsible of soot formation. Achieving a high ignition delay is thus a key factor for PCCI combustion. In order to further increase this parameter, the use of EGR plus the adoption of fuels characterized by a low cetane number are extremely helpful. Several papers have been published on PCCI combustion mode and the techniques to achieve a premixed mode and reduce exhaust emissions [58]–[76]; some of the main conclusions are discussed in the following.

In order to find out where and how partially premixed charge compression ignition (PPCCI) occurs a map that shows the changes in combustion characteristics with injection timing and EGR was created in [58]. The development from early injection PPCCI over conventional diesel combustion to late injection PPCCI has been studied. A comparison between ultra-high EGR early injection PPCCI and late injection PPCCI has been made and similarities have been ascertained. Moreover the authors studied the connection between combustion related parameters and emissions and suggest that mixing timing, cylinder pressure rate maximum and CA50 can be used as controlled outputs in a closed loop system with indirect control of emissions and efficiency. A low-temperature, premixed combustion concept to achieve simultaneous reductions in the NO_x and smoke emissions of a small DI diesel engine is proposed in [60]. The authors state that the combination of a low compression ratio, high injection pressure and EGR gas cooling can lead to more than 98% NO_x reduction and less than 1 BSU smoke concentration in an operating region near to stoichiometric air-fuel ratio. Partially premixed compression ignition is investigated in [61] as well. The authors found that, in gasoline – diesel mixtures, an increased proportion of gasoline reduced smoke emissions at higher operating loads through an increase in charge premixing resulting from an increase in ignition delay and higher fuel volatility. Their results confirm that a combination of fuel properties, exhibiting higher volatility and increased ignition delay, would enable a widening of the low emission operating regime, but that consideration must be given to combustion stability at low loads. A study on dual mode combustion concept with premixed diesel combustion was conducted in [65]. The authors proposed dual mode combustion to promote the

practical implementation of premixed diesel combustion. Under high load operations, exhaust emissions reductions are achieved by conventional diesel combustion with an after treatment system (e.g.; DPF, DeNO_x catalyst). Under low load operations, when after treatment systems are ineffective due to low exhaust temperatures, engine out exhaust emissions can be virtually reduced to zero using premixed diesel combustion. This approach results to be facilitated by "high turbulent mixing rates," small-hole nozzles, high injection pressure and injection timing near TDC. The importance of cetane number to achieve premixed combustion mode is studied in [66]. The authors state that in this combustion mode, where the injection event is separated from combustion, if the combustion phasing is the same for two of the tested fuels (an n-heptane fuel, two fuels in the diesel volatility range and three in the gasoline volatility range have been considered), their emissions behavior at a given condition will be similar regardless of the differences in volatility and composition. Thus PPCI operation with low smoke and NO_x becomes much easier to be achieved with fuels in the gasoline auto - ignition range. However PPCI operation also leads to higher CO and HC and higher heat release rates at high loads. These problems can be significantly alleviated by managing the mixing through injector design and injection strategies (e.g. multiple injection). In [67] the authors investigated the use of gasoline in premixed combustion and found that, for a given set of operating conditions (intake pressure and temperature, EGR level, fueling rate), gasoline produces a much higher ignition delay compared to diesel, for a given phasing of heat release. This facilitates premixed combustion and can result in significantly lower smoke and NO_x. The research activity conducted in [68] showed that a good fuel candidate to properly run partially premixed combustion from maximum load to idle is a fuel in the boiling point range of gasoline with an octane number of about 70. By combining this type of fuel with an appropriate EGR and λ strategy, it is possible to simultaneously achieve: very high efficiency, very low emissions and low maximum pressure rise rate in the whole load range without any drawback in combustion control. In [69] the authors propose a study on premixed LTC strategy with blends of diesel and gasoline. These blends are characterized by a low cetane number and thus produce a long ignition delay beneficial for in-cylinder air/fuel mixing. The authors state that while a conventional NO_x - soot trade - off exists for pure diesel with respect to intake oxygen concentration, soot emissions become insensitive to it when gasoline proportion increases. Results of an experimental investigation demonstrating the potential of employing blends with low cetane number to simultaneously reduce NO_x and smoke have been discussed in [70]. The authors state that because of the higher resistance to auto - ignition, blends of diesel and gasoline at different volume fraction may provide more time for the mixture preparation by increasing the ignition delay. The result produces the potential to operate under partially premixed low temperature combustion with lower levels of EGR without

excessive penalties on fuel efficiency. The major advantages of fuels characterized by higher resistance to auto ignition are related to smokeless conditions, improved NO_x emissions at moderate injection pressure and earlier injection timings with respect to commercial diesel allowing a recovery on thermal efficiency. In [71] the authors investigated blends of 20% and 40% of n-butanol in conventional diesel to achieve premixed combustion. The joint action of a longer ignition delay and the higher volatility of n-butanol - diesel blends promotes the dispersion of fuel vapor within the combustion chamber resulting in an almost smokeless combustion with the opportunity of operating at moderate injection pressures (100-120 MPa) and exhaust gas recirculation ($O_{2int}=19.5-19.0\%$). In addition, injection pressure is another parameter which has to be taken into account in order to enhance mixing of fuel and air. In fact increased injection pressure is found to enhance the early mixture formation process, resulting in increased heat release peak and generally decreased soot luminosity. The spatial distribution of soot luminosity is characterized by increased luminosity observed from the squish volume at the lower injection pressures [75].

1.4 After treatment systems

In recent years the turbocharged diesel engine has become more popular for passenger cars and even sport vehicles because of its high torque, reliability and efficiency but sophisticated exhaust after treatment systems are required to comply with increasingly stricter emission standards. An effective solution to remove all the species of pollutant from a diesel engine is reported in figure 1.9 and comprises a diesel oxidation catalyst (DOC) coupled with a diesel particulate filter (DPF), an injection system for urea and a selective catalyst reducer (SCR).

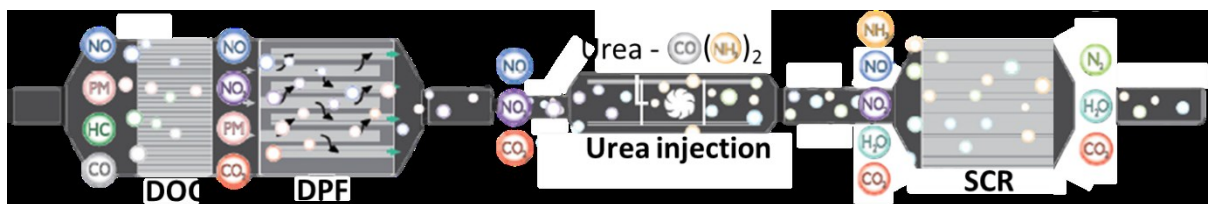


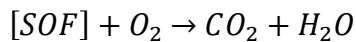
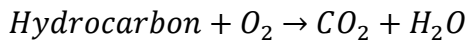
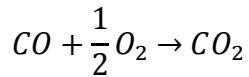
Figure 1.9: Scheme of a complete diesel after treatment system

The most common after treatment systems to reduce exhaust emissions from diesel engines, including the ones shown in figure 1.10, are described in the following.

Diesel Oxidation Catalyst (DOC)

Modern catalytic converters consist of a monolith honeycomb substrate, coated with a platinum group metal catalyst, packaged in a stainless steel container. The honeycomb structure with many

small parallel channels presents a high catalytic contact area to the exhaust gasses. As the hot gases pass through the catalyst, carbon monoxide, gas phase hydrocarbons and the soluble organic fraction (SOF) of diesel particulate matter are converted into harmless substances: carbon dioxide and water. The conversion takes place through the following reactions:



Diesel exhaust gases contain a concentration of O_2 , necessary for the mentioned reactions to take place, in the range 3 - 17%, depending on the engine load. This means that high oxygen concentration conditions, as well as high temperature (catalyst activity increases with temperature), are favorable towards the exothermic conversion of CO and HC in CO_2 and water. The conversion efficiency trends for CO and HC against temperature are given in figure 1.10. A minimum exhaust gas temperature of about $200^\circ C$ is necessary for the catalyst to "light off" while, at temperatures above $400^\circ C$, conversion efficiency, still depending on the catalyst size and design, can be higher than 90%.

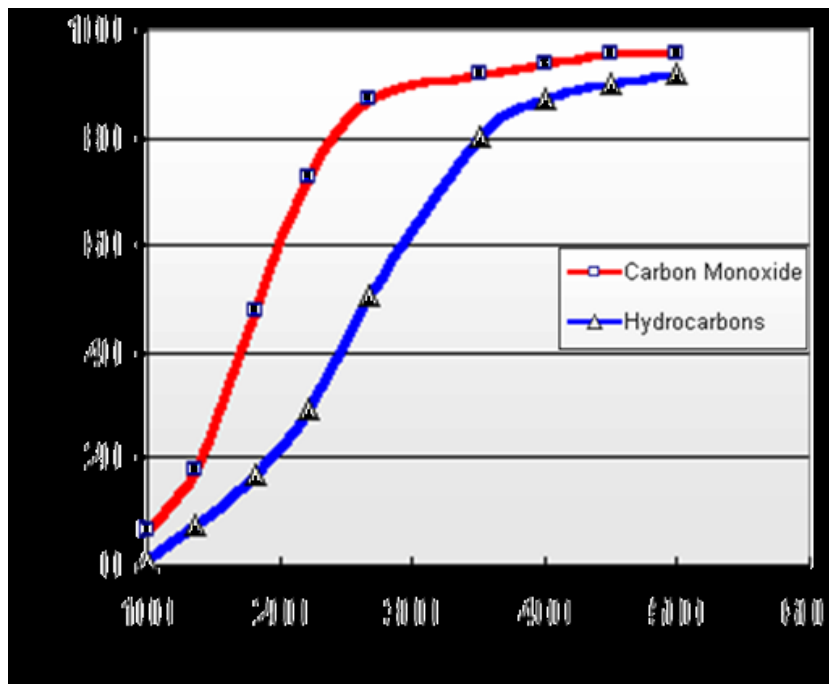


Figure 1.10: Catalytic Conversion of Carbon Monoxide and Hydrocarbons [77]

Also the conversion of diesel particulate matter is an important function of the modern diesel oxidation catalyst. The catalyst exhibits a very high activity in the oxidation of the soluble organic fraction of diesel particulates with conversion values that may reach and exceed 80%.

Diesel Particulate Filter (DPF)

A diesel particulate filter (DPF) is a device designed to remove particulate matter from the exhaust gas of a diesel engine. Such filters are made of ceramic (cordierite, silicon carbide or sintered metals) honeycomb materials. Ceramic wall-flow filters are able to remove almost completely all particulates, including fine particulates with diameter of less than 100 nanometers (nm) with an efficiency of >95% in mass and >99% in number of particles over a wide range of engine operating conditions. The soot is removed by physical filtration using a honeycomb structure with the channels blocked at alternate ends. The exhaust gas is thus forced to flow through the walls between the channels and the particulate matter is deposited as a soot cake on the walls. The deposition of such particles determines an increase of the measured pressure difference between filter input and output and the continuous flow of soot would eventually block the filter with, as a consequence, problematic exhaust gas flow; therefore, when the pressure difference exceeds a threshold value, a “regeneration” of the filter is required. The regeneration consists of burning-off the collected particulates with consequent formation of water and CO₂. In order to burn the particulates with oxygen, high temperatures are required at the DPF inlet. One of the most successful methods to achieve these temperatures and consequently start the DPF regeneration is to incorporate an oxidation catalyst (DOC) upstream the filter in order to take advantage of its exothermic reactions. In particular, the patented *Continuously Regenerating Trap* (CRT) system which is reported in figure 1.11, is composed of a platinum catalyst (which is also a normal converter for HC and CO) in front of the filter. The system takes advantage of the capability of nitrogen dioxide to burn soot at lower temperatures (around 270°C), typical of diesel exhaust. With the catalyst placed upstream the filter, the generated NO₂ travels with the exhaust gas into the filter where it combusts the trapped soot in a “continuous” way.

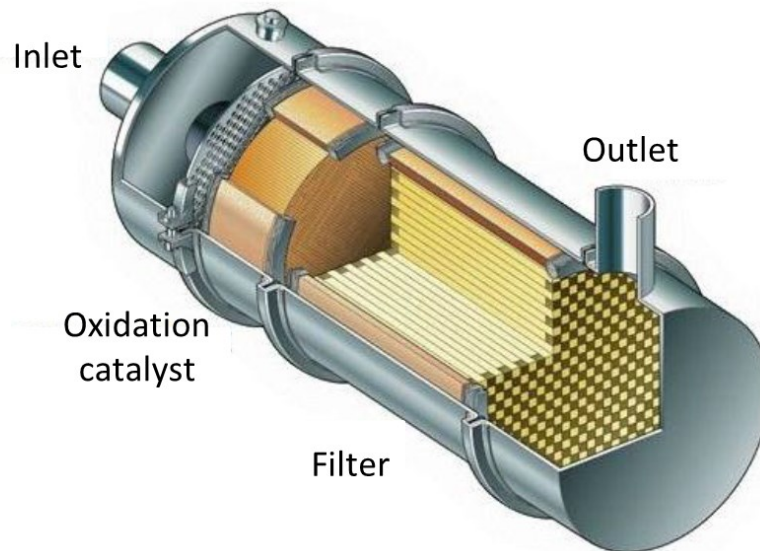


Figure 1.11: Scheme of a Continuously Regenerating Trap [78]

The system is also called "passive" because it does not require additional heat sources; on the other hand, being a non sulphur tolerant catalyst, it does require fuel with low sulfur content. Any application though, in which it cannot be guaranteed that the exhaust gas conditions will be suitable for a passively regenerating system, will require some active regeneration. Almost all active filter regeneration techniques operate by raising the temperature of the filter to around 600°C. This is the temperature at which the particulate matter (PM) collected in the filter, will combust in oxygen. In details, when the measured pressure difference between filter inlet and outlet exceeds a fixed value and a regeneration process is required, the engine ECU automatically activates a post injection strategy. The additional injections are activated late during the expansion stroke in order to determine only evaporation of the fuel (no combustion) which undergoes, in the DOC, exothermic reactions that produce the required temperature increase. The CRT system can form part of actively regenerated DPF systems in which the HC content of the exhaust stream is periodically enriched by in-cylinder post injection. Even in cases in which some active regeneration is necessary, it is desirable to maximize the amount of passive regeneration that can be achieved since it requires no additional energy and fuel.

FAP

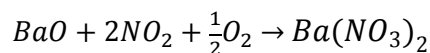
Designed in 2000 by PSA Peugeot-Citroen, this particulate filter system is characterized by the necessity of using an additive to the diesel fuel called Eolys. It is composed of cerium oxide Ce_2O_3 (also known as "glycerin") and allows particulates agglomeration with formation of macromolecules, easier to be trapped. This additive also allows to lower regeneration temperatures down to 450°C (against 600°C of the DPF with particulate matter combusted in oxygen) giving the

chance, in a wider range of operating conditions, to regenerate the filter without the need of post injections. The additive is stored in an additional tank (about five liters) located near to the main tank and is only refillable using special tools because of being quite corrosive thus requiring particular handling. It is automatically added (controlled by the engine ECU) to the diesel fuel at fill ups.

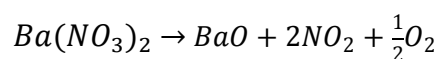
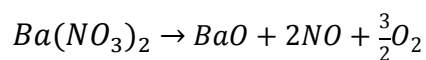
Lean NO_x Trap (LNT)

The concept of NO_x absorbers has been developed based on acid-base wash coat chemistry. It involves storage of NO_x on the catalyst wash coat during lean exhaust conditions and release during rich operation and/or increased temperatures. Depending on the NO_x release strategy they can be classified as “active” or “passive”. In active absorbers, stored NO_x is periodically released, with a typical frequency of about once per minute, during a short period of rich air-to-fuel ratio operation, called NO_x absorber regeneration. The released NO_x is catalytically converted to nitrogen, in a process similar to that occurring over three-way catalysts (TWC) widely used in stoichiometric gasoline engines. On the other side passive NO_x absorbers, a more recent and simpler variant of the technology, adsorb NO_x during vehicle cold start and release it under high exhaust temperature conditions to be converted over a downstream NO_x reduction catalyst. Hence, passive absorbers are not a stand-alone NO_x control technology.

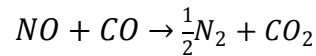
LNT is an active NO_x absorber. Under lean operating conditions extensive NO_x accumulation occurs on the catalyst surface (made of alkali metals or alkaline earth metals e.g. barium) due to NO_x adsorption in the form of nitrates or nitrites. The following equation represents adsorption of NO₂ in the form of barium nitrate if barium oxide is used as storage material:



Since the storage capacity is limited, the trap requires a periodical regeneration to prevent clogging. The regeneration can be carried on in two different ways: injecting an extra amount of fuel directly into the cylinder late during the expansion stroke or in the exhaust manifold by means of an additional injector. In both cases the aim is to consume the oxygen in excess in the exhaust line thus creating, for short intervals (2-5s), a rich mixture where nitrates NO₃ species become thermodynamically unstable and decompose, producing NO or NO₂, according to the equations:



Finally under rich conditions, the nitrogen oxides are reduced by HC, CO and H₂ to N₂ over the reduction catalyst, in a conventional three-way catalyst process. One of the possible reduction paths is described by the following equation:



It is worth to underline that the actual chemical and physical processes are more complex and not fully explained by the mentioned equations [79]. Since the exhaust gas of a diesel engine, depending on the diesel quality, might contain small amounts of sulfur (S) coming from the fuel and lubricating oil, NO_x absorbers also show some undesired reactivity with barium sulfate (BaSO₄) production. This causes gradual saturation of the barium sites with sulfur and loss of activity towards the adsorption of NO₂. BaSO₄ can be thermally decomposed but sulfates of barium or other adsorbents are more stable than the corresponding nitrates and require higher temperatures to desulfate (above 600°C). For this reason, sulfur deactivation is a major problem in the development of NO_x absorber systems and the periodical rich conditions required for denitration and desulfation increase fuel consumption up to 10% if compared to completely lean combustion mode.

Selective Catalyst Reduction (SCR)

Selective Catalytic Reduction (SCR) is one of the most cost-effective and fuel-efficient technologies available to reduce diesel engine emissions. This is designed to permit nitrogen oxides (NO_x) reduction reactions to take place in an oxidizing atmosphere. The SCR system (figure 1.12) consists of a supply pump, a dosing system ran by the ECU, an injector mounted in the exhaust pipe and the SCR.

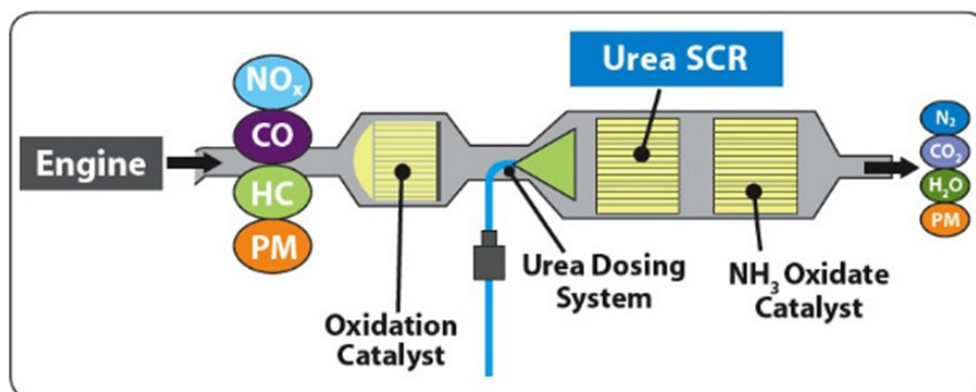
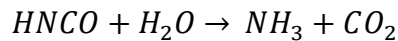
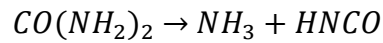


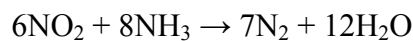
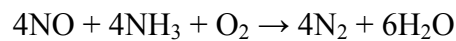
Figure 1.12: Selective Catalyst Reduction system [80]

The reductant source is usually automotive-grade urea, otherwise known as Diesel Exhaust Fluid (DEF). DEF is carried in an onboard tank which must be periodically replenished by the operator

based on vehicle operation. For light-duty vehicles, DEF refill intervals typically occur around the time of a recommended oil change, while DEF replenishment for heavy-duty vehicles and off-road machines and equipment will vary depending on the operating conditions. The injected urea solution, with chemical formula $\text{CO}(\text{NH}_2)_2$, reacts with the water contained in the exhaust gases through thermolysis in the engine exhaust line to produce the oxidizing ammonia according to the following reactions:



Once ammonia has been produced, it sets off further reactions converting nitrogen oxides (NO and NO_2) into nitrogen, water and tiny amounts of carbon dioxide (CO_2) mainly according to the following equations:



The SCR technology alone can achieve a NO_x reduction up to 90 percent and is often combined with a diesel particulate filter to achieve PM emission reductions as well. Temperature (reaction kinetics of NH_3 with NO_x is very sensitive to its variations) and amount of injected urea are the two main parameters which have to be precisely controlled in an SCR system.

The introduced stricter emission limitations for NO_x and particulates in mobile diesel applications may require the combinations of active after treatment systems like DPF, SCR with urea and LNT. The combination of these systems is currently being widely studied and several papers have been published. In [81] a combination of LNT+SCR enabling on-board synthesis of ammonia (LNT) which is then removed on the SCR catalyst, is proposed. The main application for this kind of system can be light-duty vehicles, where LNTs are already used and the low temperature de NO_x is a main target.

Diesel Particulate- NO_x Reduction system (DPNR)

The Diesel Particulate- NO_x Reduction (DPNR) system from Toyota has the potential of simultaneously reducing NO_x and PM. The system, shown in figure 1.13, is composed of a filter substrate made of cordierite (a special ceramic with excellent response properties to thermal shock).

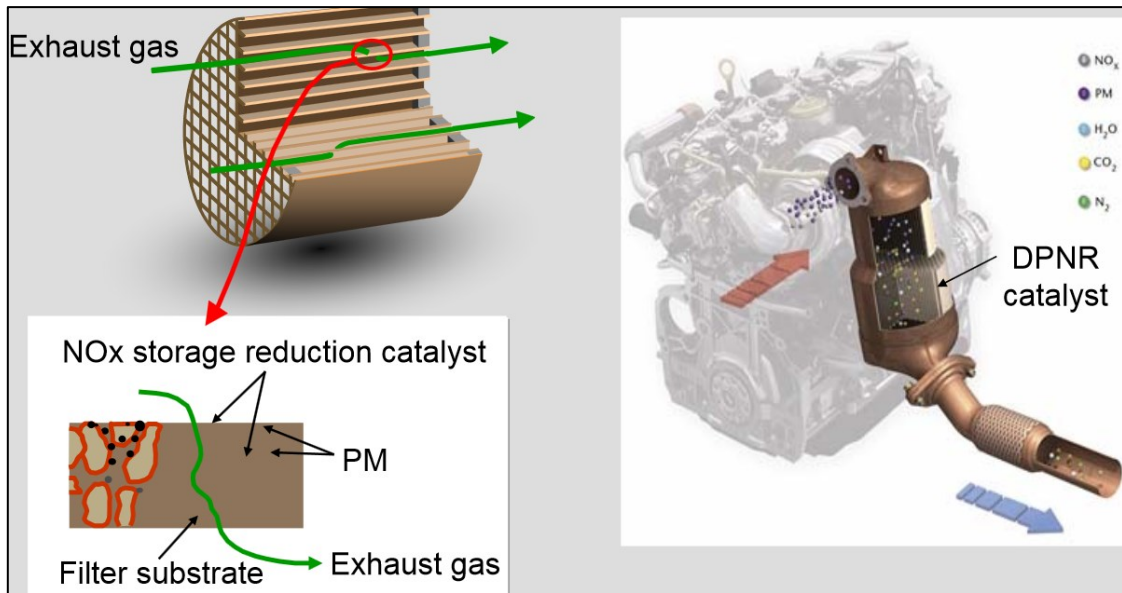


Figure 1.13: Diesel Particulate – NO_x Reduction system [82]

The honeycomb structure filter forces the gas path through the structure walls in order to collect the particulates on its surface. Moreover the system comprises an exhaust port injector installed after the turbine and activated to start the filter regeneration process and temperature and pressure sensors at the DPNR inlet and outlet. The system features a newly developed, highly porous ceramic filter coated with a catalyst exclusively developed by Toyota which allows NO_x storage and reduction. During conventional lean-burn combustion, particulate matter is oxidized using active oxygen created when NO_x is temporarily stored inside the catalytic converter. In a second phase, the engine is switched to low-oxygen rich combustion mode through the activation of the exhaust port injection. In this condition the stored NO_x is reduced producing more active oxygen available to further oxidize particulate matter inside the catalytic converter. Unlike other soot filters, it is a servicing-free system; this means that no periodic replacement of any component is scheduled during the entire vehicle life. In addition it doesn't necessitate the use of any fuel additive. The only requirement, in order to achieve maximum efficiency and avoid a deterioration of the catalyst, is the use of diesel fuel with less than 10ppm of sulphur.

1.5 Alternative fuels

Biodiesel

Biodiesels are ethylic or methyl esters of acids with long chain derived from a broad variety of resources such as vegetable oils (soybean, canola, sunflower, palm, cotton, mustard and algae), animal fats and waste cooking oil. It is rapidly biodegradable, non-toxic and, when used as a fuel

for vehicles, safer in the event of a crash because of its higher flash point (with respect to conventional diesel). A transesterification process is required to reduce the viscosity of the raw oil and produce biodiesel fuel for diesel engines [83]. A scheme of the raw oil to biodiesel conversion process is reported in figure 1.14.

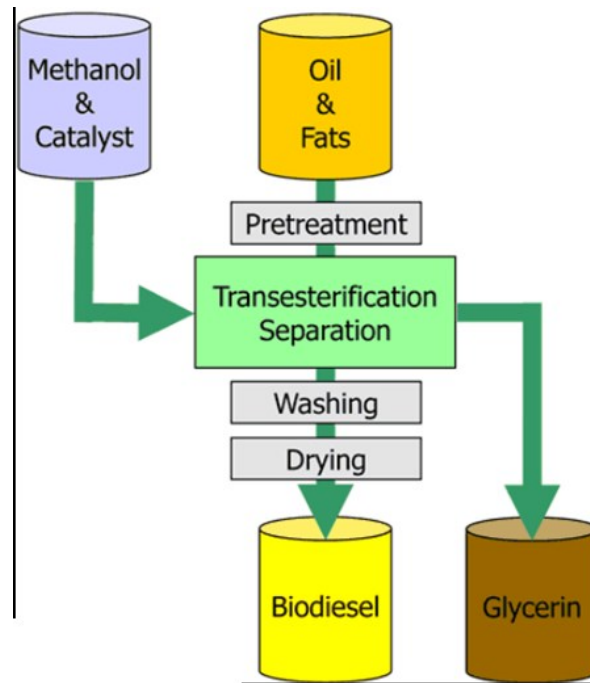


Figure 1.14: Raw oil or fats to Biodiesel process [84]

The transesterification process is the reaction of a triglyceride (fat/oil) with an alcohol to form esters and glycerol. A triglyceride has a glycerin molecule with three long chain fatty acids attached. During the esterification process, the triglyceride is reacted with alcohol in the presence of a catalyst, usually a strong alkaline like sodium hydroxide. The alcohol reacts with the fatty acids to form the mono-alkyl ester (or biodiesel) and crude glycerol. In most production methanol, with production of methyl esters (figure 1.15) or ethanol, with production of ethyl esters are the used alcohols, base catalyzed by either potassium or sodium hydroxide.

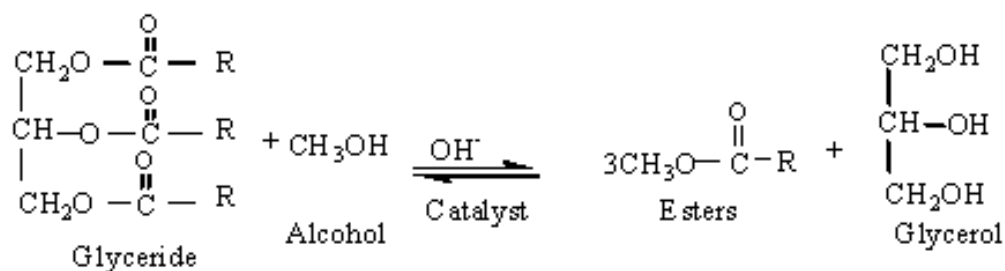


Figure 1.15: Chemical process for methyl ester biodiesel

The alcohol/catalyst mix is charged into a closed reaction vessel and the oil or fat is added. The system from here on is totally closed to the atmosphere to prevent the loss of alcohol. The reaction mix is kept at a temperature above the boiling point of the alcohol (around 160 °F) to speed up the reaction taking place. Excess alcohol is normally used to ensure total conversion of the fat or oil. Once the reaction is complete, the two major products are glycerin and the ester (biodiesel). They are characterized by two different density values and can therefore be gravity (or by means of a centrifuge) separated with glycerin moving to the bottom of the settling vessel. The excess alcohol in each phase, removed with a flash evaporation process or by distillation is then re-used. Water and alcohol are removed to produce 80-88% pure glycerin that is ready to be sold as crude glycerin. In more sophisticated operations, the glycerin is distilled to 99% or higher purity and sold into the cosmetic and pharmaceutical markets. Once separated from the glycerin, the biodiesel results in a clear amber-yellow liquid with a similar viscosity of the conventional diesel one. In some systems the biodiesel is distilled in an additional step to remove small amounts of color bodies to produce a colorless biodiesel. Prior to its use as a commercial fuel, the finished biodiesel must be analyzed using sophisticated equipment to ensure it meets any required specifications. It is important that a complete reaction took place and that glycerin, the catalyst and the alcohol are completely removed from the new-born fuel.

In a 1912 speech Rudolf Diesel said: "The use of vegetable oils for engine fuels may seem insignificant today but such oils may become, in the course of time, as important as petroleum and the coal-tar products of the present time." Biodiesel is nowadays available at gas stations blended with conventional diesel. Current fuel standards allow up to 7 % (in volume) of FAME (Fatty-acid methyl ester). It has good lubricating properties, a cetane number comparable to low sulfur diesel and a calorific value of 37 MJ/kg which is about 10% less than conventional petrodiesel. It has a high boiling point (unfavorable for evaporation) and a significantly higher flash point ($>130^{\circ}\text{C}$) than conventional diesel (64°C) which is unfavorable for the formation of an ignitable mixture in air. Moreover biodiesel is characterized by a higher density ($\sim 880 \text{ kg/m}^3$) than diesel ($\sim 850 \text{ kg/m}^3$), contains no sulfur and PAH, doesn't require changes to the engine structure and it is often used as an additive to Ultra-Low Sulfur Diesel (ULSD) fuel to aid with lubrication, as the sulfur compounds in petrodiesel provide much of the lubricity [85]. Table I.II summarizes the main properties of biodiesel from sunflower and cottonseed.

Fuel properties	Diesel fuel	Sunflower ME	Cottonseed ME
Density at 20 °C, kg/m ³	837	880	885
Cetane number	50	50	52
Lower calorific value, MJ/kg	43	37.5	37.5
Kinematic viscosity at 40 °C, mm ² /s	2.6	4.4	4
Boiling point	180–360	345	345
Latent heat of evaporation, kJ/kg	250	230	230
Oxygen, % weight	0	10.9	10.9
Stoichiometric air–fuel ratio	15.0	12.5	12.5
Molecular weight	170	284	284

Table I.II: Main properties of biodiesel from sunflower and cottonseed with respect to conventional diesel [86]

There is a wide agreement in the literature that biodiesel and its blends generally decrease the emissions of both CO and HC especially at high engine loads. Due to the lack of sulphur and PAHs, biodiesel usage decreases the carbon particulate emissions and increases the SOF (Soluble Organic Fraction), resulting in reduced visible smoke and opacity [87], [88]. The shift of PM toward higher SOF content, as well as the absence of sulphur, makes biodiesel compatible with diesel oxidation catalysts, which can maximize PM benefits. Therefore it appears that there is a potential to reduce gaseous and smoke emissions using biodiesel blends, when an engine and its auxiliary systems (injection system, EGR) have been optimized. The dynamic processes of injecting mineral diesel fuel and its mixtures with biodiesel, such as rapeseed and soybean, and their effects on diesel engine performance and emissions have been investigated in [89]. Blends of 50% in volume of rapeseed and soybean oils in diesel (RME50 and SME50) have been characterized in terms of fuel injection rate, spatial-temporal evolution of the jets and engine tests. The authors state that engine test bench analysis, performed at constant power output, highlighted a higher specific fuel consumption for the RME50 and SME50 compared to the diesel one mainly because of their lower energy content. Regarding emissions, the authors found similar levels of NO_x and CO and reduced PM emissions with the diesel/biodiesel blends. In [90] rapeseed oil methyl ester (RME), neat and blended with diesel in different percentages, has been investigated on a multi-cylinder light-duty diesel engine which included the various latest technologies for low emission (e.g. common-rail injection system, cooled-EGR system, variable geometry turbocharger (VGT) and after treatment systems). The authors state that an NO_x emission linear increase with increasing percentage of RME in diesel has

been detected while an increase in oxygen content in the fuel caused a drastic reduction of engine-out smoke emission. In [91] the authors state that a modification of the engine is required when using biodiesel. In fact they found that biodiesel blending determined problems related to oil dilution in vehicles equipped with DPF. The authors investigated the effects of biodiesel blending on exhaust emission from commercial vehicles and found an increase in NO_x emissions with particular reference to a vehicle equipped with urea-SCR system. Moreover, on one hand reduced PM emission from the vehicles not equipped with DPF has been achieved. On the other hand, though, PM emission from vehicles equipped with DPF increased because of an increase in SOF emission.

n-Butanol

Alcohol fuels are produced through biological mechanisms as well as petrochemical pathways, are characterized by molecular oxygen and less carbon than diesel, higher vapor pressures (leading to enhanced evaporative emissions) and low energy density. In addition they show a lower cetane number, which leads to increased ignition delay when used as alternative fuels in diesel engines. Alcohol fuels such as methanol (CH₃OH), ethanol (C₂H₅OH), propanol (C₃H₇OH) and butanol (C₄H₉OH) can be used with fossil-based fuels in various percentages for diesel engines as a clean alternative fuel source. Besides, low percentages of alcohol in diesel fuel do not require any modification to the engine fuel system. Ethanol and methanol, though, show low solubility with diesel particularly at low temperatures and ethanol is characterized by low viscosity which leads to lubricity problems. On the other hand, the physical and chemical properties of butanol indicate that it has the potential to overcome the limitations brought by low-carbon alcohols like ethanol and methanol. It is much less evaporative and corrosive, releases more energy per unit mass (35.1 MJ/kg vs 26.8 for ethanol and 19.9 for methanol), has a lower auto-ignition temperature and vapor pressure, a higher miscibility (no phase separation when blended with diesel) and cetane number (12, while CN=8 for ethanol and 3 for methanol) thus being more suitable as an additive for diesel fuel [92]. Butanol can be produced by fermentation of biomass, such as algae, corn, and other plant materials containing cellulose that could not be used for food and would otherwise be wasted. Butanol has four isomers, reported in table I.III, characterized by having the same amount of heat energy but different molecular structures.

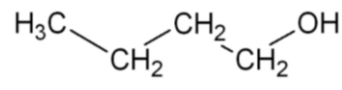
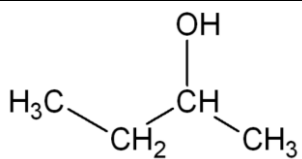
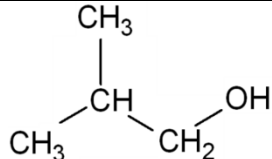
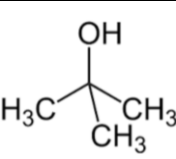
n-butanol	sec-butanol	i-butanol	t-butanol
			

Table I.III: Different molecular structures of the four butanol isomers

Table I.IV, instead, summarizes the main alcohol fuels properties with respect to conventional diesel and some of the main results concerning the use of alcohols are reported in the following.

	Diesel	n-Butanol	Methanol	Ethanol
Cetane number	40–55	12	3	8
Density (g/ml)	0.86	0.81	0.796	0.790
Auto-ignition temperature (°C)	200–220	385	470	434
Lower heating value (MJ/kg)	42.5	35.1	19.9	26.8
Boiling point (°C)	180–230	117.7	64.5	78.4
Stoichiometric ratio	14.3	11.21	6.49	9.02
Latent heating (kJ/kg)	270	581.4	1109	904
Flammability limits	1.5–7.6	1.4–11.2	6.0–36.5	4.3–19
Saturation temperature (°C)	–	20	20	20
Saturation pressure (kPa)	–	0.6	11.83	5.93

Table I.IV: Main alcohol fuels properties with respect to conventional diesel ones [93]

An experimental study has been conducted in [93] to investigate the influence of n-butanol addition with multiple injections on engine performance and emissions. The authors adjusted the EGR rate to keep NO_x emission at 2.0 g/kWh and different n-butanol volume ratios were blended in diesel. They achieved results showing a significant reduction in soot and CO emissions without a deep impact on BSFC and conclude that n-butanol oxygenated addition does not have a major influence on NO_x and can further improve emissions if combined to an optimized triple-injection strategy. In [86] the authors tested a 70-30% diesel/bio-diesel and a 75-25% diesel/n-butanol blends with respect to conventional diesel and found that peak or cumulative values of NO emission increased for the two fuel blends compared with the neat diesel fuel case and that the increase in NO emission was greater for the bio-diesel blend compared with the n-butanol one. In addition the authors experienced a decrease in smoke emissions for the two fuel blends (with maximum reduction achieved with the n-butanol blend) due to the relative fuel-bound oxygen mass playing a key role. Different blends of n-butanol in diesel were investigated in [94], [95] and engine

performance plus exhaust emissions were analyzed. The smoke density was significantly reduced with the use of the butanol–diesel fuel blends with decreasing smoke values achieved increasing the percentage of butanol in the blend. Contrarily to results found in [86], the NO_x emissions were found to be slightly reduced with the use of the butanol–diesel blends with increased reduction attained with increasing percentages of butanol in the blend. Moreover CO emissions were reduced while unburned hydrocarbons (HC) emissions were increased. Finally slightly increasing specific fuel consumption and marginally lower exhaust gas temperatures were found with the n-butanol blends. The authors conclude that n-butanol can be safely and advantageously used up to high blending ratios with conventional diesel because of reduced engine out emissions, noticeable thermal efficiency and high solubility. An important effect of n-butanol content in the fuel blends on engine performance and emissions has been even noticed in [96]. The authors investigated the performance and exhaust emissions of a single cylinder DI diesel engine at constant engine speed and four different engine loads. They conclude that n-butanol can be easily blended with diesel without phase separation and that its use determines a slight increase both in brake specific fuel consumption (because of the n-butanol inferior lower heating value) and in brake thermal efficiency. The authors even noticed that exhaust gas temperature, CO, smoke opacity and NO_x emissions (contrarily to other publications) were reduced with respect to reference diesel fuel. On the other side an increase in HC emissions was found.

Poly(oxymethylene)dimethylethers (POMDME)

Several studies on the use of oxygenated fuels have shown a reduction of particulate matter and recommend the use of oxygenates to suppress the C-C bonds and therefore the soot precursor species [97]. However, some of them, e.g. Dimethyl ether (DME), are not appropriate for diesel engines because of their properties (e.g. vapour pressure and ability to produce methane). DME has been studied in several research centres [98]–[103] and if on one hand allows an almost smokeless combustion, on the other hand requires significant modifications to the fuel injection system in diesel engines because of its low viscosity, low lubricating capability and being in a gaseous state under atmospheric conditions (thus requires to be stored under pressure). DME shows poor solubility in diesel fuel blends and high vapor pressure. Therefore, oxygenates with higher viscosity and boiling point are definitely more attractive. Poly(oxymethylene) dimethyl ethers (POMDME or OME in abbreviated form) are characterized by a $\text{CH}_3\text{-O-(CH}_2\text{-O)}_n\text{-CH}_3$ general structure, with a mass fraction of oxygen within the molecule up to almost 50%. These fuels can be obtained from methanol in a process chain described in detail in [104]–[107]. The first fuel of the POMDME family is dimethoxymethane (DMM or OME1, POMDME with only one $\text{-O-CH}_2\text{-}$ group) which

has been investigated both blended with commercial diesel and pure, still though with some fuel system modifications. DMM is still more volatile than diesel, having its boiling point at 42°C and therefore problems related to vapour lock may occur. In [108] the authors investigated a 15% DMM in diesel blend in a direct injection diesel engine and found great benefits in exhaust emission reduction. However they state that it is not possible to substitute this fuel into existing engines without modifications to fuel system. In [109] the same blend in several speed/load conditions was investigated and a PM reduction at any investigated operative point was found while no significant reduction in NO_x emissions was noticed. In [110] the authors achieved ultra-low emission and efficient diesel combustion with pure DMM and a combination of high EGR plus a three-way catalyst. In [111] a pure OME1 fuel with additives to enhance viscosity, lubricity and cetane number was tested. Engine testing proved the possibility of a soot reduction without a corresponding increase in NO_x emissions. However the authors found a growing output of methane near stoichiometric conditions. Because of the low cetane number (CN), high volatility and weak viscosity and lubricity of OME1, higher OMEs (n=3,4,5) are considered to be more suitable for application in a diesel engine as neat substance. In [104], for instance, the authors state that, due to their physical properties, POMDMEs with n ranging in between 2 and 5, can overcome the disadvantages given by DME and DMM, particularly regarding injection system modifications due to higher viscosities and higher boiling points. Table I.V reports the main properties of the POMDME family fuels.

	CDF	DME	DMM	POMDME		
				n=2	n=3	n=4
Melting point (°C)	-	-141	-105	-70	-43	-10
Boiling point (°C)	170 – 390	-25	42	105	156	201
Viscosity (25°C) (mPa*s)	2.71	-	0.58	0.64	1.05	1.75
Density liquid (25°C) (kg/l)	0.83	-	0.860	0.960	1.024	1.067
Cetane number	55	55	29	63	70	90
Oxygen content (wt%)	-	34.7	42.1	45.3	47.1	48.2

Table I.V: Physical properties of conventional diesel (CDF), DME, DMM and POMDMEs [104]

The POMDMEs are characterized by the presence of activated methylene groups bounded to oxygen atoms ($-O-CH_2-$) which leads to the formation of hydroperoxides in an early stage of the combustion. These hydroperoxides decompose into OH radicals which subsequently degrade soot precursors by oxidative processes. Their higher viscosities and boiling points allow the blending in diesel without modifications to the injection system. In addition POMDMEs show a good

miscibility with diesel (the optimal chain length for a POMDME-diesel blend is with $n=3-4$; for $n=2$ a low flash point is shown while longer chains determine the risk of precipitation at low temperatures. This may clog filters or other parts of the fuel system) and because of their low vapor pressures, no pressurized tank or fuel system is needed. POMDMEs with $n = 3-5$ are characterized by a cetane number in the range 70-100, higher than diesel one (55). POMDMEs are therefore very attractive as alternative fuels for diesel engines [104]. As shown in table I.V, POMDMEs present an oxygen content in the range 42-53 wt%. This means that small amounts of this oxygenated in diesel could still allow a high heating value coming from the diesel, taking advantage at the same time, of the oxygen content coming from POMDME. Unfortunately POMDMEs are characterized by requiring an expensive production process, with respect to other oxygenates, because of a higher finishing grade. In the near future, though, an optimized production technology could decrease the cost facilitating, in this way, the possibility of a large scale production.

In [104] the production process for POMDME is explained in detail; these oxygenates can be obtained from methanol in a process chain which is illustrated in figure 1.16. In a first process step formaldehyde is obtained by dehydrogenation of methanol. The trioxane process consists of the trimerisation of formaldehyde which is usually catalyzed by H_2SO_4 and a work up of the reactor outlet, for example by a pressure-swing distillation sequence. The preferred production method for methylal from formaldehyde and methanol is a heterogeneously catalyzed reactive distillation. Subsequently both formaldehyde based products trioxane and methylal are converted to POMDMEs.

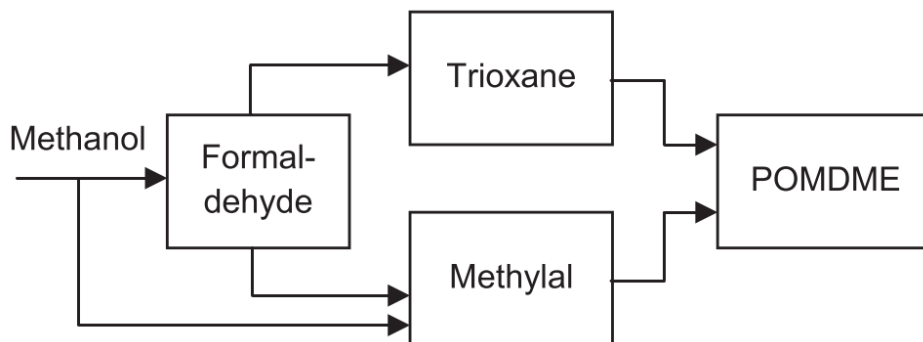


Figure 1.16: POMDME process chain [104]

Just few papers on the use of pure or blended POMDME fuels have been published [112]–[116]. Pellegrini et al. state that, comparing a 7.5% POMDME in diesel blend with commercial diesel, at fixed NO_x emission level, a significant reduction of PM is achieved. At the same time, though, higher PAH emissions were found, because of the higher EGR rate and lower exhaust gas temperature that reduced the DOC activity when operating with the oxygenated fuel. The authors

even noticed a reduction of the number of particles above 30 nm at engine speeds above 2000 rpm with POMDME. In addition a 3-4% power loss and increase in specific volumetric fuel consumption was found [115].

1.6 Structure and objective of the activity

The present activity had, as main objective, the investigation of different oxygenated fuels properties on combustion evolution and achievable performance and exhaust emissions from diesel engines to bring a further scientific contribution in reducing in-cylinder emissions. The activity has been conducted in two phases that will be discussed in this dissertation. Each chapter will contain both phases, presented in different sections.

The first part of the present study has been carried on at Istituto Motori, Italian National Research Council in Naples and focused on comparing performance and engine out emissions from conventional diesel and alternative fuels. In particular the experimental investigation has been performed on a light duty diesel engine, turbocharged DI four cylinder for automotive applications equipped with a common rail injection system. The engine has been fueled with different biodiesel in diesel blends, two gasoline - diesel mixtures and one butanol – diesel. Their results have been compared to conventional diesel ones. Even though no molecular oxygen content is present in the gasoline – diesel blends, they have been investigated because of the low cetane number of gasoline that is helpful to achieve a premixed combustion mode (PCCI), as reported in several previous works (e.g. [61], [66], [67]). In particular in [66], the authors state that in a PCCI combustion mode, where the injection event is separated from combustion, if the combustion phasing is the same for two of the tested fuels (the authors considered an n-heptane fuel, two fuels in the diesel volatility range and three in the gasoline volatility range), their emissions behavior at a given condition will be similar regardless of the differences in volatility and composition. PCCI has been studied because of its potential to increase the air-fuel mixing reducing, in this way, the locally rich regions in the combustion chamber responsible for soot formation. The effects of PCCI and molecular oxygen have been both investigated and will be discussed in the present dissertation with the aim of providing further knowledge on advantages introduced with oxygenated fuels, with the PCCI combustion mechanism and, particularly, with the combination of PCCI and different oxygenated and non – oxygenated (but with low cetane number) fuels. In this way the present activity tries to provide further understanding on whether specific fuel characteristics are exalted with PCCI to achieve the maximum exhaust emission reduction, with particular reference to particulate matter.

The second part of this study has been, instead, conducted at the Aerothermochemistry and Combustion Systems Laboratory, ETH Zurich, Switzerland. Different oxygenated fuels have been investigated in a constant volume chamber with large optical access. In particular Poly(oxyethylene) dimethyl ethers (POMDME) with a $\text{CH}_3\text{-O-(CH}_2\text{-O)}_n\text{-CH}_3$ general molecular structure have been studied focusing, with respect to combustion evolution, both on the fuels properties and the temperature at start of combustion. In order to study the combustion evolution and soot formation and oxidation processes, optical techniques such as OH chemiluminescence and two dimensional two color pyrometry (2D2CP) have been applied. Moreover soot emissions from the different investigated fuels have been analyzed by means of a fast particle spectrometer. The deeper knowledge of the oxygenated fuel effect on soot formation/oxidation processes provided by this activity has been then applied to a second investigation on a single cylinder “heavy duty” direct injection diesel engine. The aim of this final activity has been to achieve a complete overview of the impact of POMDME-diesel blends on engine performance and exhaust emissions. Great attention has been reserved to the analysis of the different engine out emissions: soot as well as nitrogen oxides, unburned hydrocarbons, carbon monoxide and carbon dioxide.

Chapter 2

Experimental Procedure

Introduction

The different experimental facilities used during the present study and the investigated fuels are described in the following paragraphs. Moreover, paragraph 2.2 includes the theory and mathematical expressions allowing the calculation of the k_L factor (proportional to the absorption coefficient per unit of soot cloud thickness and the flame thickness) used as an index of the in-cylinder soot mass concentration.

2.1 Automotive GM diesel engine

The first part of the study has been conducted on a turbocharged, water cooled, 4-valve, 4-cylinder DI diesel engine (figure 2.1) from General Motors, installed at the Istituto Motori – Italian National Research Council.

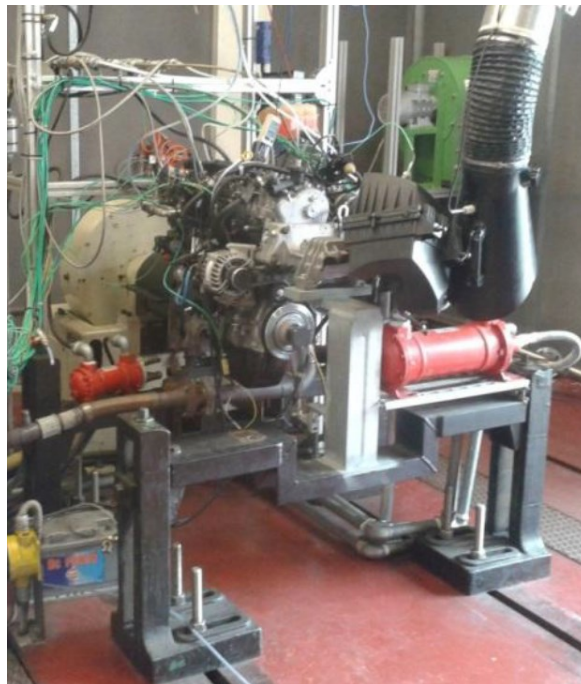


Figure 2.1: Automotive four cylinder diesel engine test bench

Engine set-up

The 95 hp engine fulfills Euro V emission standards and is equipped with an EGR system, a common rail injection system and 7 hole - 0.12 mm nozzle diameter solenoid injectors. It is characterized by a 1248 cm³ displacement (bore = 69.5mm, stroke = 82mm) and a compression ratio of 16.8:1. The INCA (Integrated Calibration and Measurement System) software has been used for the engine management (e.g. load, injection pressure and injection timing). This software gives the possibility of reading the ECU variables, managing its parameters, building up its calibration and acquiring results. Moreover, a piezo-quartz pressure transducer ($\pm 0.1\%$ accuracy) to detect the in-cylinder pressure signal, several pressure and temperature sensors in different parts of the engine and a current probe to acquire the energizing current to the injector (pressure transducer and current probe only for cylinder number 2) have been installed. The intake air has been supplied to the engine at constant temperature (293 K) by means of an air handling unit (conditioning system); intake and exhaust O₂ concentrations were checked by two O₂ sensors. An eddy current dynamometer, capable of absorbing powers up to 190 kW and convert them (Joule effect) in heat dissipated through a water cooling system, has been connected to the engine. On the eddy-current dynamometer a force transducer has been installed in order to measure the engine torque. For the acquisition of the in-cylinder pressure signal and the energizing current to the injector an AVL Indimodul data recording system, integrated with the Indicom software which allows to calculate the instantaneous and cumulative heat release curves through the first law of thermodynamics, has been used. A sketch of the experimental set-up is shown in figure 2.2 while the accuracy of the main acquired quantities is reported in table II.I.

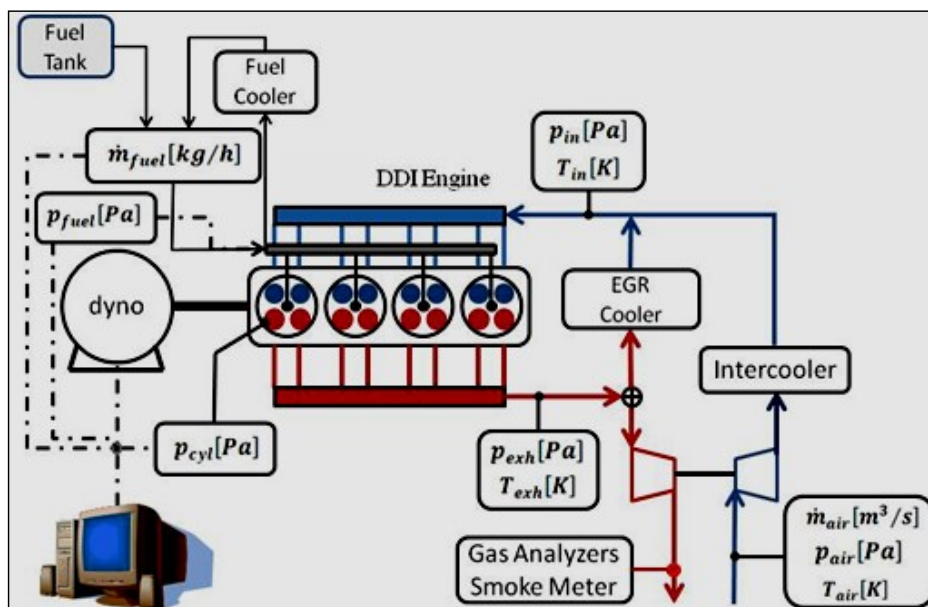


Figure 2.2: Sketch of experimental engine set-up

Engine Speed	± 1 rpm
Torque	± 1 Nm
Air Mass Flow Rate	$\pm 1\%$
Specific fuel consumption	$\pm 5\%$

Table II.I: Accuracy of the main acquired quantities

Exhaust emissions have been measured by means of the following analyzers:

- an ABB Limas 11 for NO_x exhaust emissions, belonging to the Non Dispersive Ultra Violet (NDUV) category. Its working principle is based on an ultraviolet ray source generating a beam of light passing through an optical filter (in order to select the specific wavelength exciting the molecules to be detected) and into the cell where the engine exhaust gas is inflated. The UV light passes through the gas and reaches a light absorption detector. Following the Beer – Lambert law, the energy absorption results to be proportional to the number of absorbing molecules.
- an ABB Uras 14 for O₂, CO and CO₂ emissions. CO and CO₂ are measured by means of a Non-Dispersive Infra-Red (NDIR) detector: each constituent gas in a sample absorbs some infra - red at a particular frequency. By shining an infra-red beam through a sample cell (containing CO or CO₂) and measuring the amount of infra-red absorbed by the sample at the specific wavelength, a NDIR detector is able to measure the volumetric concentration of CO or CO₂ in the sample. In addition O₂ is measured by means of an electrochemical oxygen sensor.
- an AVL 415 Smoke Meter (0.1% value resolution) for smoke measurements. The Smoke Meter uses the filter paper absorption method: the shades of gray imprinted on the paper are detected and associated to an FSN (filter smoke number) by means of a photoelectric meter.

Investigated fuels

The investigation focused on fuels characterized by molecular oxygen and/or a low cetane number in order to enhance premixing with air. The baseline diesel fuel has been the European low sulphur (max 10 ppm) commercial diesel with a cetane number of 52 and its results have been compared with:

- an RME biodiesel fuel, denoted B100
- a blend, denoted B30, composed of 70% baseline diesel and 30% RME by volume
- a blend, denoted B60, composed of 40% baseline diesel and 60% RME by volume
- a blend, denoted BU30, composed of 70% of diesel and 30% n-butanol by volume.

Further, two additional investigated blends were obtained by mixing diesel and gasoline (ON=95) in order to evaluate results coming from fuels with no molecular oxygen but characterized by a high ignition delay:

- a first blend, denoted G30, composed of 70% baseline diesel and 30% gasoline by volume.
- a second blend, denoted G60, composed of 40% baseline diesel and 60% gasoline by volume.

Table II.II shows the main characteristics of the tested fuels. Their main differences are related to the cetane number, density, volatility and the net heat value, of particular interest for local mixing preparation, charge fuel distribution within the combustion bowl and thermal efficiency.

FUEL PROPERTIES							
	Diesel	B30	B60	B100	G30	G60	BU30
Density@15°C [kg/m ³] ASTM D4052	840	853	866	883	810	780	828
Viscosity@40°C [mm ² /s] ASTMD445	2.5	3.0	3.6	4.3	2	1.5	2.2
Cetane Number ISO4264	52	52.1	52.2	52.3	41.3	30.6	43.9
Net Heat Value [MJ/kg]	42.9	40.9	39.3	37.1	43.1	43.2	39.9
C content [%] ASTM D5291	86	84	81.6	78.5	85.6	85	79.9
H content [%] ASTM D5291	12.7	12.1	11.6	10.8	13.5	14.2	13
O ₂ content [%] ASTM D5291	-	3.2	6.3	10.5	-	-	6.5
IBP [°C] ASTM D86	160	209	257	322	-	-	120
Distillation 50% Vol. [°C] ASTM D86	280	297	314	337	220	160	230
Distillation 90% Vol. [°C] ASTM 5291	338	340	341	343	328	317	328

Table II.II: Main properties of the different fuels

Operating conditions

The experimental investigation conducted on the automotive 4 cylinder 4 valve DI diesel engine focused, with respect to the operating conditions, on exploring the effect of combustion phasing (CA50) and oxygen concentration at intake on engine out emissions and performance. Tests have been performed at 2500 rpm and 0.8 MPa BMEP, one of the operating points of the reference multi-cylinder engine New European Driving Cycle (NEDC). The investigation has focused on a comparative report of the engine performance and emissions exploring a set of operating conditions (Table II.III) with commercial diesel and alternative fuels.

CA50 [cad atdc]	O ₂ at intake [%]	Inj. pressure [MPa]	Boost pressure [MPa]
18, 21	17, 19	140	0.16

Table II.III: Operating conditions

A single injection strategy has been chosen for the tests and the engine load has been fixed at the constant value of 0.8 MPa for the different investigated fuels (characterized by different energy content) by managing the injection duration. The combustion phasing (CA50) has been set, within ± 0.1 ca, by adjusting the start of injection (SOI) and its values have been chosen in order not to exceed the 2% of the IMEP coefficient of variation, selected as the engine stability limit. It is helpful to remark that with SOI it is intended the start of the energizing current to the solenoid injector and not the start of the actual fuel delivery. In fact, because of the hydraulic and electronic delays a lag between the timing of the energizing current to the solenoid and the actual fuel delivery from the nozzle is present; this value has been estimated from the instantaneous fuel flow rate measurements to be about 300 μ s (~ 4.5 cad at 2500 rpm).

2.2 Constant volume cell set-up

Cylindrical constant volume chamber set-up

The second phase of the activity has been carried on a cylindrical constant volume chamber (CCVC) with large optical accesses. Its air path contains an autoclave, a connecting inlet tube, the chamber itself (figure 2.3) and an exhaust tube while an external compressor is used to achieve suitable in-cell pressures before combustion. This is connected to an autoclave via a pressure control valve to reduce the pressure to a set point value. The autoclave is characterized by a

considerably larger volume compared to the cell body and feeds it via the connecting inlet tube as soon as a cycle is initiated. This pressure reservoir, the inlet tube and the chamber are equipped with pressure and temperature sensors as well as heating elements which allow temperatures up to 800 K within the chamber. Moreover, in order to emulate engine-like conditions at start of main injection combustion, a pilot injection can be applied to further increase, through its combustion, pressure and temperature values prior to the main injection event.

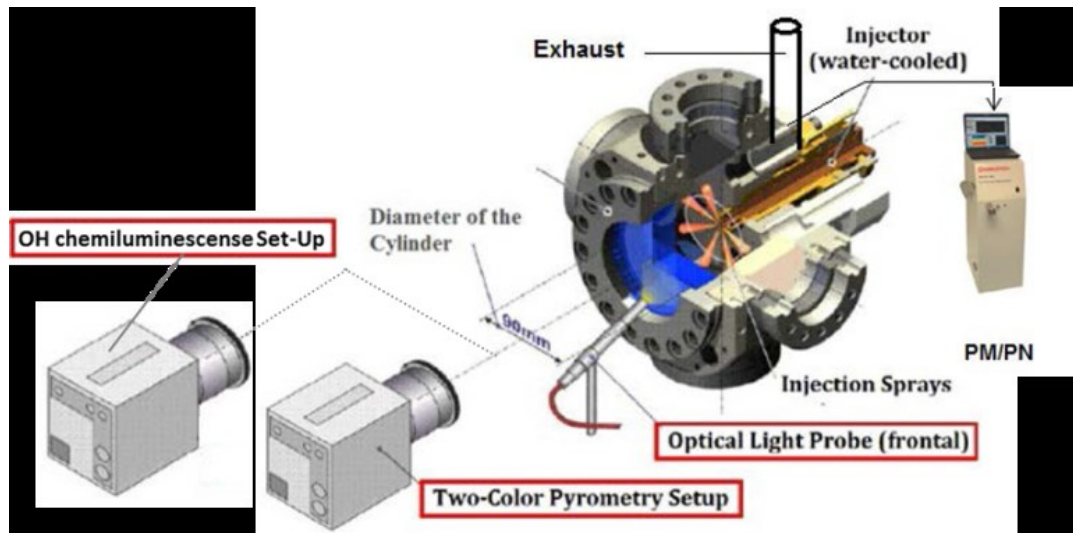


Figure 2.3: Experimental apparatus (cell, optical set-up and particle spectrometer) [117]

The fuel pressure is achieved by a pneumatic high pressure pump, which is able to generate fuel pressures up to 1600 bar, connected to a rail and a passenger car Bosch piezo injector (8 holes, 0.108 mm nozzle diameter). In order to have optical access to the complete combustion volume, the originally cubic-formed vessel has been retrofitted with steel cylindrical walls, concentric to the axis of the injector. Due to the insertion of these cylindrical walls, the optical access is limited to the front window but allows a complete view of the combustion chamber. Because of heat losses (figure 2.4), the in-cell pressure trace presents a decreasing trend after the combustion event meaning that a variation of exhaust valve opening timing determines different values of gas pressure being released in the exhaust. Part of the exhaust volume is sampled and analyzed using a Cambusion DMS 500 fast particle spectrometer.

Investigated fuels

The investigated fuels, which main characteristics are reported in Table II.IV, have been:

- Commercial diesel as the reference fuel;
- Dimethoxymethane (OME1 or DMM);

- OME2 (POMDME with n=2) pure and blended in diesel in different percentages (5, 30 and 50% in volume, identified in the following with the abbreviations OME2-5%, OME2-30% and OME2-50% respectively);
- A mixture of POMDME mainly comprising n=2,3,4 (abbreviated form: OME2/3/4, characterized by the following composition: 33.1 wt-% OME2, 37.9 wt-% OME3, 27.4 wt-% OME4, 0.3 wt-% OME1, 1.2 wt-% Trioxane).

The OME2 and OME2/3/4 fuels were synthesised from the educts Trioxane and DMM at the University of Kaiserslautern. Trioxane has been dissolved in DMM (2 kg per kg Trioxane), and dried ion-exchange resin Amberlyst 46 (of Rohm and Haas, 50 g per kg Trioxane) has been added as heterogeneous catalyst. The mixture has been stirred at ambient conditions for two days and then separated from the catalyst by filtration. The reaction product which comprises OME of varying chain length and residues of Trioxane has been fractionated in a batch still under reflux into the investigated fuels. Details on the formation reactions including a quantitative model of the chemical equilibrium and the reaction kinetics are given in [107].

FUEL PROPERTIES								
	Diesel	DMM	OME2-5%	OME2-30%	OME2-50%	OME2	OME3	OME4
Density@25°C [kg/L]	0.84	0.85	0.85	0.88	0.9	0.96	1.03	1.07
Viscosity@25°C [mPa s]	2.5	0.58	2.41	1.94	1.57	0.64	1.05	1.75
Cetane Number	52	29	-	-	-	63	70-124	90-148
Energy density [MJ/kg]	42.1	23.4	-	-	-	<22	<22	<22
O ₂ content [wt%]	-	42.1	2.6	14.8	24.4	45.3	47.1	48.2
Normal Boiling point [° C]	170-390	42	104	104	104	104	155	200

Table II.IV: Main properties of the different fuels [106], [118]–[120]

Operating conditions

In order to operate in engine-like conditions, the cell has been preheated during the experiments by means of several electrical resistances which assured, before start of combustion, a constant temperature of around 713K for the cell walls. In addition, for any investigated condition and fuel, two injections have been activated, the first of them (pilot injection) with the only purpose of further increasing the cell temperature prior to start of main combustion. Moreover a modification of the dwell time has been performed in order to determine different temperatures at start of main

combustion. In fact, as shown in figure 2.4, the cell pressure, due to heat losses, is characterized by a decreasing trend (after the combustion process) over time.

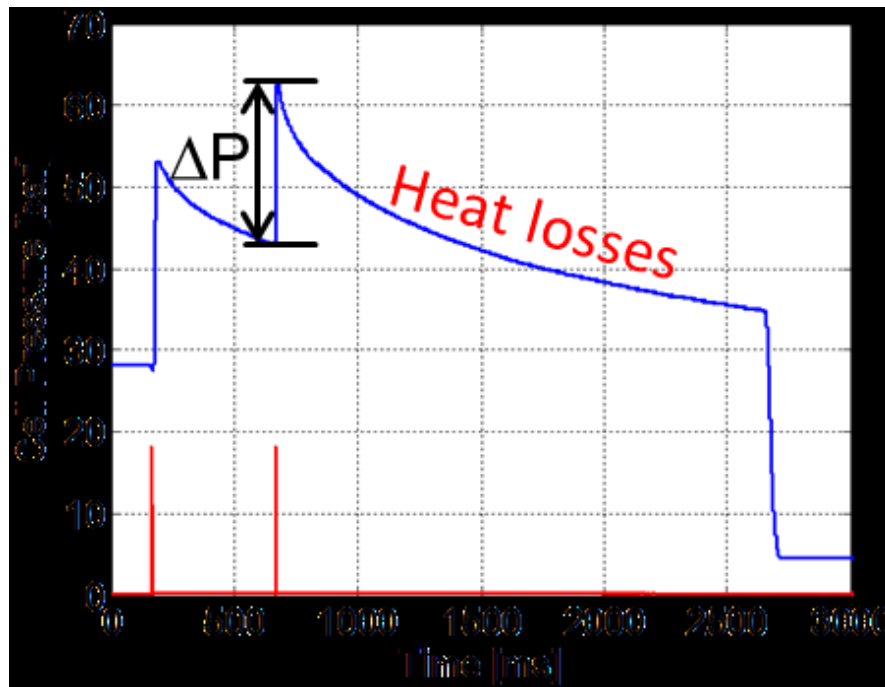


Figure 2.4: In cell pressure and energizing signal to the injector

Different temperatures at start of main combustion (SOC), which lead to a modification in ignition delay and therefore premixed combustion fraction variation, have been investigated in order to evaluate, for the different fuels, their influence on soot formation. Considering the different fuels energy and oxygen content, a calibration of injection duration has been performed for each fuel to achieve the same injected energy (4.1 kJ per injection) and thus the same $\Delta P=20$ bar (figure 2.4). The peak pressures from the main injection ranged between 73 bar at the highest $T@SOC$ (1150K) and 62 bar at the lowest one (830K).

Optical set-up

The optical set-up (sketch in figure 2.5) that has been adopted for two dimensional two colour pyrometry (2D2CP) and OH-chemiluminescence measurements comprises two cycle resolved CCD cameras; a LaVision HSS6 has been used for the 2D2CP measurements while a LaVision HSS5, connected to an IRO image intensifier, has been adopted for OH-chemiluminescence acquisition.

Chemiluminescence is a cheap and non-intrusive method for monitoring the combustion event in environments such as combustion engines. It is the radiation of flames emitted in the ultraviolet and visible bands. Most of this emission is caused by electronically excited intermediate species such as OH^* , CH^* or C_2^* formed during chemical reactions. In particular, the electronically excited state

OH* presents a peak of radiation at 310 nm. It is of interest trying to correlate this emission radiation to the heat release rate in order to acquire information on the combustion evolution.

The 2D2CP optical set – up comprises a system of lens and mirrors to split the light into two beams and filter it at two different wavelengths, as reported from Barro et al. in [117]: the emitted light from the cell window enters the system through a zoom lens with a variable focal length of $f = 18 - 125$ mm. The diverging light beam is defocused (infinite focal length) with the $f = 127$ mm lens and progresses to the first dichroic beam splitter (cold mirror). Wavelengths below 700 nm are rejected and wavelengths above 700 nm transmitted. Afterwards the rejected beam passes through a 640 nm bandpass filter with 2 nm full width at half maximum (FWHM) and the transmitted beam passes through a 740 nm bandpass filter with 4 nm FWHM. The redirection of the beams is accomplished with two adjustable precision mirrors. With a second dichroic mirror (hot mirror) the two beams are combined. A second camera lens with a focal length of $f = 105$ mm has been used to focus the beams precisely on the CCD-chip (charged coupled device) of the camera. The intensity of the incoming light can be adjusted with the aperture of the lens.

Because of the 2D2CP set – up (as shown in figure 2.5) the second high speed camera, used for OH chemiluminescence acquisition, could not be set in front of the cell window. For this reason only the light coming from part of the cell could be reflected on the mirrors (filtering the light at 309 nm) reaching the HSS5 camera.

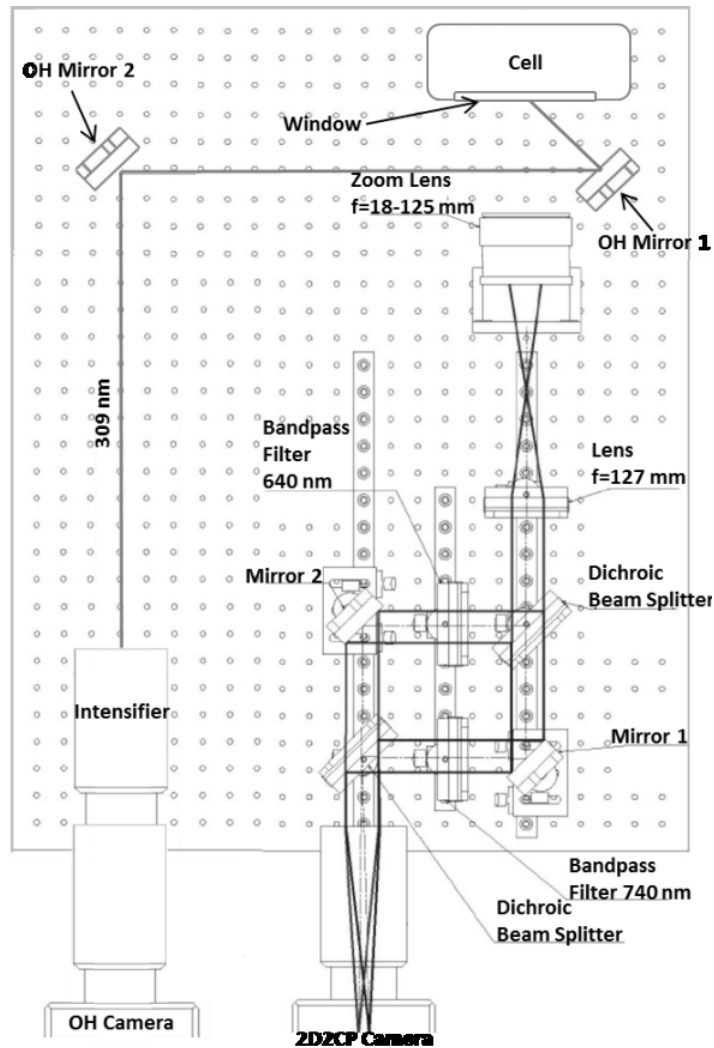


Figure 2.5: Optical set-up for 2D2CP and OH chemiluminescence

The 2D2CP technique allows calculating the kL factor which is used as a measure of the in-cylinder soot mass concentration. It is equal to the absorption coefficient per unit of soot cloud thickness k (the law of Lambert-Beer demonstrates its proportionality to the soot volume fraction) times to the flame thickness L [121]–[123]. Assuming that the volume changes linearly with the flame thickness, kL provides a value which corresponds to the actual in-cylinder soot mass. If optical properties close to black body for black carbon and a homogeneous soot cloud containing only black carbon are assumed, the soot concentration must be proportional to the ratio of the optical properties of the soot cloud and the black body properties. It is worth to underline, though, that the kL -evolution provides a rough estimation of the in-cylinder soot mass evolution and thus information about the soot formation and oxidation processes.

kL factor

In the following the algorithm used for the calculation of the kL value and the soot temperature is shown. Figure 2.6 reports the black body radiation for different temperatures and wavelengths and shows as the intensity of radiation increases for increasing black body temperatures and is characterized by a bell shape curve with respect to the wavelengths.

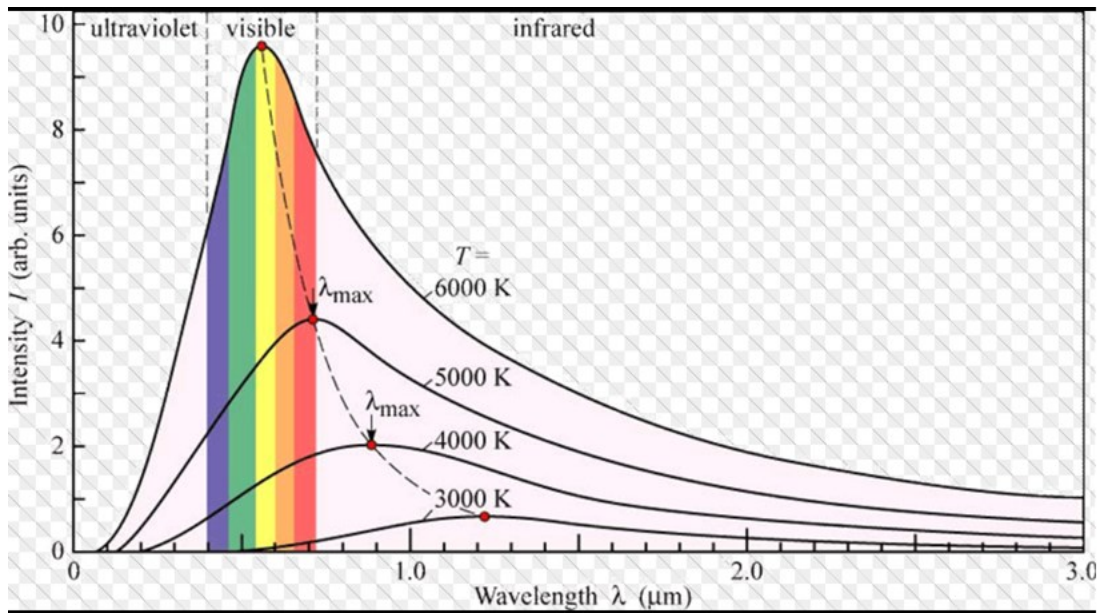


Figure 2.6: Black body radiation [124]

Knowing the intensity of radiation, the wavelength-specific black body temperature (T_{BB}) can be derived for according to Planck's law (eq.1).

$$i(\lambda, T) = \frac{2C_1}{\lambda^5 \left(e^{\left(\frac{C_2}{\lambda T} \right)} - 1 \right)} \quad (1)$$

where:

$C_1 = h \cdot c$ (h is the Planck constant and c is the speed of light)

$C_2 = h \cdot c / k_b$, (k_b is the Boltzmann constant).

If a diffuse body x characterized by a temperature T and emitting an intensity of radiation i is considered, the apparent black body temperature (eq.2) is defined as the temperature of the same body x emitting the same intensity i but with black body properties (maximum emissivity: $\varepsilon = 1$). Since the emissivity of a non-black body is below 1, the apparent black body temperature needs to be lower than the soot cloud temperature.

$$i(\lambda, T_{BB}) = i(\lambda, T) \quad (2)$$

Considering equations 1 and 2, since the emissivity of a diffuse body ($\varepsilon(\lambda)$ independent of the direction) is the ratio between its radiation and the ideal black body radiation (with the two bodies being at the same temperature), it can be written:

$$\varepsilon(\lambda, T) = \frac{i(\lambda, T)}{i_B(\lambda, T)} = \frac{i(\lambda, T_{BB})}{i_B(\lambda, T)} = \frac{\lambda^5 \left(e^{\left(\frac{C_2}{\lambda T}\right)} - 1 \right)}{\lambda^5 \left(e^{\left(\frac{C_2}{\lambda T_{BB}}\right)} - 1 \right)} \quad (3)$$

The kL factor can be calculated using the wavelength – dependent correlation of a soot – containing flame emissivity (eq. 4) proposed by Hottel and Broughton in 1932 [125]:

$$\varepsilon(\lambda) = 1 - e^{-\frac{kL}{\lambda^\alpha}} \quad (4)$$

where

k is the absorption coefficient per unit of flame thickness

L is the geometrical flame thickness along the optical axis

α is an experimentally derived exponent: 1.39 in [125] and 1.38 in [126].

In their work the authors presented a proof of the possibility of determining both the true temperature and the total emissivity of a luminous flame from a pair of apparent temperatures obtained with an optical pyrometer, using color screens of two different effective wavelengths successively.

Combining eq. 3 and 4 and solving for kL , it is possible to write:

$$kL = -\lambda^\alpha \ln \left(1 - \frac{\left(e^{\left(\frac{C_2}{\lambda T}\right)} - 1 \right)}{\left(e^{\left(\frac{C_2}{\lambda T_{BB}}\right)} - 1 \right)} \right) \quad (5)$$

Now, considering equation 5 for two different wavelengths λ_1 and λ_2 the following equation is obtained:

$$\left(\frac{1 - \left(e^{\left(\frac{C_2}{\lambda_1 T} \right)} - 1 \right)^{\lambda_1^\alpha}}{e^{\left(\frac{C_2}{\lambda_1 T_{BB1}} \right)} - 1} \right) = \left(\frac{1 - \left(e^{\left(\frac{C_2}{\lambda_2 T} \right)} - 1 \right)^{\lambda_2^\alpha}}{e^{\left(\frac{C_2}{\lambda_2 T_{BB2}} \right)} - 1} \right) \quad (6)$$

After solving, for two different wavelengths, equation 1 for T (in this case T is the apparent black body temperature), T_{BB1} and T_{BB2} are calculated; this makes the soot cloud temperature T in equation 6 the only unknown. Once T is calculated, it can be inserted in equation 5 to derive kL.

For the soot mass calculation, as reported in [123], using Kirchoff's law to combine the approach of Hottel and Broughton and the law of Lambert-Beer [121], it can be written:

$$\varepsilon(\lambda) = 1 - e^{-\frac{kL}{\lambda^\alpha}} = 1 - \tau = 1 - e^{-C_{ext}(\lambda)N_v L} \quad (7)$$

where

τ is the transmissivity of the soot particle

C_{ext} is the extinction coefficient: area behind a single particle which cannot be reached by a parallel light source due to absorption, scattering and diffraction. This area is not equal to the geometrical cross section area, increasingly larger for very small particles.

L is the geometrical flame thickness along the optical axis

N_v is the particle number per unit of volume.

Equation 7 can be simplified into:

$$\frac{kL}{\lambda^\alpha} = C_{ext}(\lambda)N_v L \quad (8)$$

Assuming:

$$c_{soot} = f_v \cdot \rho_{soot} = \frac{\pi}{6} d^3 N_v \rho_{soot} \quad (9)$$

where

c_{soot} is the soot concentration

f_v is the soot volume fraction

ρ_{soot} is the soot density

d is the soot particle diameter

kL can be expressed as a function of the soot concentration:

$$kL = C_{\text{ext}}(\lambda) \frac{6c_{\text{soot}}}{\pi d^3 \rho_{\text{soot}}} L \lambda^\alpha \quad (10)$$

or as equation 11, where the wavelength has been cancelled out, since the only remaining wavelength-dependent parameter is $C_{\text{ext}}(\lambda)$:

$$kL \propto c_{\text{soot}} L \quad (11)$$

As previously mentioned, with the assumption of a linear change of the cylinder volume with respect to the layer thickness L , equation 11 can also be expressed as a correlation between kL and the actual in-cylinder soot mass within the optical view field:

$$kL = f \cdot m_{\text{soot}} \quad (12)$$

However, it is not trivial to find the factor f , since it is dependent on the actual soot particle size, the particle density and the extinction coefficient, which all change during the combustion cycle. Applying these algorithms for three different wavelengths (3-colour pyrometry) results in 3 soot temperatures and 3 kL evolutions which have to match in case of correct calibration. This means that the 3-colour pyrometry technique gives the possibility of a calibration check, which is not possible with only two colours. In order to apply the 3-colour pyrometry technique, a miniaturized optical light probe (OLP) developed through a collaboration between ETH Zurich, Kistler AG and Sensoptic AG [127], has been used. The OLP (figure 2.7) is an optical fiber allowing the light radiation coming from the cylinder to reach a light sensor after being amplified within a specific amplifier. Its dimensions are suitable to fit the probe in an engine glow plug bore.

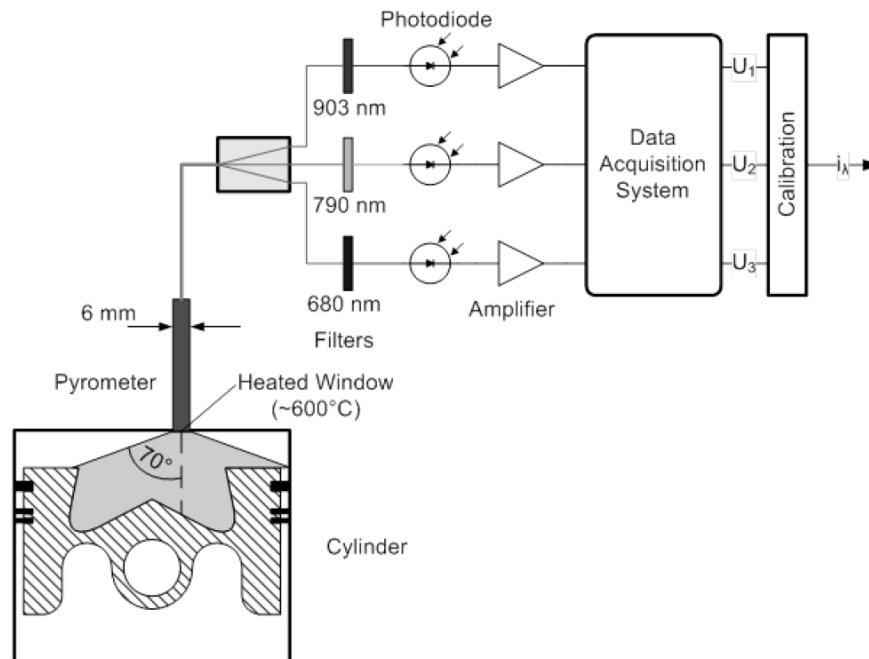


Figure 2.7: Schematic overview of the 3 – colour – pyrometry method [123]

The OLP features at its tip a sapphire lens maintained at 600°C during engine operation through an externally controlled heating system in order to avoid massive contamination of the lens from particulate matter. In fact to achieve a constant soot radiation signal, the lens, which permits a 140° viewing angle, must be kept as clean as possible. The light travelling through the optical fiber is filtered at three different wavelengths (680nm, 790nm, 903nm), with the intensity of each of them being recorded at every time step and amplified before the data acquisition system. At this point a wavelength calibration from the amplified voltage to a known uniformly emitted intensity is required. For this purpose a tungsten lamp, in combination with an integrating sphere (to cover the whole OLP view field) is used. Once the calibration has been successfully carried on, the wavelength specific black body temperature (T_{BB}) can be derived for each wavelength (680nm, 790nm and 903nm) according to Planck's law (eq.1). In order to achieve an optimized calibration (minimum error between the 3 pairs of kL and temperature), an algorithm which tunes the calibration factors (between output voltage and intensity) has been applied. An example of the calibration procedure is reported in figure 2.8 showing temperature and kL values before calibration on the left hand side and the calibrated ones on the right hand side.

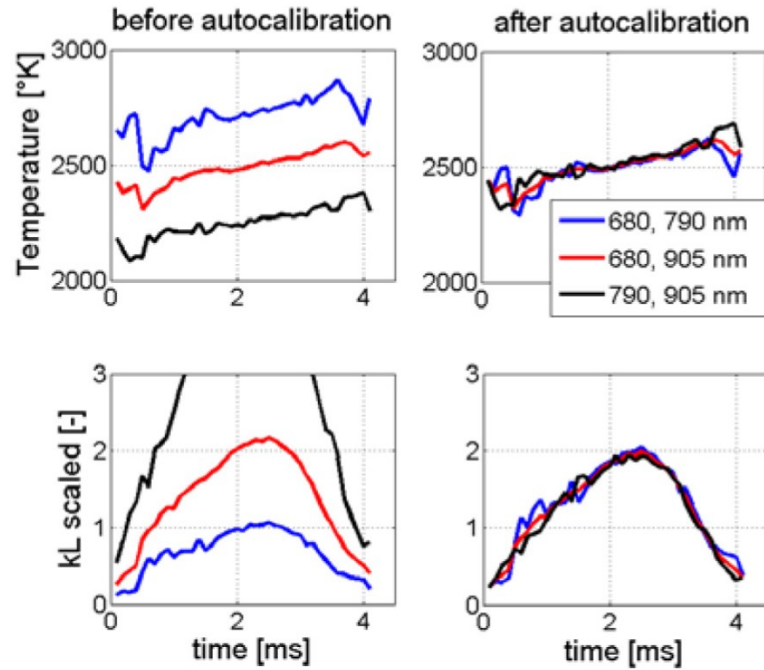


Figure 2.8: Auto – calibration procedure for temperature and kL value [117]

Nevertheless there are several factors restricting the applicability of a miniaturized pyrometer. Firstly the soot radiation is only captured within the angle of view (140°) but spatially averaged over the complete view field, since the OLP contains only one photodiode per wavelength. Moreover the fraction of the total in-cylinder soot contributing to the signal depends on the installation position of the OLP and the presence of cold zones which determine a low soot radiation that might not be captured by the pyrometer. Regarding the soot particles, they are assumed to be monodisperse and spherical. This is based on the simplification that the soot primary particles are round and further agglomerations have a chain-like structure which does not change the surface to volume fraction. Furthermore, spatially inhomogeneous distribution of the soot can lead to an additional error while regions containing no soot at all determine a “dilution” of the averaged captured radiation intensity.

Correlations between a characteristic kL-end value to the exhaust soot emission have been performed in [128], [129].

2.3 MTU-396 Single Cylinder Diesel Engine

Engine set-up

The last part of the present study has been conducted on an experimental single-cylinder DI diesel engine (figure 2.9) located at the ETH Zurich. It is based on a MTU 396 series engine and is equipped with a common rail injector system capable of injection pressures up to 1600 bar and an 8 hole Ganser 218 solenoid injector. The engine is connected to a Zöller – Kiel AG B-300 AC dynamometer characterized by a maximum absorbable power of 260 kW and a maximum speed of 7500 rpm.

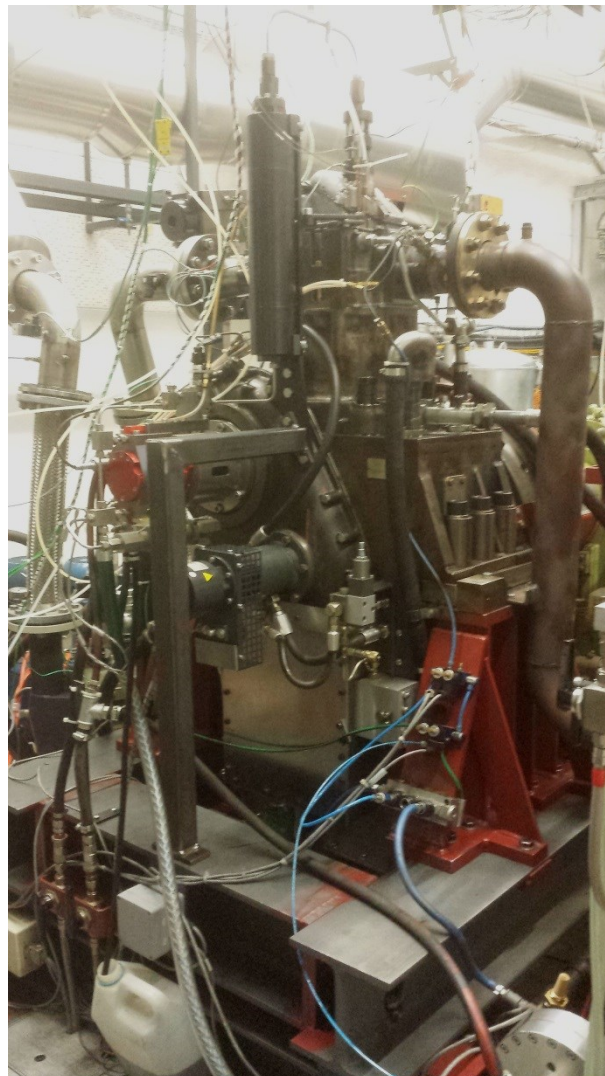


Figure 2.9: MTU-396 Single Cylinder Diesel Engine

An external compressor able to supply pressurized air up to 5 bar is connected to the engine intake while a heating/cooling system allows conditioning the intake air in a 17 – 100°C temperature

range. Moreover, the experimental engine, which main characteristics are reported in table II.V, is provided with an exhaust gas throttle allowing the exhaust gas back pressure management.

Parameter	Unit	Value
Number of Cylinders		1
Bore	mm	165
Stroke	mm	185
Compression Ratio		13.7
Speed Range	rpm	800 – 2100
Number of valves		4 (3 with extra access)
Maximum in-cylinder pressure	bar	155

Table II.V: MTU – 396 single cylinder engine specifications

Even though the original cylinder head configuration is a 4-valve design, in order to insert a water-cooled sensor adaptor allowing the placement of an additional optical sensor, one of the two exhaust valves has been removed. The removal of an exhaust valve did not significantly deteriorate the cylinder scavenging because of the specific intake/exhaust configuration allowing an independent setting of inlet and exhaust pressure values. The engine management (e.g. load, injection pressure and injection timing) has been carried on using the dSpace software. A piezo-quartz pressure transducer ($\pm 0.1\%$ accuracy) to detect the in-cylinder pressure signal, several pressure and temperature sensors in different parts of the engine and a current probe to acquire the energizing current to the injector are installed. For the acquisition of the in-cylinder pressure signal, intake and exhaust pressures and the energizing current to the injector a Trans AS data recording system has been used while the data post – processing has been carried on with Matlab.

In order to investigate alternative fuels, which could be extremely expensive, not disposable in large amounts or aggressive towards some components (e.g. gaskets) of the engine high pressure pump (constructed at the ETH Zürich specifically for the MTU engine), an external fuel high pressure system has been conceived and assembled as part of the dissertation activity. The purpose of this system is to allow the engine warm-up phase (which requires quite a long time) with commercial diesel, switch to the alternative fuel once a stationary condition with the desired operating parameters has been achieved, perform the measurements and switch back to commercial diesel for the engine cooling down and shut off phases.

A scheme of the whole system is shown in figure 2.10 while a picture of the engine with the external injection system is reported in figure 2.11. The external system consists of a tank for the alternative fuel, a dedicated fuel balance and a low pressure pump which sends the fuel to the high

pressure pump. This is an automotive derivate series production pump driven by a 3kW electric motor. The pressurized fuel is stored in a rail (automotive derivate as well) connected to the engine main rail. In between the engine high pressure pump, the external rail and the main rail, two NOVA pneumatic valves are installed. They are controlled by an electro-valve and allow the opening/closure of the diesel or alternative fuel line. In addition, two security valves are installed before the pneumatic ones in order to ensure the fuel discharge in case of over-pressure.

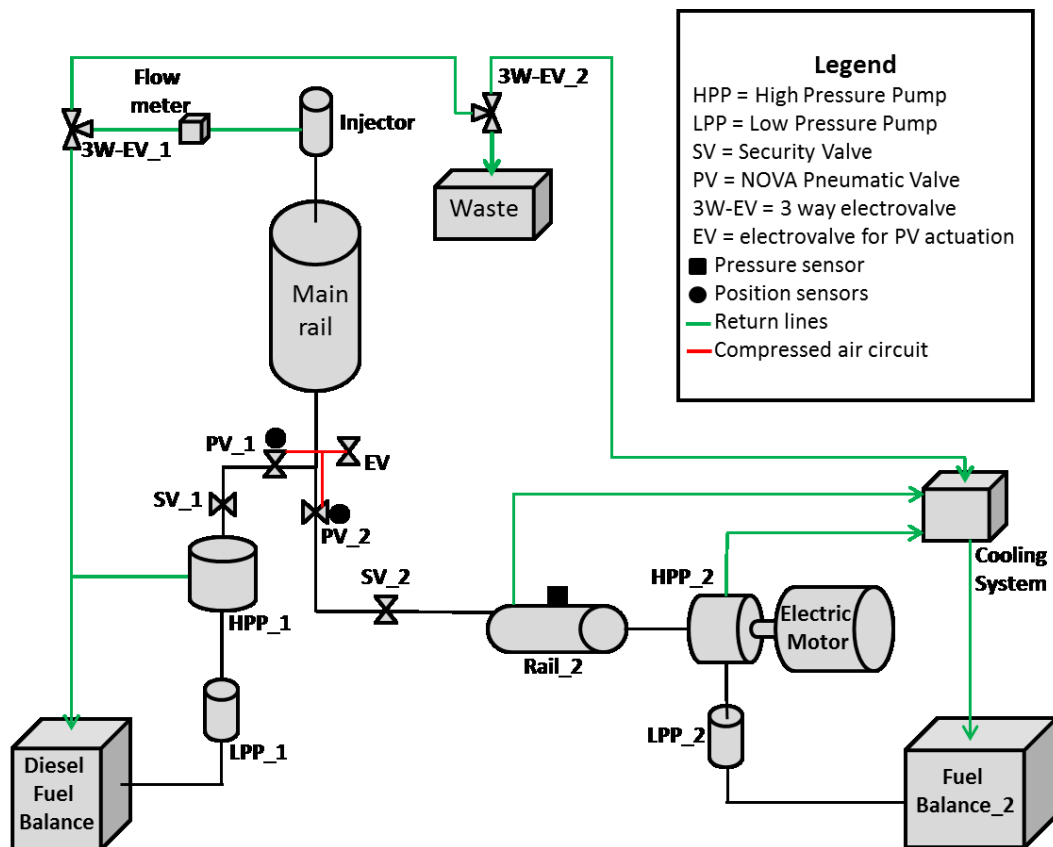


Figure 2.10: Scheme of the engine plus external injection systems

Moreover, a BIOTECH flow meter and two BURKERT three way electro-valves have been mounted on the injector return line. The flow meter, resistant to aggressive fuels, has the purpose of measuring the backflow from the injector in order to check its correct behavior over time. In case of unexpected behavior of the injector, the backflow would vary and this would be recognized by means of the flow meter. It outputs a frequency signal which is then transformed, through dSpace, in a flow rate. In addition, a mechanical security device (mounted on the injector) blocks the fuel line if a prefixed amount of injected fuel is exceeded (in case the injector tip would stuck in open position). The purpose of inserting the two three way electro-valves, instead, is connected to the need of connecting the injector return line to the diesel fuel balance, to the additional fuel balance or to a waste tank. The two valves are mounted in series so that the first sends the fuel to the diesel

balance or to the second valve which allows the connection to the second fuel balance (when the second fuel is being used and fuel consumption measurements are being taken) or to the waste tank. This reservoir is used to store the injector backflow in a first transient phase, after having switched fuels. In fact, once the fuel lines are switched by means of the pneumatic valves, the alternative fuel will be delivered to the main rail which is still, though, full of diesel. Depending on the operative conditions, a certain amount of time is required to replace all the diesel fuel with the alternative one in the main rail. During this time the exact composition of the fuel in the main rail is not known thus the return line cannot be connected to the fuel balance.

In order to avoid pressure waves in the fuel high pressure pipes, fuels may only be switched once the pressure in the automotive rail is equal to the pressure in the main rail. The pressure regulation valves mounted on the automotive rail and high pressure pump are actuated through a PWM signal coming from dSpace. The whole external system, including a PID controller to achieve a desired rail pressure, the electro-valves actuation and the pneumatic valves has been built in Simulink and managed through dSpace.

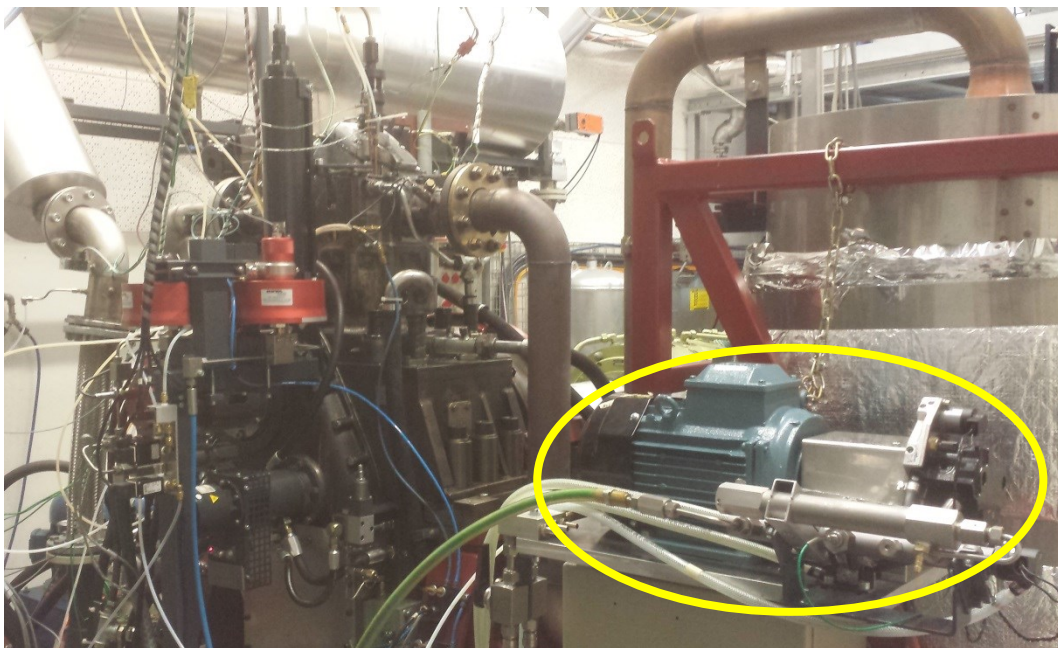


Figure 2.11: MTU-396 Single Cylinder Diesel Engine with external injection system

The electric motor, the automotive high pressure pump and rail and the overpressure security valve are highlighted in figure 2.11 while the pneumatic valves, flow meter and three way electro-valves on the injector return line are shown in figure 2.12.

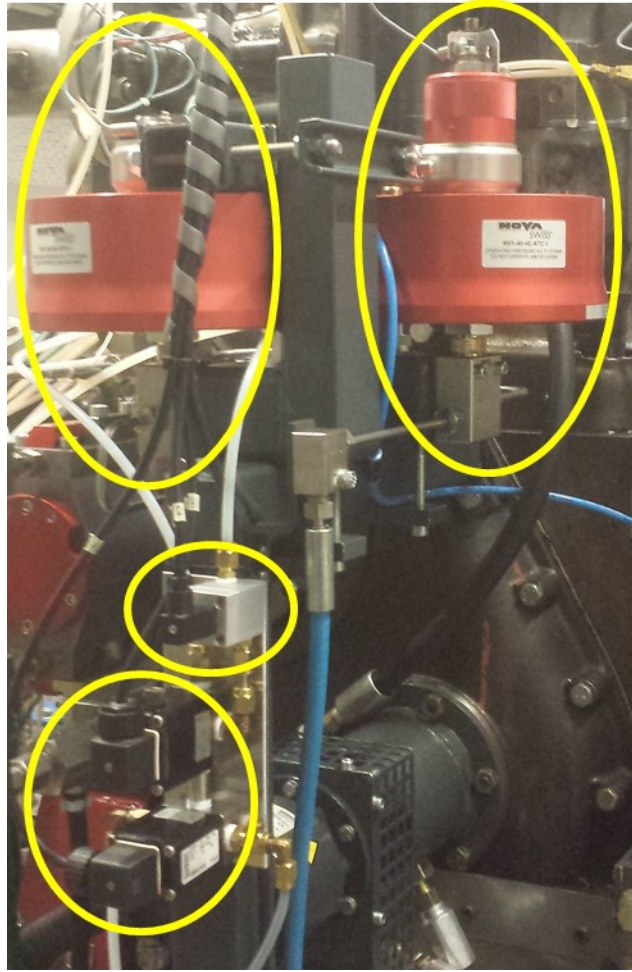


Figure 2.12: Pneumatic valves, flow meter and the two three way electro-valves on the injector return line

Exhaust emissions have been measured by means of the following analyzers:

- An ECO PHYSICS CLD 82 for NO_x exhaust emissions, belonging to the CLD category. Its working principle is based on the reaction between NO and O_3 (ozone). This reaction produces photons which are detected by a photo multiplier tube (PMT). The CLD output voltage is proportional to NO concentration.
- An ABB MultiFID14 for HC, belonging to the FID category. The sample gas is introduced into a hydrogen flame. Any hydrocarbons in the sample will produce, when they are burnt, ions which are detected using a metal collector. The current across this collector is thus proportional to the rate of ionisation which in turn depends upon the concentration of HC in the sample gas.
- An ABB Uras 26 for CO and CO_2 emissions. These emissions are measured by means of a Non-Dispersive Infra-Red (NDIR) detector: each constituent gas in a sample absorbs some infra - red at a particular frequency. By shining an infra-red beam through

a sample cell (containing CO or CO₂) and measuring the amount of infra-red absorbed by the sample at the specific wavelength, a NDIR detector is able to measure the volumetric concentration of CO or CO₂ in the sample.

- An ABB Magnos 206 for O₂ based on the magneto-mechanical measuring principle. It takes advantages of the paramagnetism distinguishing oxygen. Because of this physical property, oxygen molecules are attracted by a strong magnetic field which can be used in detection. Therefore a paramagnetic sensor is used to measure the oxygen concentration. It consists of two spheres arranged in the form of a dumbbell suspended in a symmetrical, non-uniform magnetic field. When the surrounding gas contains oxygen, the dumbbell spheres rotate out of the magnetic field by the relatively strong attraction of oxygen. A light beam focused on a mirror attached to the dumbbell reflects asymmetrically onto two photo diodes resulting in a voltage shift. The voltage difference produces a current used to drive the dumbbell back to the original position. The current flow required to maintain the null position is directly proportional to the oxygen concentration.
- An AVL 415 Smoke Meter (0.1% value resolution) for soot measurements. The Smoke Meter uses the filter paper absorption method: the shades of gray imprinted on the paper are detected and associated to an FSN (filter smoke number) by means of a photoelectric meter.

Investigated fuels

The investigation focused on the comparison between the reference diesel fuel and two blends composed of 90% baseline diesel – 10% POMDME by volume and 95 % baseline diesel – 5% POMDME by volume respectively. The POMDME fuel (characterized by the following composition: 0.55 wt-% Methylal, 0.07 wt-% Methanol, 0.05 wt-% Ethanol, 41.51 wt% OME2, 15.5 wt-% OME3, 27.52 wt-% OME4, 8.74 wt-% OME5, 4.58 wt-% OME6, 2.15 wt-% OME7 and 0.33 wt-% Trioxane) presented an oxygen overall mass fraction of 0.46 g/g, an energy content below 22 MJ/kg and a density of 1012.96 kg/m³ at 25°C. At the same temperature of 25°C, instead, the commercial diesel density is 840 kg/m³. Therefore the two investigated blends, denoted in the following as 5% POMDME and 10% POMDME, are characterized by an oxygen mass fraction of 2.74 and 5.44 wt-% respectively.

Operating conditions

The experimental investigation conducted on the single cylinder MTU diesel engine focused on exploring the effect of fuel and oxygen concentration at intake on engine out emissions and performance. Tests have been performed at 1050 rpm and two BMEP values, 8 and 10.5 bar. Table II.VI reports the investigated operating conditions.

SOI [cad atdc]	O ₂ at intake [%]	BMEP [bar]	Intake Pressure [bar]	Exhaust Pressure [bar]	Injection pressure [bar]
-12, -9, -6	15, 18 and 21	8	1.5	1	800
-12, -9, -6	15, 18 and 21	10.5	2	1.5	1000

Table II.VI: Operating conditions

A single injection strategy has been chosen for the tests and, in order to fix the BMEP at the constant values of 8 and 10.5 bar for fuels characterized by different energy content, the duration of injection has been tuned for each fuel. The tuning has been conducted for the conditions without EGR and the same injection duration has then been kept for conditions with EGR.

Chapter 3

Experimental Results

The analysis of the experimental results is shown in the following discussing at first the comparison of different oxygenated blends with respect to commercial diesel in a premixed combustion mode in order to present which advantages are introduced with oxygenated fuels, which ones with the investigated innovative combustion mechanism and which benefits can be achieved combining the two aspects. Afterwards the investigation moves to the study of a specific oxygenated fuel family characterized by a high molecular oxygen content: the poly(oxymethylene) dimethyl ethers. These fuels, their properties and the benefits connected to their use are at first analyzed by means of optical techniques in a cylindrical constant volume chamber and, subsequently, in a diesel single cylinder engine in order to compare performance and exhaust emissions with respect to commercial diesel.

3.1 Automotive Diesel Engine results

Rate of heat release analysis

The discussion of the achieved results is presented starting from the analysis of the instantaneous heat release traces, averaged on 250 cycles reported in figures 3.1 - 3.4. The figures, displaying the energizing current to the solenoid injector as well, demonstrate as for each investigated operating condition, a premixed combustion mode has been attained. Thus the discussion mainly focuses on the analysis of fuels characterized by different properties (such as cetane number, net heat value, fuel volatility and oxygen content) releasing energy, through a premixed combustion mode. The heat release computation has been performed with a simplified approach based on the first law of thermodynamics assuming constant gamma (C_p/C_v). The assumption allows calculating, from the cylinder pressure signal, the energy released with the combustion of the air/fuel mixture and this value includes the fraction that is then dissipated through heat losses. The values of rate of heat release (RoHR), reported in the following plots, have been calculated as $\text{kJ/m}^3\text{deg}$, being for the specific engine $100\text{kJ/m}^3\text{deg} = 31.2 \text{ J/deg}$. Results refer to four different operating conditions with two levels of oxygen at intake (17 and 19%) and two combustion phasings ($CA_{50}=18$ and 21 cad atdc) being considered.

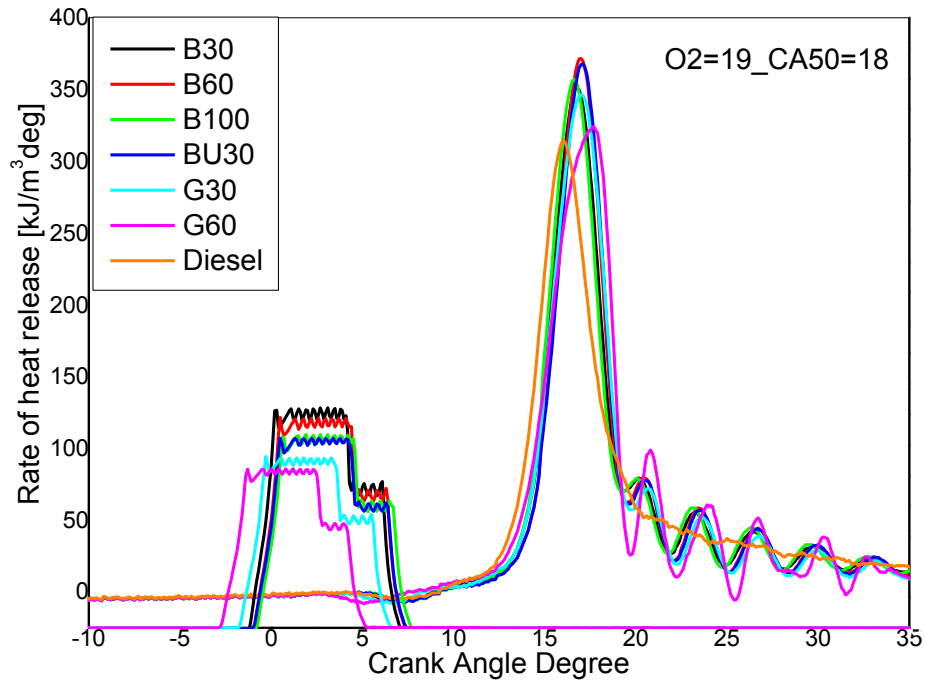


Figure 3.1: Instantaneous rate of heat release traces for the investigated fuels at

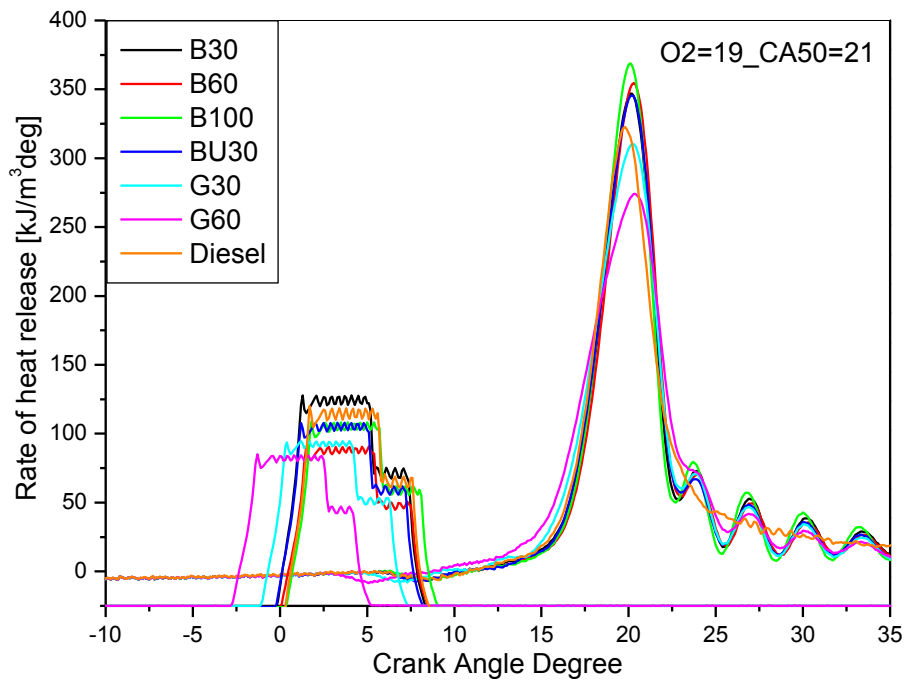
 $O_{2int}=19\%_{CA50}=18$


Figure 3.2: Instantaneous rate of heat release traces for the investigated fuels at

 $O_{2int}=19\%_{CA50}=21$

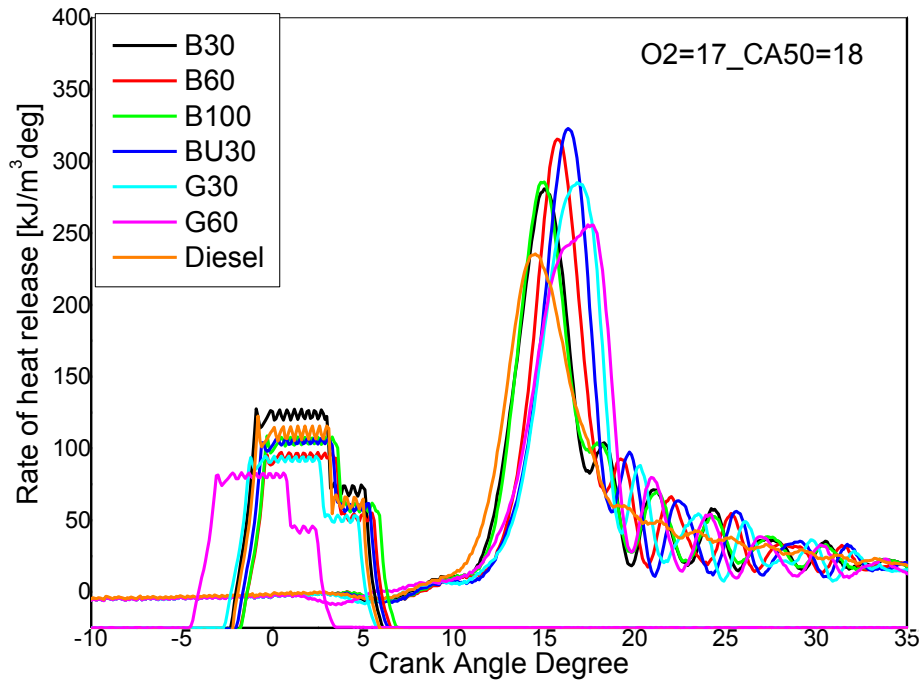


Figure 3.3: Instantaneous rate of heat release traces for the investigated fuels at $O_{2int}=17\%_{CA50}=18$

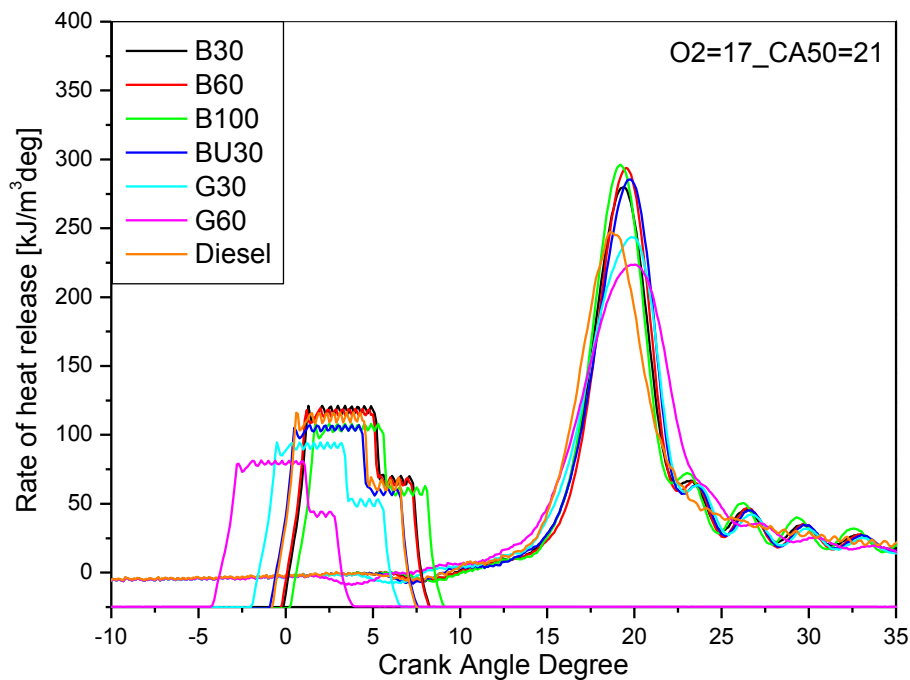


Figure 3.4: Instantaneous rate of heat release traces for the investigated fuels at $O_{2int}=17\%_{CA50}=21$

As illustrated in the figures above, the management of injection timing and EGR has allowed a combustion process characterized only by the premixed peak meaning that the whole amount of fuel is introduced in the combustion chamber prior to the start of combustion and allowing an enhanced air-fuel mixing. Once auto-ignition conditions are achieved, the entire injected fuel suddenly burns causing a high rate of heat release and a short premixed combustion duration (less than 10 cad). It is important to underline that the different fuel properties (cetane number, volatility and net heat

value) would have determined variability in combustion phasing with the consequent difficulty in comparing results from the investigated fuels. For this reason a management of the start of injection and injected fuel amount has been performed, achieving, for the different fuels, constant combustion phasing and BMEP values.

Exhaust emission and performance results

The main result that has to be discussed is the possibility of reducing smoke emissions with the adoption of a premixed combustion mode joint with the use of fuels characterized by the presence of molecular oxygen and/or low cetane number. With this purpose results of smoke emissions are shown in figure 3.5. In order to show the correlation between soot detected at the exhaust and cetane number, the different fuels on the x-axis are reported in a specific way (from the one characterized by the lowest CN value to the one with the highest). Results show that, for any tested fuel, an increase in oxygen at intake, associated with a retarded combustion phasing, determines the maximum reduction of smoke emissions. In fact almost smokeless combustion has been achieved for the $O_2=19\%$ _CA50=21 cad atdc operating condition with the different fuels except commercial diesel (which determines the highest smoke emission values).

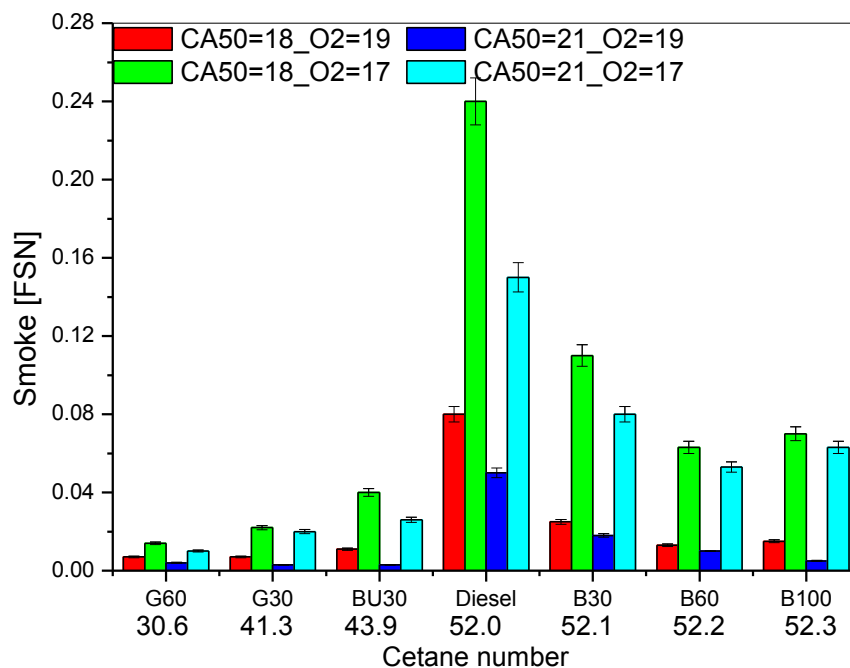


Figure 3.5: Smoke emissions from the different investigated fuels

It is worth to point out that since results from figure 3.5 refer to a premixed combustion mode, in order to evaluate exclusively its potential in reducing soot emissions, the same 2500rpm, 0.8MPa BMEP and 19% O_2 at intake operating condition with commercial diesel has been ran under default ECU settings. In this case a multiple injection strategy was activated with a diffusive combustion

mode determined and an FSN measured value of more than 1. This means that a significant reduction in soot emissions is already achieved with commercial diesel if a premixed combustion mode is achieved. As a general result, figure 3.5 indicates that the use of blends composed of diesel-gasoline or -butanol, determines the maximum reduction in smoke emissions compared to the commercial diesel. In order to give an explanation of these trends, an analysis of fuels properties and combustion mechanisms has to be conducted. As reported on the x-axis of figure 3.5, G30, G60 and BU30 show the lowest cetane number which determines a longer ignition delay thus an increase of the available time for air/fuel mixing before start of combustion. The correlation between cetane number and ignition delay is shown in figure 3.6 where the ignition delay values have been calculated as the interval between the start of energizing current to injector solenoid and CA10 (crank angle degree corresponding to the 10% of total heat release).

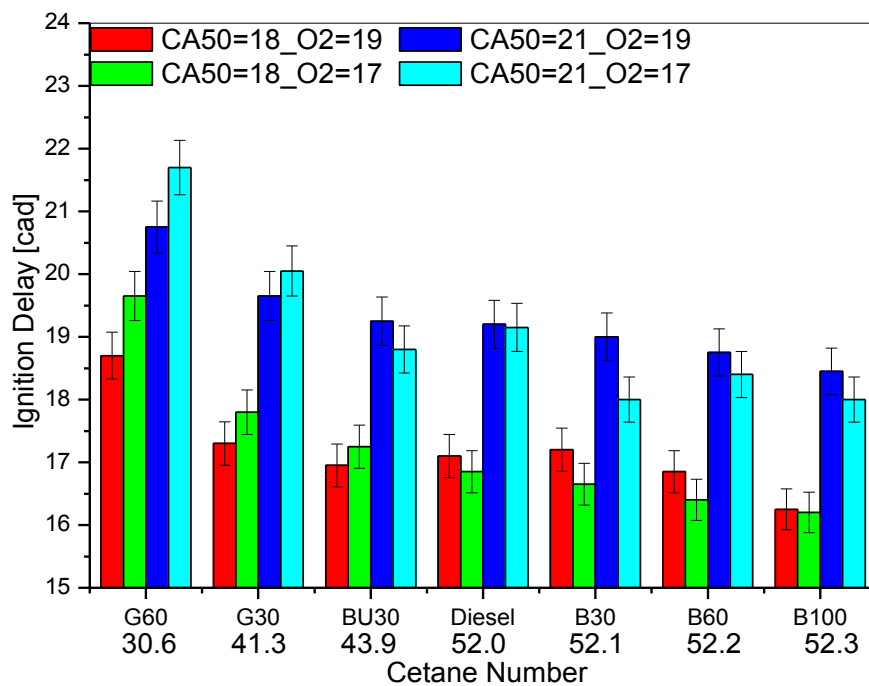


Figure 3.6: Ignition delay vs fuel blends and CN for the different test conditions

The figure shows a direct relation between ignition delay decrease and cetane number increase and its analysis actually allows to establish a correlation between soot reduction and available time for air-fuel mixing before auto-ignition. The comparison in figure 3.5 between commercial diesel and alternative fuels confirms that an increasing soot reduction may be achieved by:

- adding molecular oxygen in fuel blends characterized by similar cetane numbers. This is the case of increasing the amount of biodiesel in the diesel – biodiesel blends
- adopting fuel blends with lower amount of molecular oxygen but higher ignition delay, as for the comparison between BU30 (6.5% of oxygen in the molecule – CN = 43.9) and B100 (10.5% of oxygen in the molecule – CN = 52.3).

- adopting fuel blends with no molecular oxygen but extremely high ignition delay, as for G60 which provides the lowest soot emissions for any investigated operating condition.

Moreover, with regard to BU30, it has to be pointed out that, in addition to its molecular oxygen which allows a reduction of the locally rich regions responsible for soot formation, its low initial boiling point enhances fuel evaporation which is beneficial for mixture homogeneity. Regarding biodiesel blends the reduction of aromatic compounds (-80% of Polycyclic Aromatic Hydrocarbons with respect to commercial diesel [85]) further contributes to the lower smoke emissions compared to the mineral diesel in accordance to previous results reported in literature (e.g. [130]–[134]).

As a result the investigation has given some indications in the direction of identifying three key factors mainly responsible for soot reduction in a premixed combustion mechanism. Firstly, the higher ignition delay allows a better air-fuel mixing leading to an enhanced homogeneous mixture. The increased mixture homogeneity determines a reduction of locally rich regions where the low availability of oxygen leads to decreased oxidation rates. Therefore a second key factor to reduce soot emissions has to be oxygen availability within the fuel molecule. In addition a low initial boiling point facilitates fuel evaporation leading to enhanced mixture homogeneity.

Figure 3.7 reports results of NO_x emissions for the different investigated fuels. As a general result, minor differences have been found between the investigated fuels at fixed operating conditions while a decrease of oxygen concentration at intake from 19 to 17% has led to a NO_x reduction of about 60%. At O₂=17%, a later combustion phasing further reduced NO_x levels. In particular certain discordance is found in literature between authors (e.g. [130], [132], [134]) detecting higher NO_x values with biodiesel (vs commercial diesel) and authors finding lower ones (e.g [131]). In the present activity no significant increase in NO_x emissions, attributable to the biodiesel molecular oxygen (nor to the n-butanol one) has been detected.

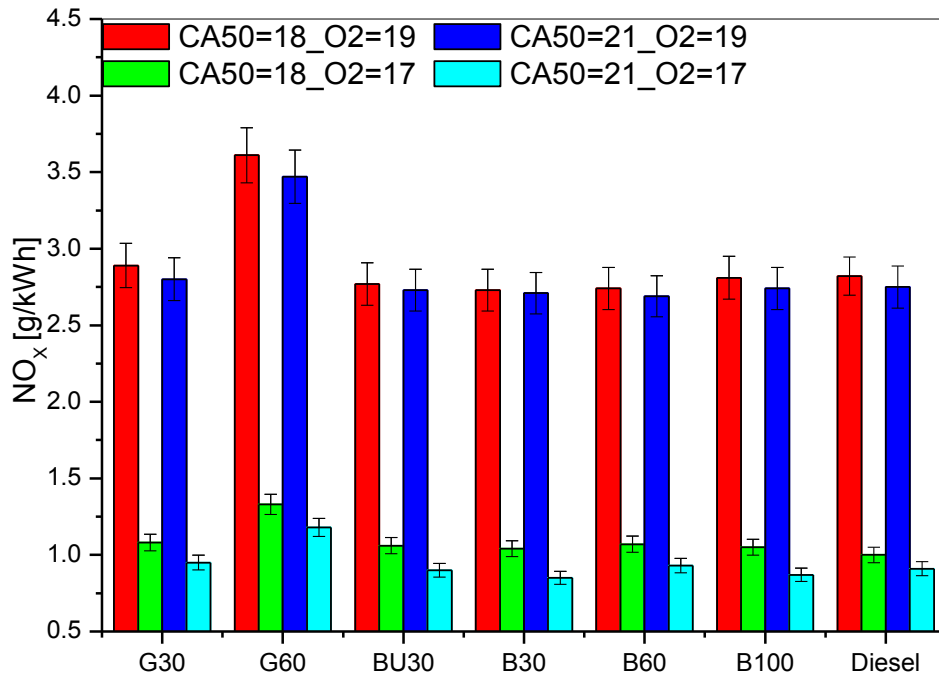


Figure 3.7: NO_x emissions from the different investigated fuels

A similar trend, with respect to the other fuels, was also observed for G30 while G60 produced higher NO_x levels for any tested condition. To explain this behavior in-cylinder temperature profiles have been reported in figure 3.8. The plot refers, as an example, to the O₂=17%_CA50=21 cad atdc test case highlighting the highest peak temperature, responsible of NO_x increase, achieved with G60.

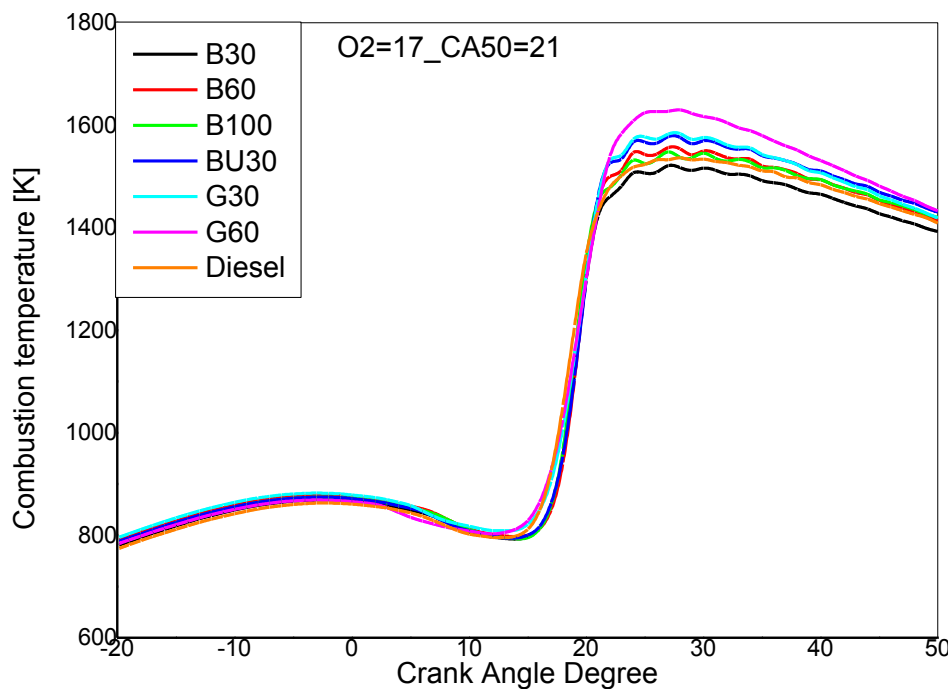


Figure 3.8: Combustion temperatures for the investigated fuels at O₂_{int}=17%_CA50=21

Finally, to highlight the operative conditions determining the maximum reduction of both NO_x and particulate matter, NO_x on the y-axis and FSN on the x-axis are reported in figure 3.9. The figure clearly shows as the best results correspond to the scatters in the bottom - left corner and that the maximum reduction of both soot and NO_x is associated to diesel-gasoline blends operating at the CA50=21_O2=17 condition (blue scatters).

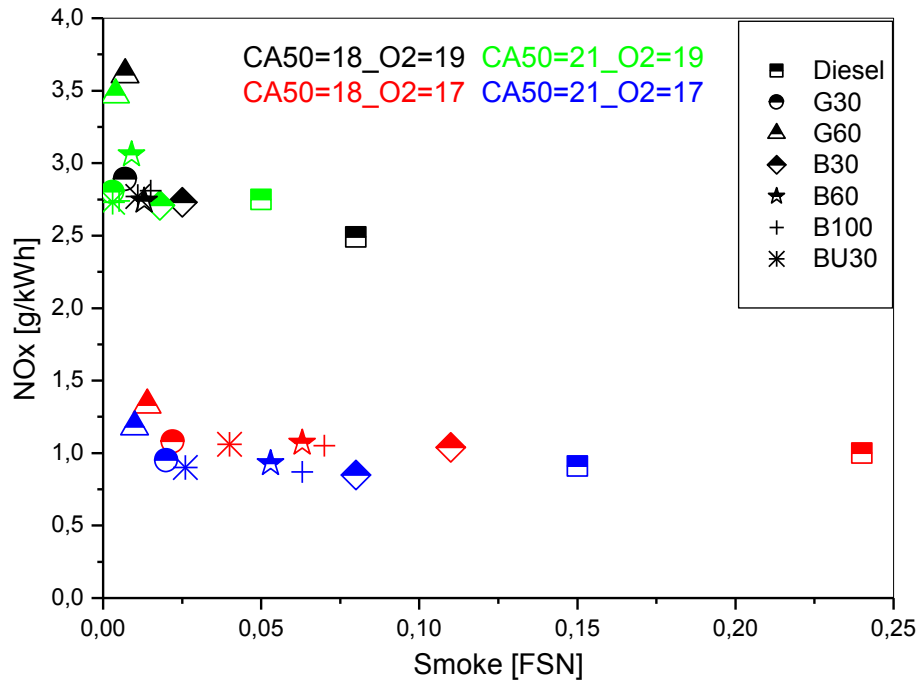


Figure 3.9: NO_x Smoke trade-off for the different fuels

It has been underlined that, for fuels characterized by different lower heating values, the injection timing has been tuned for each fuel and operative condition in order to keep a constant BMEP of 0.8MPa. The tuning results in the variation of break specific fuel consumption reported in figure 3.10. As expected, for any investigated fuel, because of lower temperatures during combustion an increase in BSFC is noticed at retarded combustion phasing (from 18 to 21 cad atdc) or decreased oxygen concentration at intake (from 19 to 17%). Increased BSFC means more fuel to be injected in order to keep a constant BMEP of 0.8MPa and thus a lower combustion efficiency. The lowest values of BSFC, for any operating condition, have been achieved with commercial diesel because of its high net heating value ($\text{NHV} = 43 \text{ MJ/kg}$) while the highest ones have been obtained with B100. In fact, RME (B100) is characterized by a low NHV ($\sim 37 \text{ MJ/kg}$) thus a higher amount of fuel must be injected in order to achieve the same output power. As expected, results underlined as a combustion phasing plus EGR management is required in order to achieve a BSFC optimization.

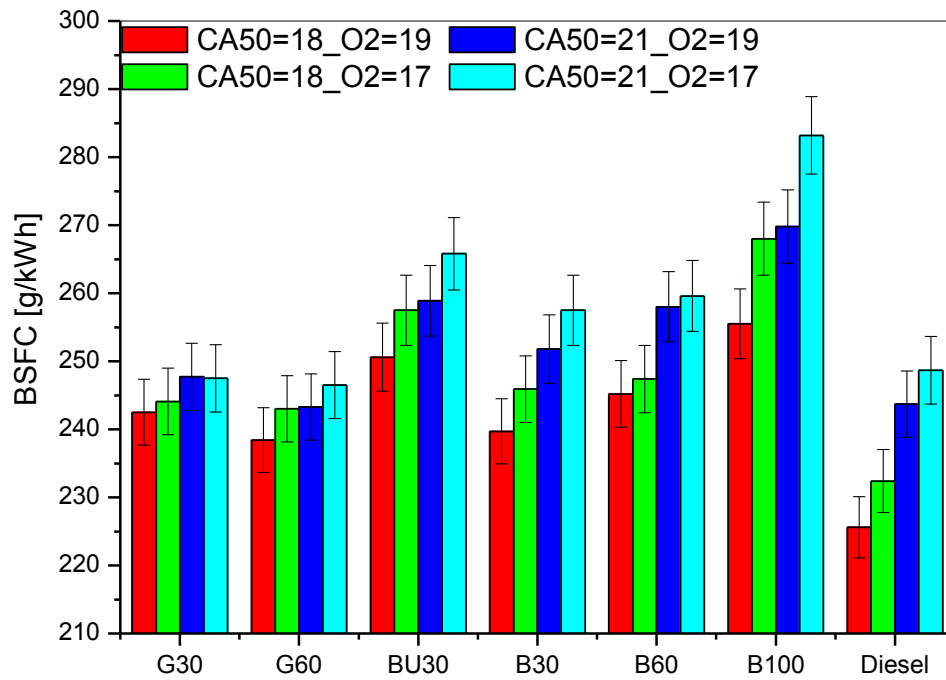


Figure 3.10: BSFC from the different fuels

From the comparison of the investigated fuels net heating values, it is clear that a different amount of released energy may be expected from them. In order to give a further analysis of the different fuels behavior and show a comparison which could be considered fairer with respect to the different fuels, figure 3.11 reports thermal efficiency (TE) values. It has been calculated as

$$TE = \frac{1}{BSFC * NHV}$$

and indicates how efficiently energy conversion is accomplished. In this case the maximum values are given by B60, B100 and commercial diesel, in particular for the O₂=19%_CA50=18 cad atdc test case. It is interesting to highlight that, at reduced percentage of O₂ at intake (17%), the B60 blend provided the best result denoting the positive contribution given by the oxygen within the blend.

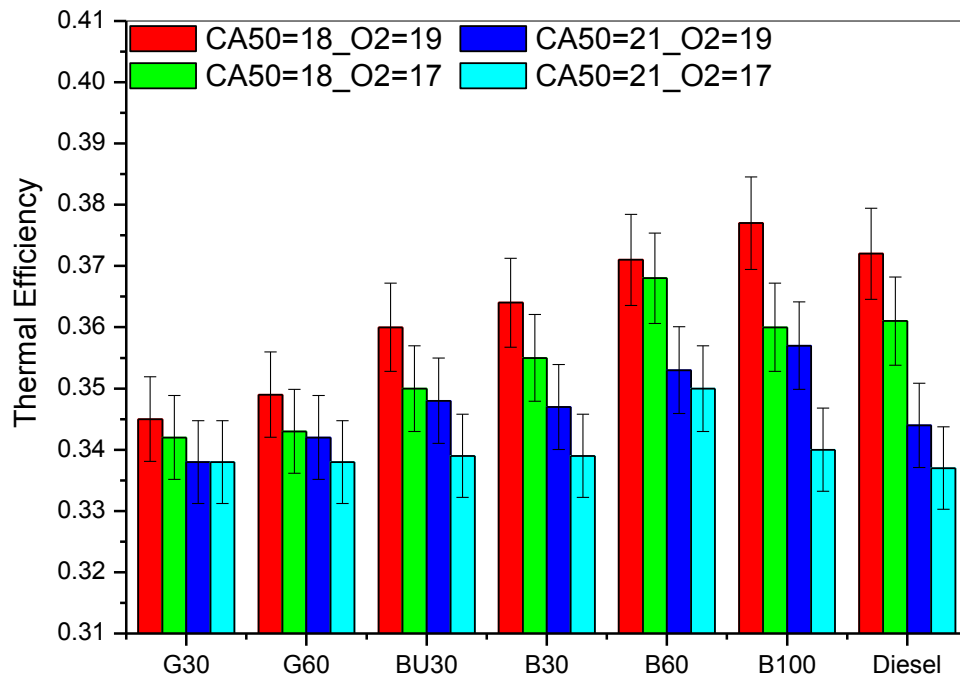


Figure 3.11: Thermal efficiency from the different fuels

Combustion noise, evaluated as the peak value of the in-cylinder pressure trace first-derivative, is a further important parameter which has to be taken into account when comparing different fuels. Results are shown in figure 3.12 and the lowest values are achieved with G60, while the different biodiesel blends and BU30 gave the highest ones. Instead with regard to the operative conditions, the effect of combustion phasing retard and increased EGR (which contributes to prolong the ignition delay) determine a strong reduction of the combustion noise peak. This fact is related to the development of combustion mainly during the expansion stroke, leading to a softer in-cylinder pressure rise and lower peak. Although the combustion phasing retard may be an effective control factor for reducing the combustion noise peak, it is limited by poor cycle-to-cycle stability. It is worth to underline that the high values displayed in figure 3.12 are explained considering that a single injection strategy has been fixed for the investigation in order to better achieve a premixed combustion mode. One of the issues, though, related to this injection strategy linked to a PCCI mode, which determines a simultaneous ignition of the whole injected fuel, is indeed high combustion noise.

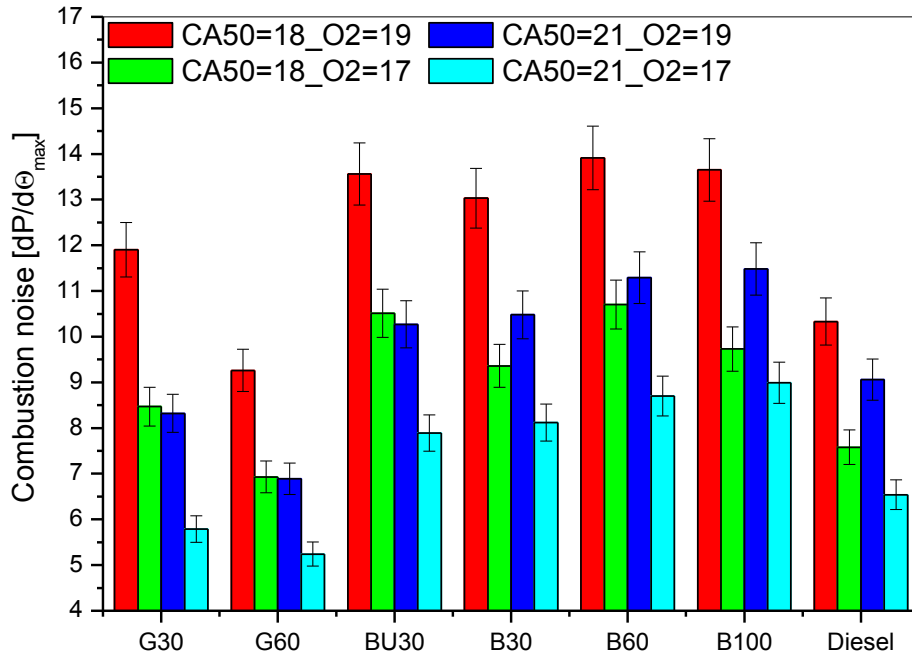


Figure 3.12: Combustion noise from the different fuels

Finally figure 3.13 shows the correlation between combustion noise and the crank angle degree at which the maximum value of the in-cylinder pressure trace first-derivative is achieved. The figure strengthens the combustion noise reduction (highlighted by the direction of the arrows) associated to increased EGR and retarded combustion phasing.

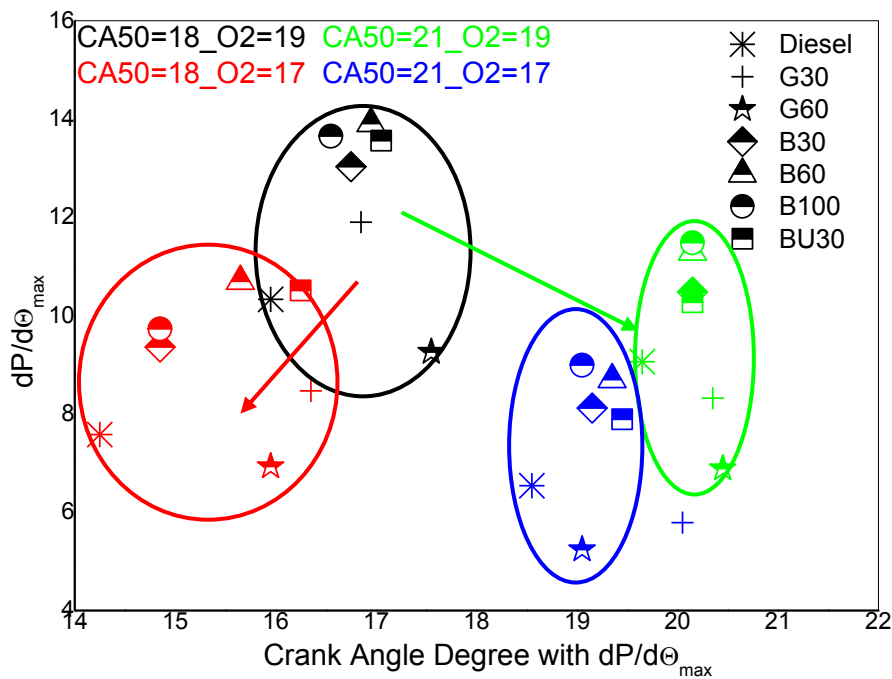


Figure 3.13: Combustion noise vs CAD ATDC with dP/dθ_{max}

3.2 Cylindrical constant volume chamber results

The results presented in the first part of the activity have given some indications in the direction of associating an important role for soot reduction to the adoption of a premixed combustion mode thus to the available time for air/fuel mixing. In order to isolate the contribution of molecular oxygen with regard to soot reduction, the discussion is continued analyzing several highly oxygenated fuels in a diffusive combustion mode, which produces high soot levels. The investigation is conducted in an optically accessible constant volume chamber in order to apply optical techniques suitable for the study of combustion evolution and soot formation and oxidation processes. Moreover a fast particle spectrometer at the chamber exhaust is used in order to analyse the soot emissions from the different investigated fuels. Results are discussed in two sections: a first section for the optical results and a second section for exhaust measurements comparing the different oxygen content effect on soot emissions.

Optical results

The investigation focuses on the impact of different oxygen content on flame temperature and soot formation/oxidation processes through the 2D2CP technique with the calculation of the kL factor. The four investigated fuels, for this specific comparison, are OME2 pure (oxygen content: 45.3% in mass), OME2-50%, OME2-30% and OME2-5%. The three blends present an oxygen content of about 24.4, 14.8 and 2.6% in mass respectively. Results from pure OME2 are not shown because no soot was optically detected for any investigated operating condition, meaning that the particulate matter from pure OME2, if any, is below the detection threshold of the technique. For each fuel four different temperatures at SOC (1150K, 1010K, 960K and 830K) have been considered. The results for the highest temperature at SOC are reported in figures 3.14 (rate of heat release and energizing signal to piezo injector) and 3.15 (kL factor and energizing signal to piezo injector). The energizing curves in figure 3.14 show longer injection duration for higher oxygen content of the blend to keep the total injected energy constant. The effect on the heat release rate results in a lower and later peak for higher oxygen content. However, the late-phase combustion after end of injection is apparently faster.

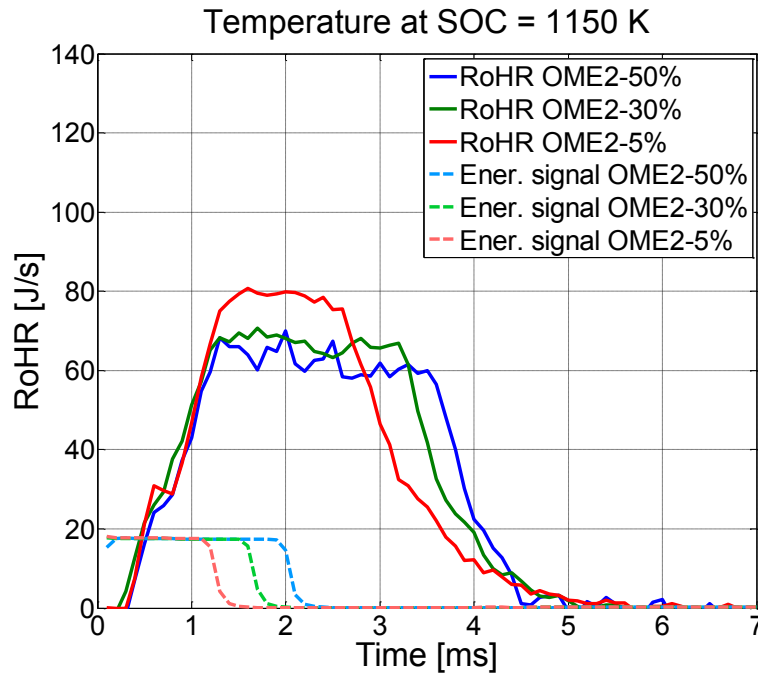


Figure 3.14: RoHR and energizing signal to the piezo injector (start at time 0) for OME2-50%, OME2-30% and OME2-5% at 1150K@SOC

A first evidence from figure 3.15 is that increasing the oxygenated fraction in the blend, a massive reduction of the peak at end of the soot formation dominated phase is achieved. This first phase is followed by a second formation/oxidation phase in which soot formation and oxidation processes roughly cancel each other out. OME2-5% shows the shortest duration of this process because it is characterized by the shortest injection duration. Finally, during the third, oxidation dominated phase, temperatures rapidly decrease and flame luminosity falls below the minimum detectable value. The second peak, corresponding to the end of the balanced soot formation/oxidation phase, particularly showed by the OME2-30% blend, is correlated to a decrease in lift-off length which brings the flame luminosity backwards towards the injector tip with an increase of the soot formation area. The lift off length is affected by temperature and fuel oxygen content. In a constant volume chamber, with the lack of expansion, shorter lift off lengths with increasing injection durations are expected. This explains the presence of the peak corresponding to the end of the balanced soot formation/oxidation phase particularly for the blends, characterized by longer injection duration because of their lower energy content.

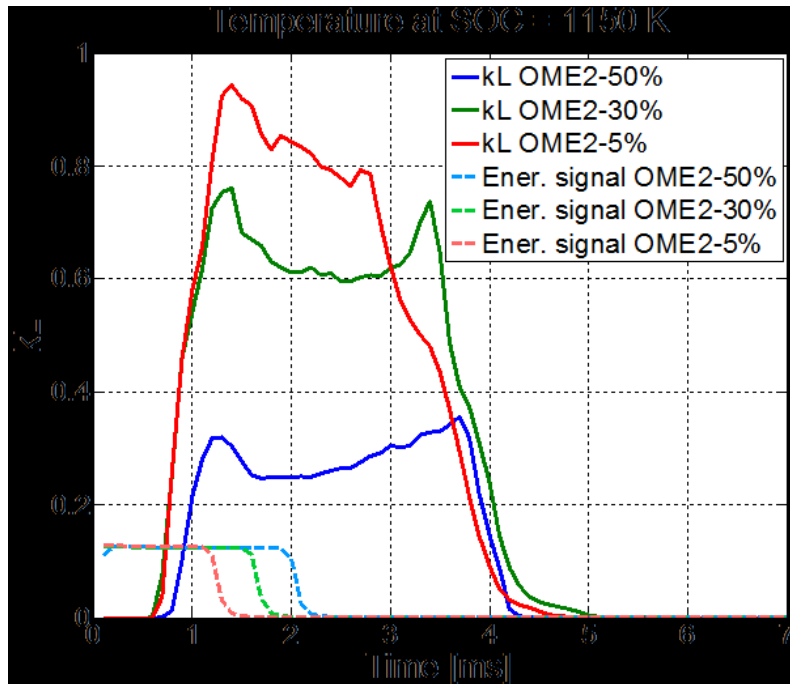


Figure 3.15: kL factor and energizing signal to piezo injector (start at time 0) for OME2-50%, OME2-30% and OME2-5% at 1150K@SOC

Figure 3.16 and 3.17 display the results at the second temperature at SOC, 960K. This temperature determines still relatively high flame luminosity for the OME2-5%. The OME2-50% blend, instead, shows a significantly shorter soot formation + oxidation process with respect to the OME2-5% blend meaning that the increased oxygen content is determining an almost complete breakdown of soot formation. The different adiabatic flame temperature, number of C-C bonds and local air fuel ratio are all correlated to soot formation reduction, determining a non-linear relation between soot formation dominated phase decrease and fuel oxygen content increase.

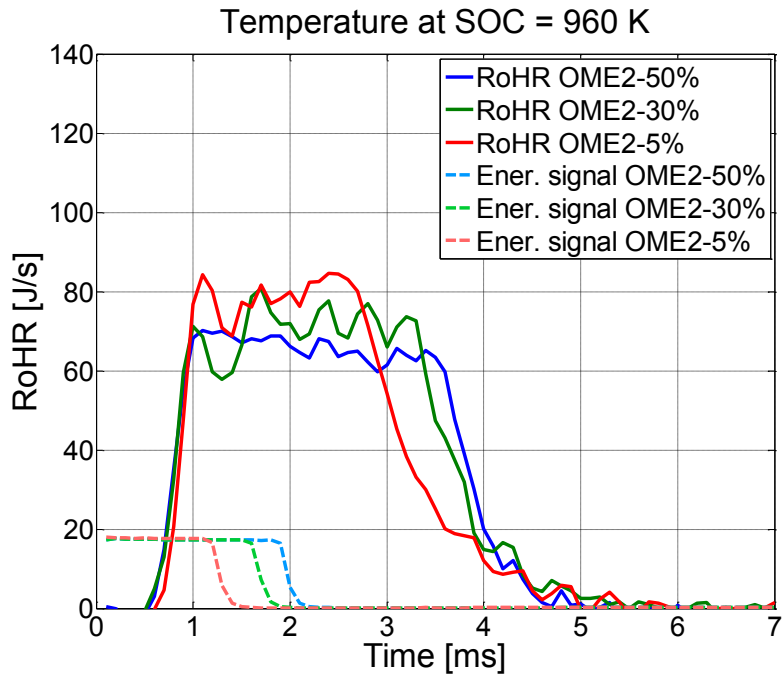


Figure 3.16: RoHR and energizing signal to piezo injector (start at time 0 for OME2-50%, OME2-30% and OME2-5% at 960K@SOC)

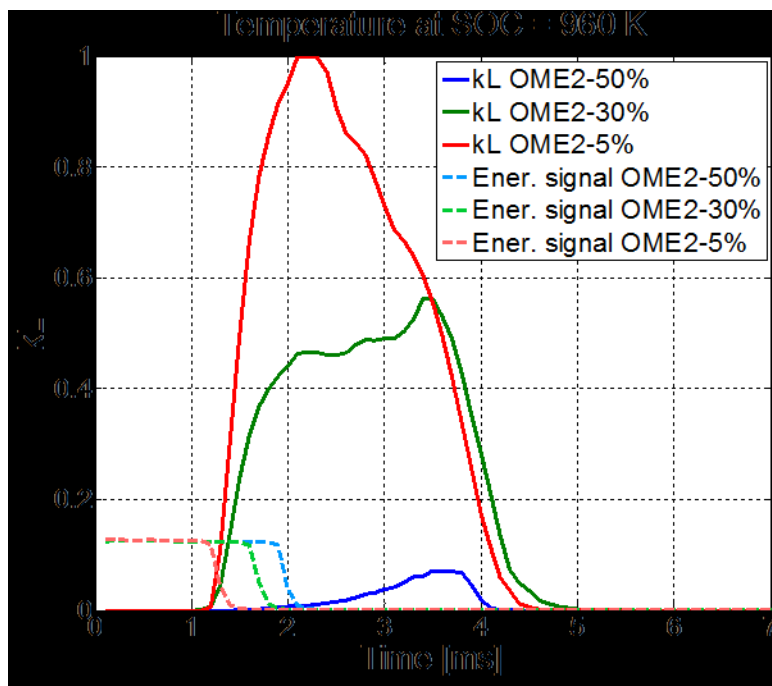


Figure 3.17: kL factor and energizing signal to piezo injector (start at time 0) for OME2-50%, OME2-30% and OME2-5% at 960K@SOC

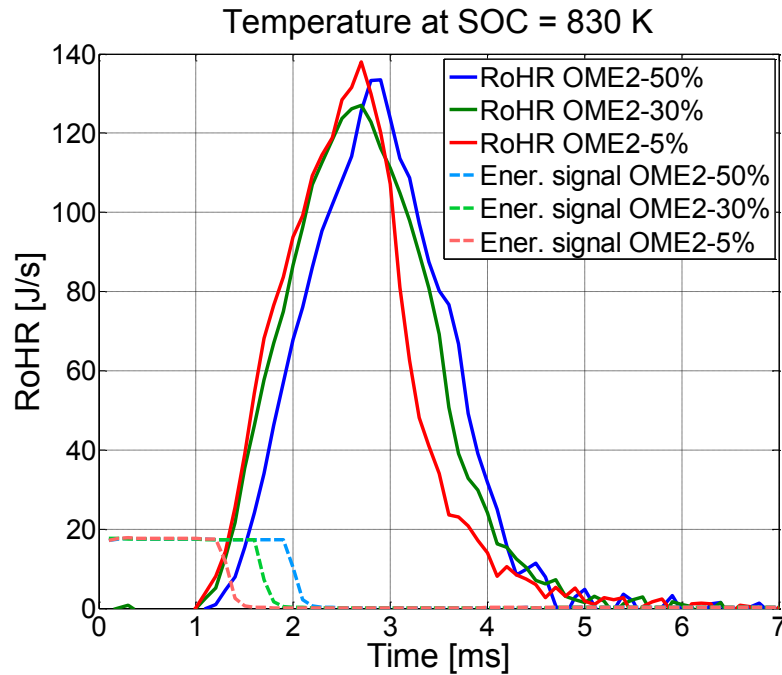


Figure 3.18: RoHR and energizing signal to piezo injector (start at time 0) for OME2-50%, OME2-30% and OME2-5% at 830K@SOC

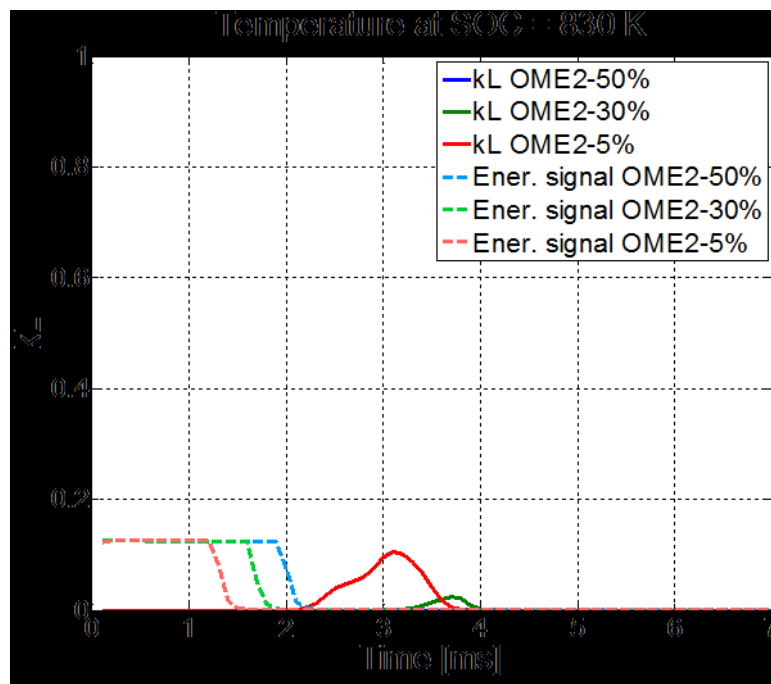


Figure 3.19: kL factor and energizing signal to piezo injector (start at time 0) for OME2-50%, OME2-30% and OME2-5% at 830K@SOC

Finally figures 3.18 and 3.19 report RoHR and kL factor curves for the lowest temperature at SOC, namely 830K. In this condition the ignition delay for each of the three blends results to be higher thus leading to a high fraction of premixed combustion, as shown in the figure. In fact, in this case, a single high pressure peak for each of the three blends is noticeable. The higher amount of time provided to the air/fuel mixing process strongly contributes to further reduce the locally rich

regions in the combustion chamber. As a result, both OME2-50% and OME2-30% show no soot formation while only a very weak kL factor is still characterizing the OME2-5% blend.

Therefore the analysis of figures 3.14 to 3.19 permits to highlight that a first key factor to decrease soot formation is related to the fuel oxygen content, independently from temperature. In [135] though, the authors state that fuel oxygen content becomes an important parameter only for a same chemical family while there is no absolute relationship between PM reduction and global fuel oxygen content when different chemical families of oxygenated fuels are considered. The authors compared different oxygenated compounds (ethers, acetals, polyacetals and carbonates) blended in diesel (5% in volume) and found a maximum reduction in PM emissions of less than 20%, with respect to a reference diesel fuel, for carbonates while ethers provided a reduction of less than 5%. In conclusion the authors found that the choice of the oxygenated compound is more important than only adding oxygen to diesel fuel. In comparison with [135], the present study provided results for an oxygenated compound characterized by no C-C bonds (each compound tested in [135] was, instead, characterized by several C-C bonds), fact that strongly reduces the tendency to soot.

In addition the effect of a higher temperature at start of combustion is related to enhanced soot formation and oxidation processes. This results in higher kL peaks at end of the soot formation dominated phase and increased slope of the soot oxidation dominated phase. Finally a reduction of temperatures @ SOC determines an increase in ignition delay with higher premixed combustion fraction. As a consequence, an enhanced air-fuel mixing before start of combustion with reduction of locally rich regions and soot formation is achieved.

For the same blends, at 1150K and 1010K @SOC, figures 3.20 and 3.21 show the evolution of one of the eight jets from the piezo injector. The evolution is seen in the image of the jet at 1.4 ms, 2.2 ms and 3.5 ms after start of injection (SOI). These three timings represent an early phase of combustion, an instant around the maximum soot formation timing and a relatively late phase of combustion respectively. The images from the two blends are overlapped, subtracted from each other and contoured by a red line for the OME2-5% blend and a blue line for the OME2-50% one. This means that white areas within both the red and blue contours state an equal intensity from the two blends. At any timing after SOI, the OME2-50% blend shows a far smaller area of soot formation, perfectly overlapped only for the first two timings. In fact at 3.5 ms after SOI, the combustion process relative to the OME2-5% blend has spread at annulus shape giving no more chance to detect the fuel jet while for the OME2-50% blend it is still visible. This inequality is due to the different injection duration characterizing the two fuels.

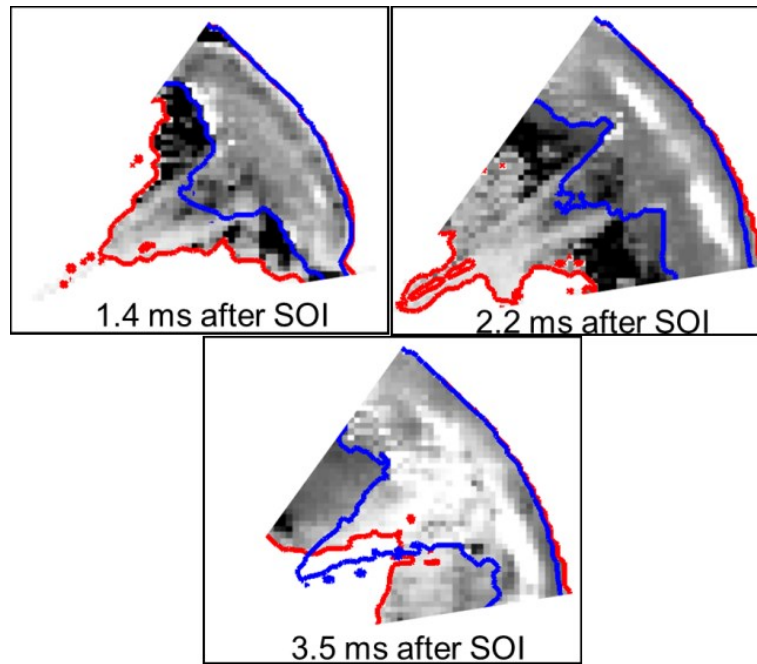


Figure 3.20: Overlapping of fuel jet for OME2-5% (contoured in red) and OME2-50% (contoured in blue) at 1150K@SOC and 1.4, 2.2 and 3.5 ms after SOI

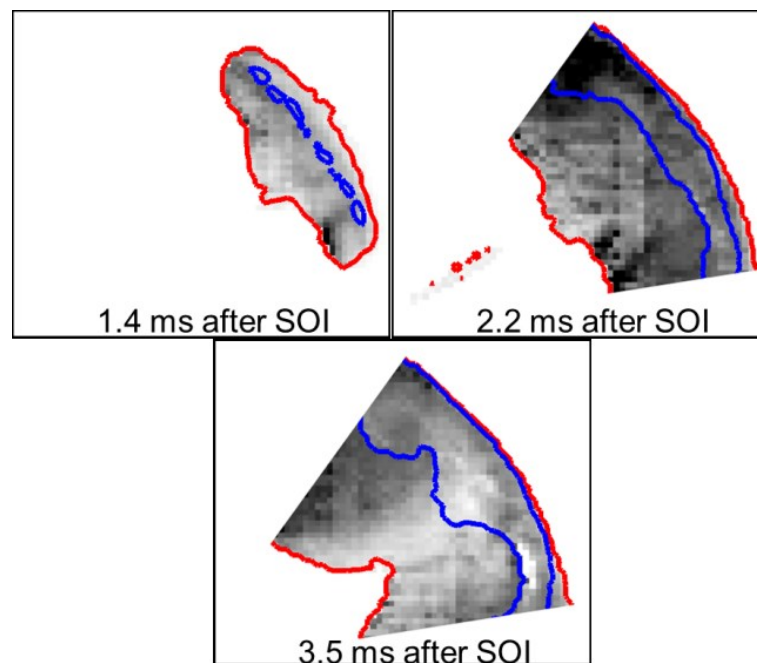


Figure 3.21: Overlapping of fuel jet for OME2-5% (contoured in red) and OME2-50% (contoured in blue) at 1010K@SOC and 1.4, 2.2 and 3.5 ms after SOI

The same scenario is shown in figure 3.21, which reports results for the 1010K at SOC operating condition. Same considerations stated for figure 3.20 are still valid in this last case. In addition a comparison between same timings and fuels from figures 3.20 and 3.21 allows to evaluate the effect of a lower temperature at SOC on soot formation. Each area contoured in red or blue in figure 3.21

is smaller than the corresponding one in figure 3.20 meaning that the k_L factor is decreasing with lower temperatures.

The following figures will show luminosity at 309 ± 5 nm wavelength (OH-peak in the emission spectrum) results for pure OME2 and OME2 in diesel blends with the aim of following the evolution of combustion precursors. Each figure displays 4 images (representing only one quarter of the cell), one for each investigated fuel, at a specific temperature at SOC. The images in each figure are shown in clockwise layout from highest to lowest fuel oxygen content. Figure 3.22 reports the results for 1150K, figure 3.23 shows the 960K condition and figure 3.24 the 830K. In order to improve the images visibility, three different luminosity scales (count of all pixel is taken as unit) are selected for the three different temperatures at SOC. If the different scales are taken into account, it clearly appears how the luminosity at 309 ± 5 nm wavelength is temperature dependent. In addition, the images from the blends (increasing brightness with lower percentage of oxygenated fuel) are characterized by a higher luminosity with respect to pure OME2. This effect is probably coming from soot (emitting all over the spectra) which emits even at 309 nm, covering, in this way, the OH signal. This means that the only fuel from which information on combustion precursors can be considered is the OME2 pure. This fuel in fact has shown a soot level below the 2D2CP detection sensitivity threshold.

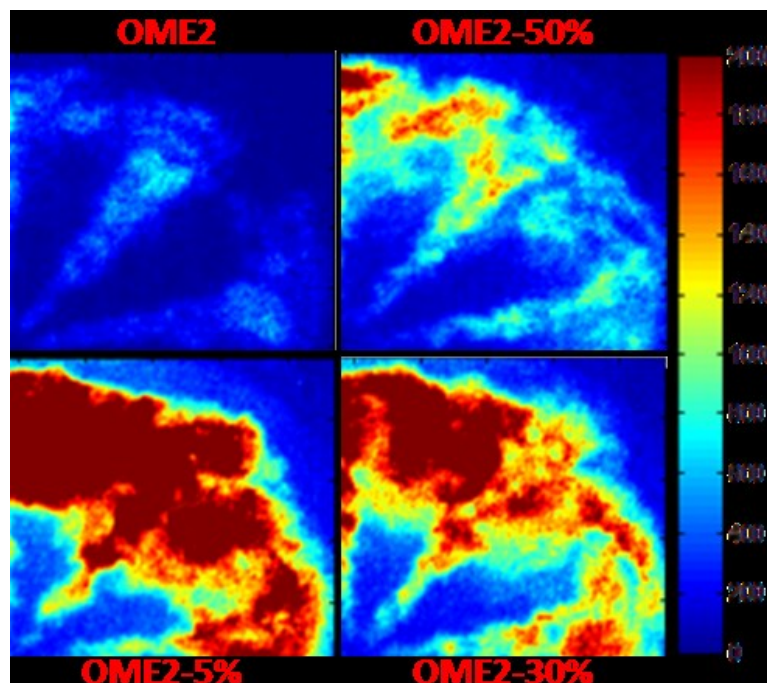


Figure 3.22: Luminosity at 309 ± 5 nm – 1150K@SOC

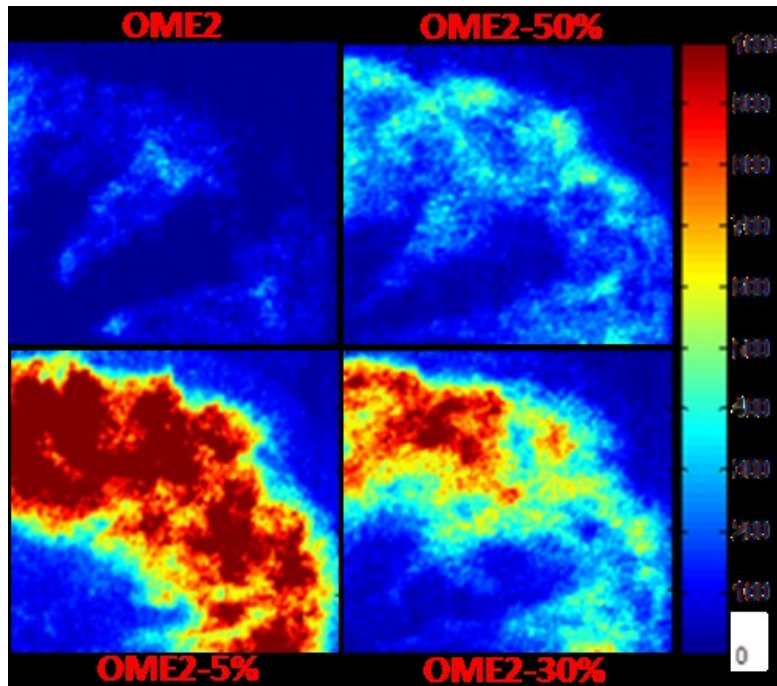


Figure 3.23: Luminosity at 309±5 nm – 960K@SOC

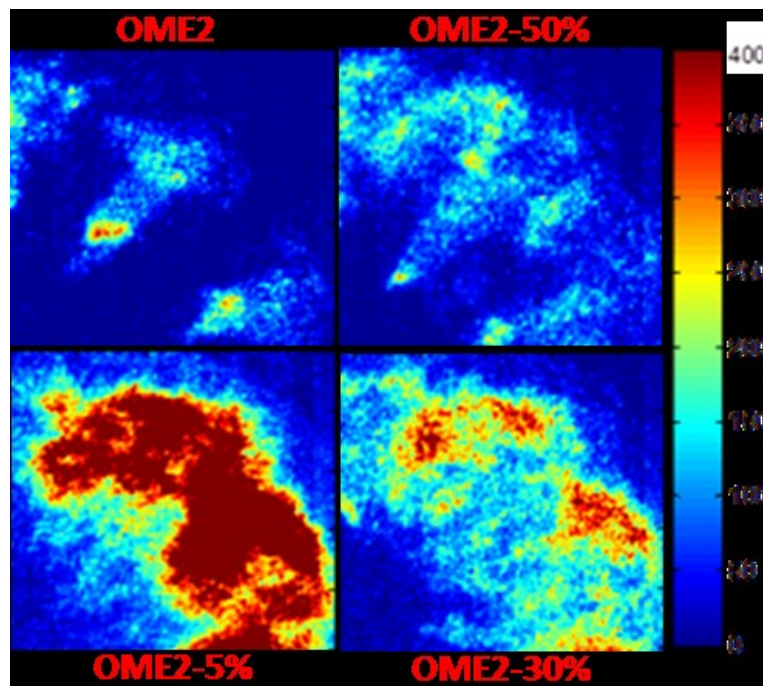


Figure 3.24: Luminosity at 309±5 nm – 830K@SOC

For this reason a comparison between the integral of OH intensity and the rate of heat release over different temperatures at SOC is shown in the next two figures (3.25 and 3.26) only for pure OME2. The aim of this comparison is to investigate whether a temperature dependency trend may be associated to the variable detected gap between start of heat release and OH signal. Each figure displays the OH intensity curve in green, the RoHR in blue and the energizing signal to the piezo injector in red. It is worth to underline that a different scale for OH intensity has been set for figures

3.25 and 3.26 in order to achieve a better signal visibility. The comparison OH-RoHR shows as the delay between start of RoHR and start of OH signal increases with the decreasing temperatures at SOC. This means that moving towards a premixed combustion mode temperatures are too low to provide a visible OH signal in the earliest phase. For this reason, probably, OH signal appears with some delay and is no longer directly correlated to the RoHR signal, as it was instead at high temperatures @ SOC.

Figure 3.25 shows two “hot” conditions (1150K and 1010K at SOC) in which a good correlation between RoHR and OH signal is noticeable. On the other hand, figure 3.26 shows two “cold” conditions (930K and 830K at SOC) in which an increasing delay of OH signal with decreasing temperature at SOC is observed.

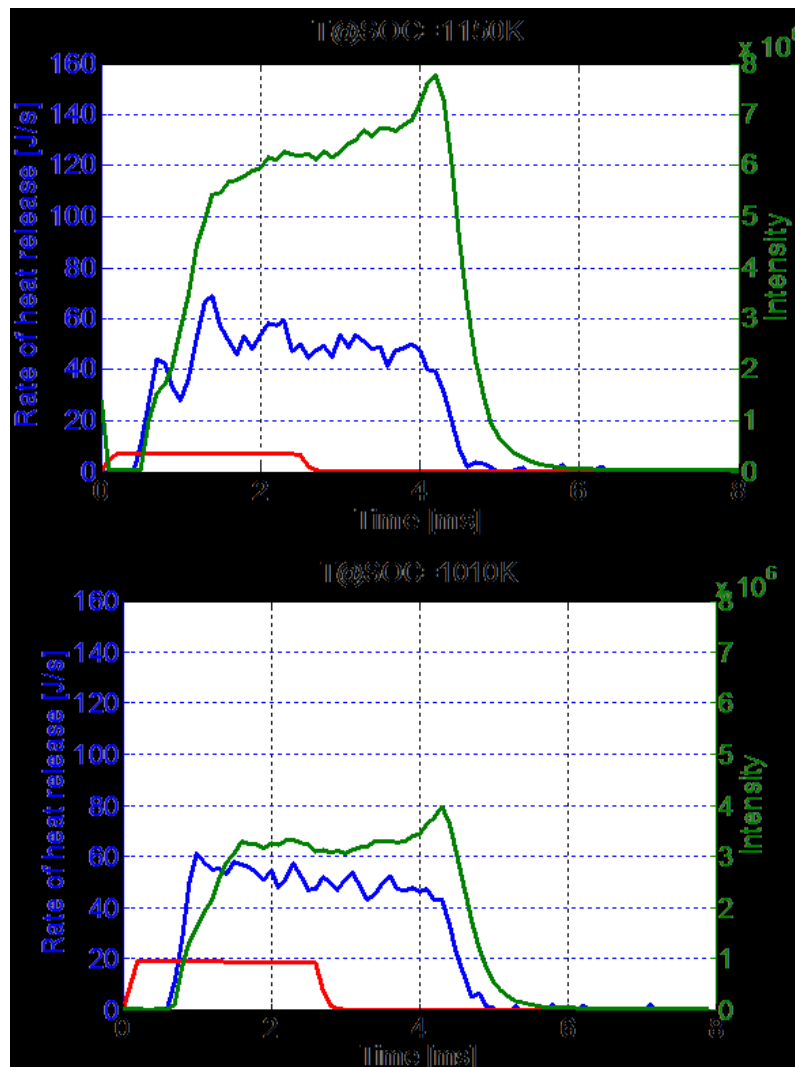


Figure 3.25: OH chemiluminescence 1150K and 1010K @ SOC for pure OME2

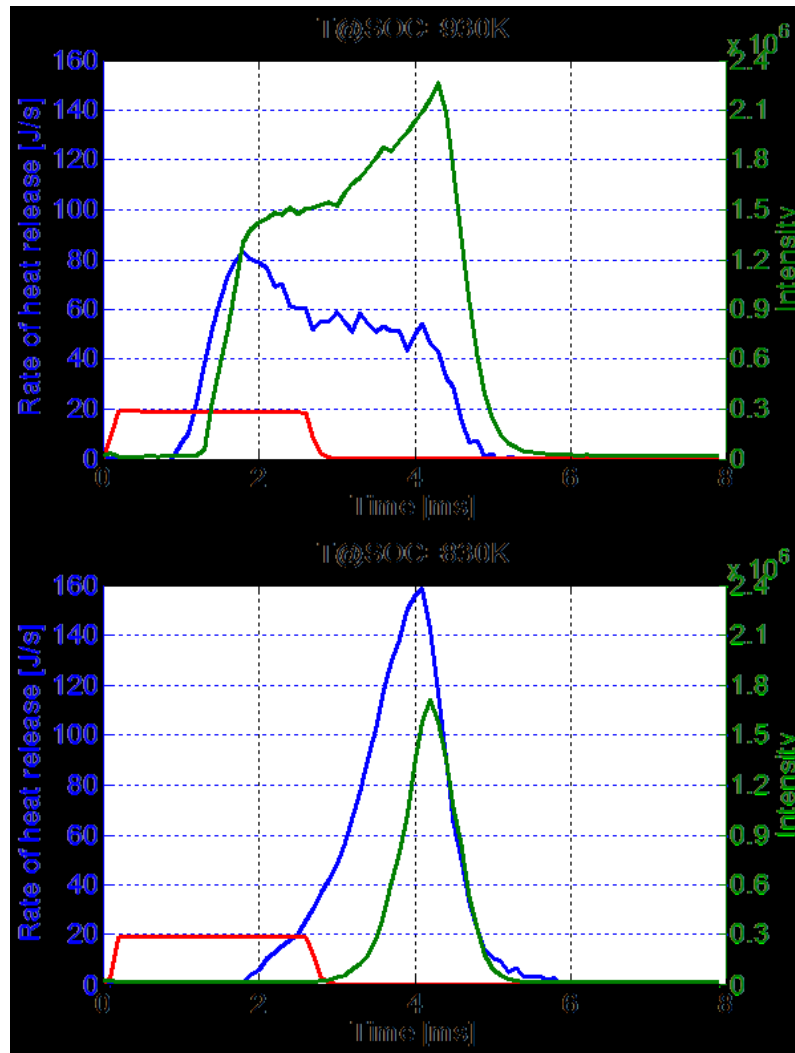


Figure 3.26: OH chemiluminescence 930K and 830K @ SOC for pure OME2

Exhaust results

In order to compare exhaust emissions results from the different investigated fuels, a Combustion DMS 500 fast particle spectrometer has been used. For each fuel the exhaust emission values presented in the following are normalized to the one of commercial diesel at 1010K@SOC. Figure 3.27 reports normalized soot values vs fuel oxygen content of the investigated fuels at the operative condition of 1010K@SOC. Error bars have been inserted in the figure in order to take into account the relatively high values of cycle to cycle variation provided by the measurements. The figure shows as an increase in fuel oxygen content determines always a decrease in soot emissions. It is worth to underline as the soot emissions reduction is not linear with the oxygen content increase, as reported in [135]. In fact since the different investigated fuels are characterized by a different adiabatic flame temperature, number of C-C bonds and local air fuel ratio (parameters correlated to soot formation), a linear correlation soot reduction – oxygen content may not be

expected. Pure OME2 and OME2/3/4 basically show an almost smokeless combustion while still some soot mass is detected with OME1.

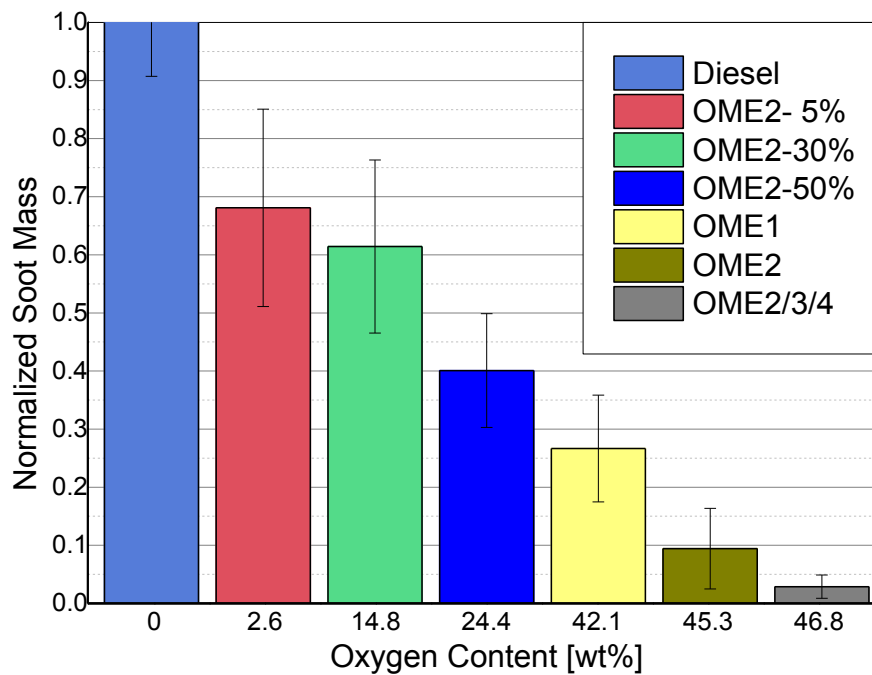


Figure 3.27: Normalized Soot Mass for the investigated fuels at 1010K @ SOC

A remarkable result, though, is related to OME2-5%: a 2.6 % oxygen content in the blend already leads to a reduction of about 30% in soot mass. This result, higher than that provided from the 5% oxygenated compounds in diesel tested in [135], is probably explained because of the absence of C-C bonds in OME2, which reduces the tendency to soot leading to a higher PM reduction.

Figure 3.28 reports the comparison of OME2, OME2/3/4 and the OME2 blends at different temperatures at SOC. The yellow arrows indicate the direction of soot reduction with respect to temperature at SOC. OME2 and OME2/3/4 lead to a reduction of more than 85% with respect to the reference diesel for any operating condition. The effect of temperature at start of combustion has to be analyzed in two different ranges: a slight trend (within the repeatability, error bar, of the measurements) towards higher exhaust soot with lower temperature is visible down to 960K. In fact, in accordance with literature, a decrease in temperature determines a decrease in soot formation on one hand but a slower oxidation process on the other hand [17]. As a result, an overall slight increase of soot detected at the exhaust is observed. A further decrease in temperature (960K to 830K), instead, determines, for all the investigated fuels, the transition towards a partially premixed combustion mode which permits a massive reduction in soot emissions due to reduced mass fraction burnt during diffusive combustion, as shown in the figure. It is worth to underline that no direct link may be established between the peak in soot emissions at exhaust (given by soot

formation – soot oxidation) described within figure 3.28 at 960K@SOC and the soot formation zone in the well-known ϕ -T diagram (i.e. in [20]).

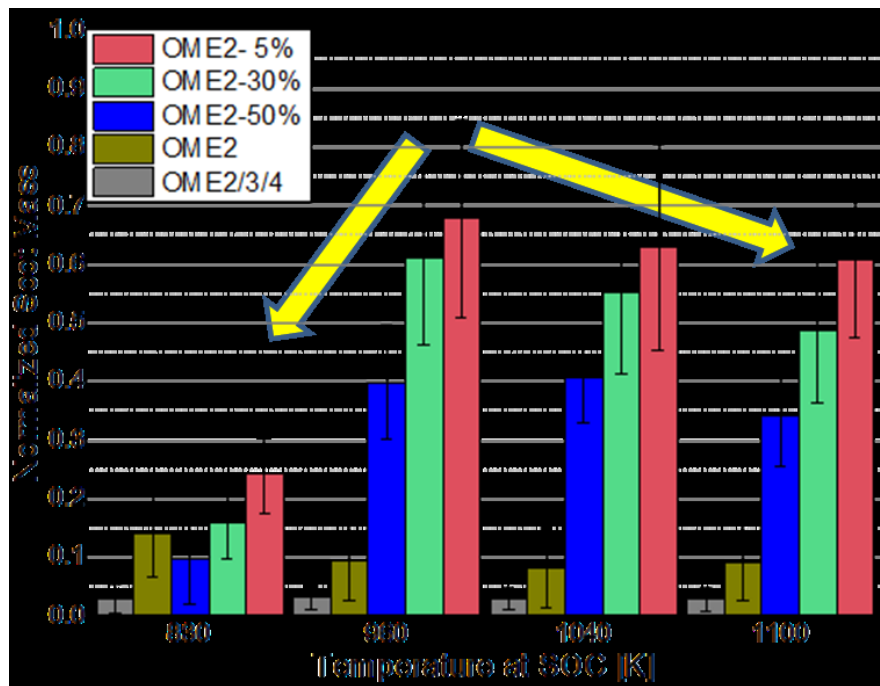


Figure 3.28: Normalized Soot Mass: OME2/3/4, OME2 pure and OME2 in diesel blends at different temperatures @ SOC

Moreover, a comparison of particle concentration with respect to particle diameter for OME2-5% and OME2 pure is reported in logarithmic scale in figure 3.29 which refers to a temperature at SOC of 1150K. In order to show the particle concentration of the two fuels on a single scale, a break on the y-axis has been introduced. The main difference which clearly appears comparing the two fuels is that the pure oxygenated fuel produces no particles bigger than 50 nm (diameter) while the combustion of OME2-5% shows a minor number of presumably volatile particles up to 20 nm (since no volatile particle remover was used) and larger particle agglomerations, up to 500 nm. This means that even for pure oxygenated fuels the first nucleation phase of the soot formation process takes place but the following agglomeration phase is strongly reduced. This effect is most probably due to the molecule oxygen content which could then oxidize the “new born” nucleation cores. In addition, as reported in [136] the larger particles from OME2-5% (bigger than 50 nm diameter) act as a sponge during the agglomeration phase thus reducing the total number of particles, even though the total mass is increased with respect to OME2 pure. Instead OME2 is characterized by volatile particles up to 20 nm and solid particles, in the range 20-50 nm, which determine most of the contribution to mass from it. It is worth to underline that no volatile particle remover has been used since their contribution to the total mass is very low.

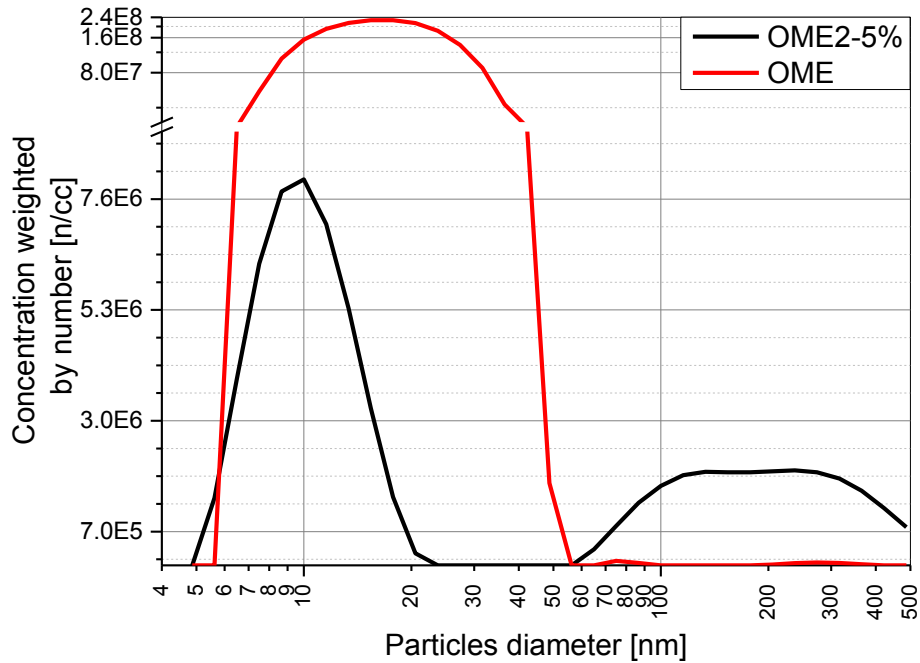


Figure 3.29: OME2-5% and OME2 pure at 1150K @ SOC: particle concentration

The discussed results demonstrated, among other, as a massive reduction of the soot formation dominated phase is achieved when increasing the oxygenated fraction in the blend and that an addition of just 5% of oxygenated fuel within commercial diesel permits a reduction in soot emissions of about 30%. With particular reference to the OME2/3/4 mixture, characterized by an oxygen content of 46.8%wt, the achieved soot reduction, with respect to commercial diesel, is more than 95%. Since this fuel is characterized by similar physical properties to diesel thus not requiring substantial modifications to the engine infrastructure, it could be therefore produced on industrial scale to be blended with conventional diesel. In this way the blend could take the advantages of both fuels: diesel high energy content and OME2/3/4 strong capability of reducing soot formation. Since the presented activity provided a deeper knowledge of the oxygenated fuel effect on soot formation/oxidation process but not a complete overview of the impact of an industrial scale producible OME-diesel blend on a compression ignition engine, results of a further investigation conducted on a single cylinder “heavy duty” direct injection diesel engine are shown in the following. The aim is to examine achievable engine performance and exhaust emissions taking into account nitrogen oxides, unburned hydrocarbons, carbon monoxide and carbon dioxide as well. A 10% OME2/3/4 in diesel blend is considered for the investigation.

3.3 MTU single cylinder engine results

Exhaust emission and performance results

Since fuels from the POMDME family (with $n > 2$) are characterized by similar physical properties with respect to commercial diesel, thus not requiring substantial modifications to the engine infrastructure, an industrial scale production could be desirable to obtain blends with diesel. In this way they could take the advantage of diesel high energy content and POMDME capability of reducing soot formation. The experimental work conducted on the MTU single cylinder “heavy duty” direct injection diesel engine aimed at examining achievable engine performance and exhaust emissions. Results for the 8 bar BMEP condition are presented in a first section, while the 10.5 bar BMEP one is discussed in a second section.

Figure 3.30 shows smoke results for the investigated fuels at BMEP=8 bar for the different O_2 contents at intake and start of injection. As expected, for any operating condition, a decrease in smoke emissions is noticed with decreasing EGR and increasing oxygen content of the blend. In addition, the figure reports the average soot reduction values (with respect to commercial diesel) obtained with 5% POMDME and 10% POMDME over the whole experimental campaign at BMEP=8 bar, 19.7 and 31.4% respectively.

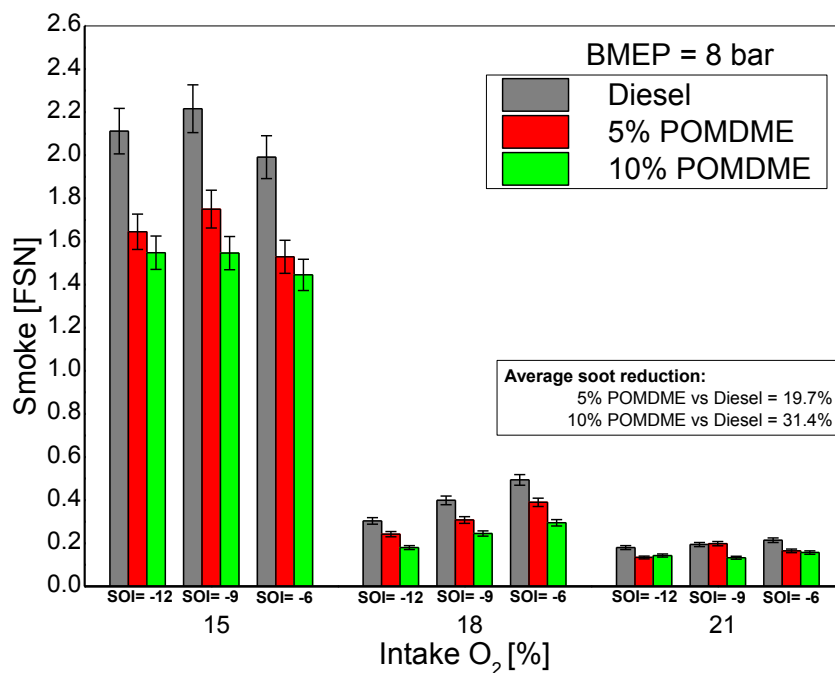


Figure 3.30: Diesel, 5% POMDME and 10% POMDME - Smoke emissions @ BMEP=8bar

No significant difference in smoke emissions is detected, instead, for the different starts of injection, probably because of the comparable premixed - diffusive combustion mode ratio achieved over the selected SOIs.

With respect to NO_x emissions (figure 3.31), a similar behavior of the different fuels in operating conditions with EGR has been observed. This allows stating that the recirculation of exhaust gases determines the major variation of this pollutant and low NO_x values are achieved even with fuels containing molecular oxygen. An increase in NO_x emissions, especially with the 10% POMDME, has been though detected under zero EGR operating conditions.

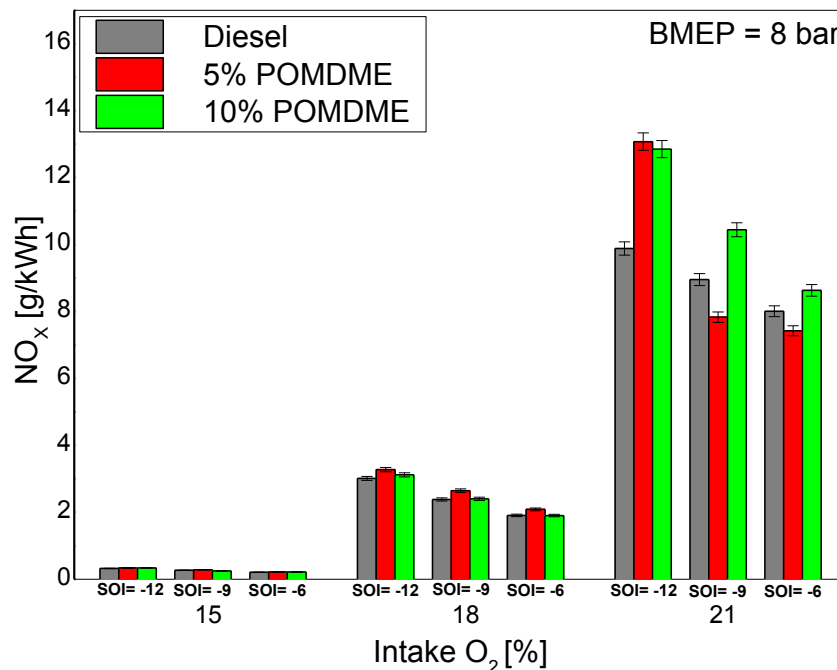


Figure 3.31: Diesel, 5% POMDME and 10% POMDME - NO_x emissions @ BMEP=8bar

In order to analyze the trade-off Soot NO_x for the different investigated fuels, results are reported in figure 3.32. The condition allowing the best compromise between the two pollutant species is the intake $\text{O}_2=18\%$ one. Within this condition, the figure clearly shows as the adoption of the oxygenated blends allows a reduction in soot associated with no significant increase in NO_x , thus achieving a better trade-off. In order to further understand the behavior of the different investigated fuels for the intake $\text{O}_2=18\%$ condition (being the most interesting one), heat release curves are shown in figure 3.33 for the SOI=-12 cad atdc case. The same considerations, though, are still valid for the other SOIs. The curves show a similar profile both in the premixed and diffusive combustion phase allowing to consider that the addition of the oxygenated fraction does not introduce deep modifications in the ignition delay, combustion behavior and combustion efficiency, as will be further discussed in the following. This explains the similar NO_x emissions,

shown in figure 3.32 even though, the presence of molecular oxygen allows, for the blends, a reduction in smoke emissions. In addition, it is worth to observe from figure 3.33, as the final part of diffusive combustion (from 370 cad atdc) seems to be slightly faster for the blends. This fact has to be connected with the higher oxygen fraction which enhances the oxidation process.

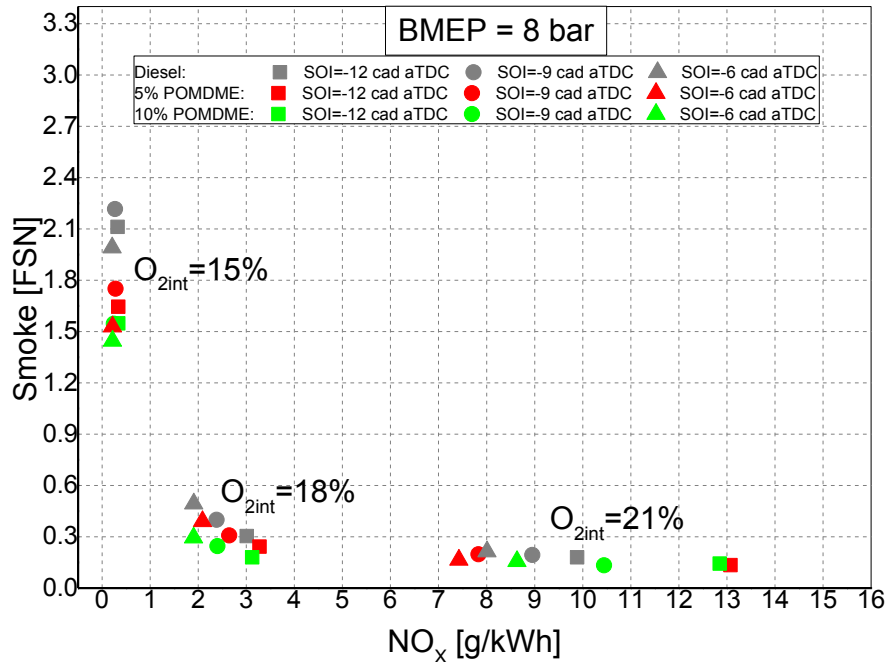


Figure 3.32: Diesel, 5% POMDME and 10% POMDME – Smoke NO_x trade off @ BMEP=8bar

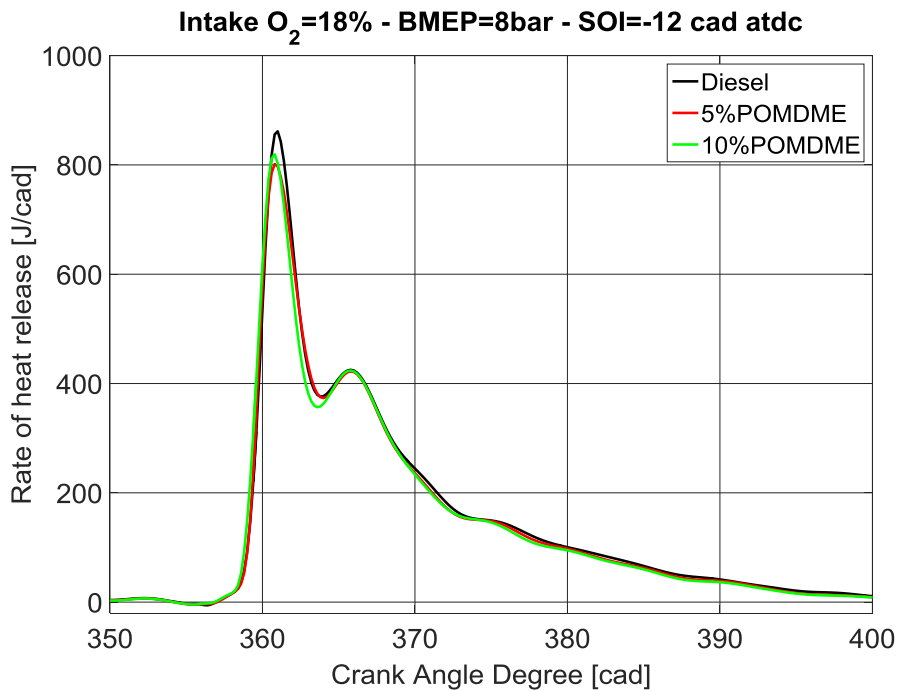


Figure 3.33: Diesel, 5% POMDME and 10% POMDME – Rate of heat release curves @BMEP=8bar, intake O₂=18% and SOI=-12 cad atdc

The discussion continues proposing the analysis of products of incomplete combustion, namely unburned hydrocarbons and carbon monoxide, to observe whether oxygenated blends could lead to a worsening of combustion efficiency. Results are reported in figures 3.34 (HC) and 3.35 (CO). HC emissions show no clear trend associated neither to the particular fuel nor to the specific operating condition. Therefore the only conclusion that can be drawn from results in figure 3.34 is related to the fact that the investigated oxygenated fuels did not determine an average increase of HC with respect to commercial diesel.

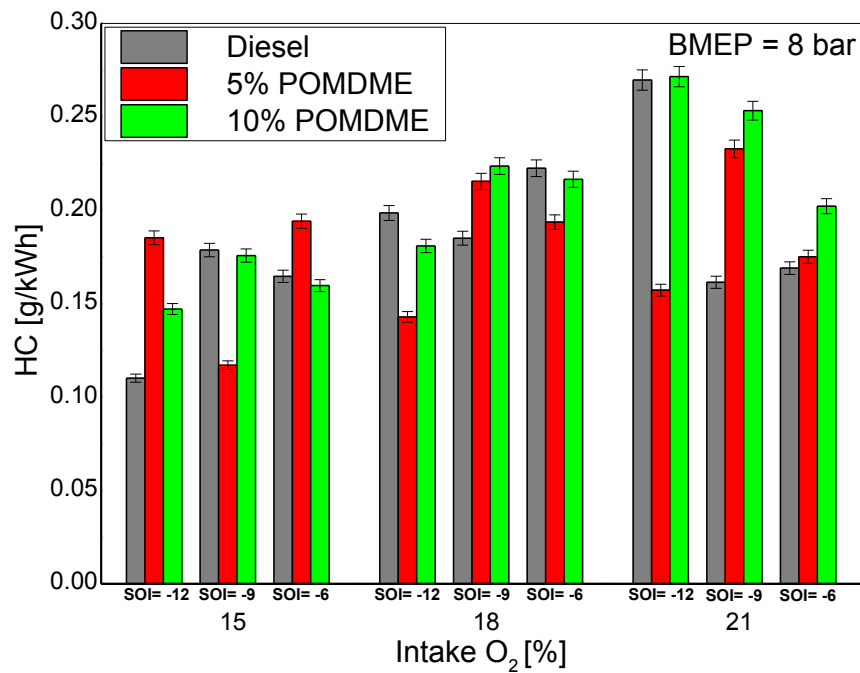


Figure 3.34: Diesel, 5% POMDME and 10% POMDME - HC emissions @ BMEP=8bar

On the other side CO emissions, shown in figure 3.35, display a clear increasing trend associated to higher EGR rates and retarded SOIs but, once more, not to the particular investigated fuel. In conclusion, it is possible to state that no significant decay of combustion efficiency, at least for the BMEP=8 bar condition, has been introduced operating the engine with the 5% POMDME nor the 10% POMDME blends.

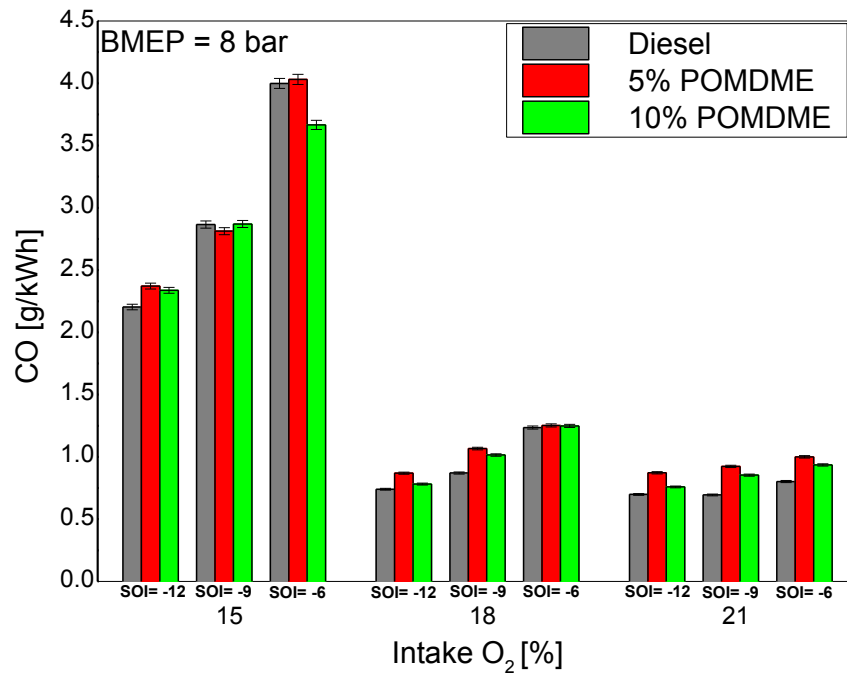


Figure 3.35: Diesel, 5% POMDME and 10% POMDME - CO emissions @ BMEP=8bar

Results of break specific fuel consumption for the different investigated fuels are discussed in figure 3.36. The low energy content of the oxygenated fuels (less than 22 MJ/kg) determine, for the two investigated blends, a higher amount of fuel that has to be introduced in the system in order to achieve the same power output. Therefore, fuel economy could be the main reason for considering, in a hypothetical industrial scale production, 10% POMDME as a maximum percentage to be blended in commercial diesel. Figure 3.36 reports BSFC trends with respect to the different fuels and operating conditions as well as the average increment (with respect to commercial diesel) detected with 5% POMDME and 10% POMDME, 2.2 and 4 wt-% respectively (considering the whole experimental campaign at 8bar BMEP). In addition, an increase in BSFC is shown for any investigated fuel when retarding the start of injection from -12 to -6 cad atdc because of a lower efficiency due to a higher fraction of the combustion process taking place during the expansion stroke. Finally, an increase in BSFC, as expected, is even noticed with increased EGR rates.

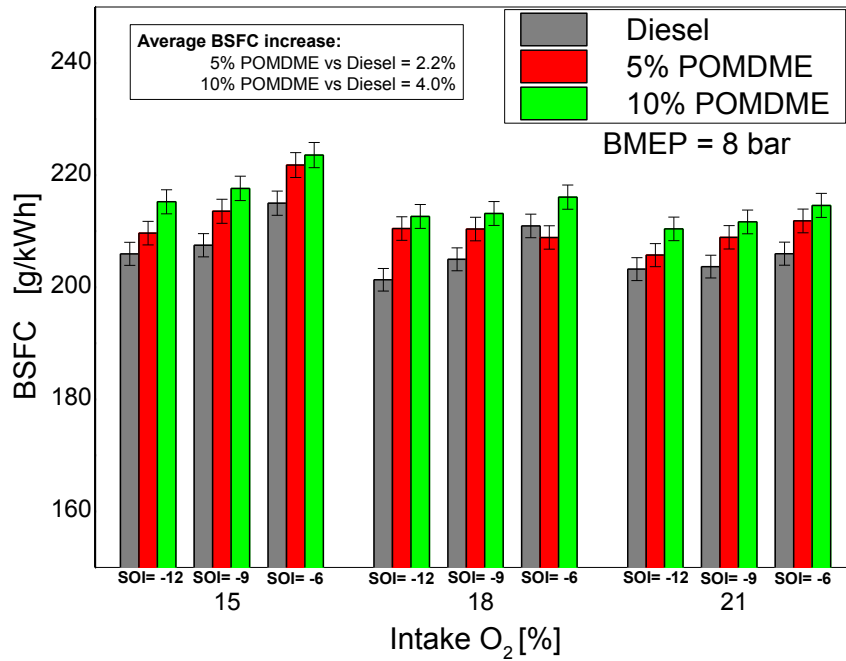


Figure 3.36: Diesel, 5% POMDME and 10% POMDME – BSFC @ BMEP=8bar

Moreover, in order to further discuss the behavior of the different fuels towards combustion efficiency, figure 3.37 reports values of CO₂ measured at the exhaust. CO₂ emissions, which give indications on the efficiency of the combustion process, range on similar values for the different fuels and SOIs. This confirms, as previously stated, that no decrease in combustion efficiency is introduced with the oxygenated blends while an increase in EGR leads to more CO₂ detected at the engine exhaust.

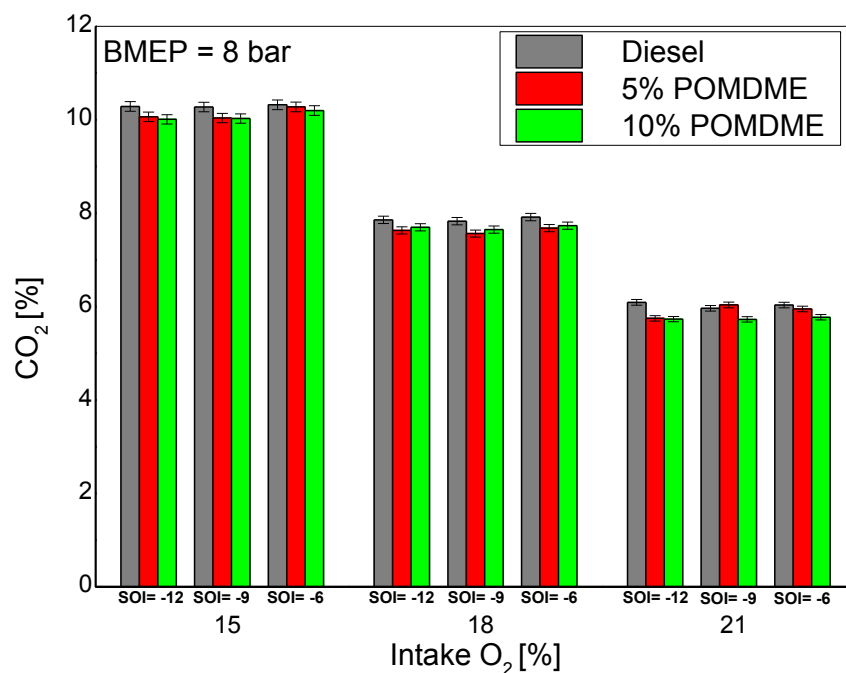


Figure 3.37: Diesel, 5% POMDME and 10% POMDME – CO₂ emissions @ BMEP=8bar

Experimental tests have been conducted, for the different fuels, with a fixed intake pressure and injection pressure while a slight variation in injection duration has been considered in order to keep the BMEP constant. Therefore, the presence of molecular oxygen in the 5% POMDME and 10% POMDME blends seems to be associable, for any operating condition, with an increase in oxygen detected at the engine exhaust (figure 3.38). As a conclusion, the higher oxygen availability provided by the blends, could allow operating at higher EGR levels, with respect to commercial diesel, still maintaining a constant value of oxygen detected at the exhaust.

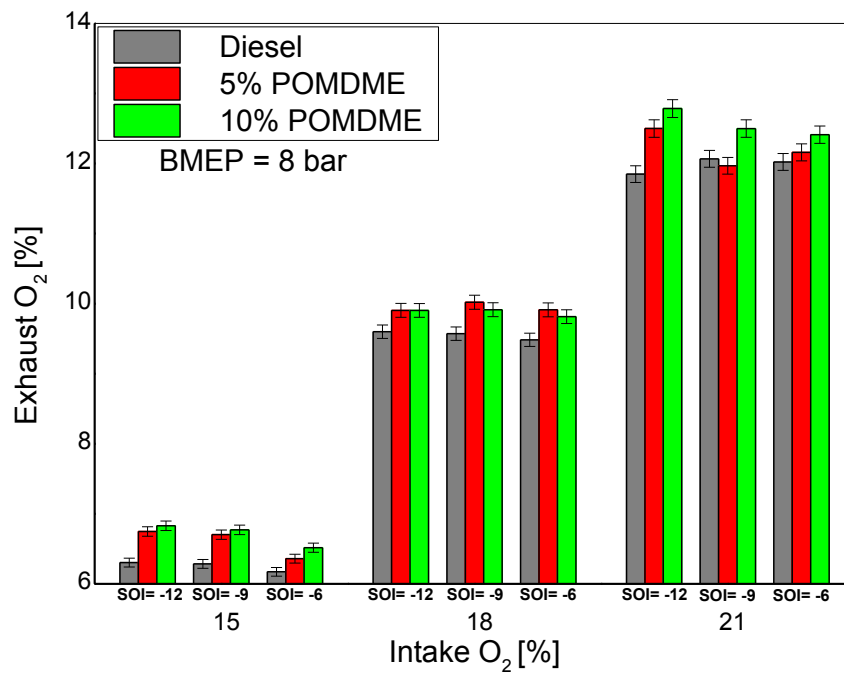


Figure 3.38: Diesel, 5% POMDME and 10% POMDME – Exhaust O₂ @ BMEP=8bar

The second part of this section discusses the main results achieved at the higher investigated load condition, 10.5 bar BMEP. The discussion focuses on smoke, NO_x and BSFC results while the other pollutants are not shown being still valid the observations discussed for the 8 bar BMEP load. As shown in figure 3.39, a reduction in soot emissions has been achieved, even at this higher load, for any operative condition when adopting the 5% POMDME and 10% POMDME blends. An average soot reduction (with respect to commercial diesel) over the whole experimental campaign at BMEP = 10.5 bar has been calculated for the two blends and the result shows that almost 35% of soot reduction is achieved with the 10% POMDME blend while more than 10% reduction is obtained with the 5% POMDME one. In addition, as discussed for the 8 bar BMEP load, still no significant difference in smoke emissions is detected for the different starts of injection. At 10.5 bar BMEP though, just a minor decrease in soot is noticed when moving from the 18% O₂ at intake condition to the zero EGR one probably because of the effect of higher temperatures favorable for

soot oxidation. A further increase in EGR, though determines a massive increase in soot for any investigated fuel. In fact, the 15% O₂ at intake condition determines a substantial reduction of combustion temperatures because of the high amount of inert gas introduced in the cylinder. As a consequence NO_x emissions are almost completely removed, as shown in figure 3.40 but the soot oxidation phase is strongly affected with unacceptable soot values detected at the exhaust.

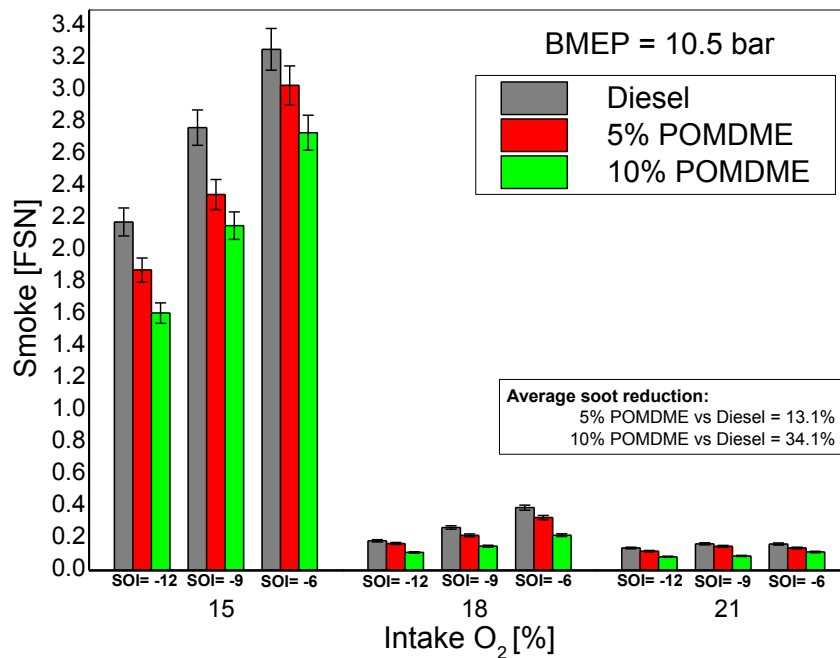


Figure 3.39: Diesel, 5% POMDME and 10% POMDME - Smoke emissions @ BMEP=10.5bar

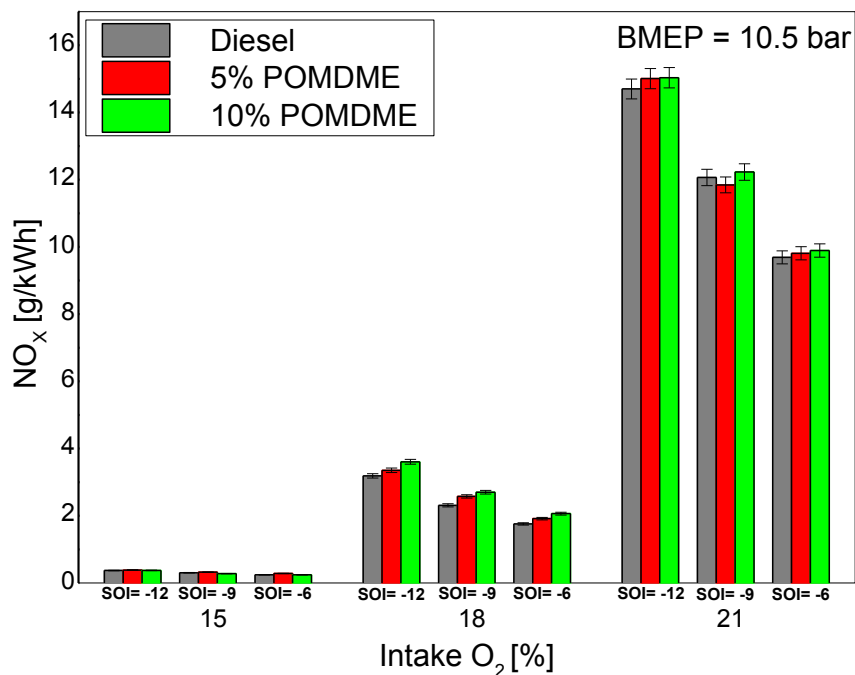


Figure 3.40: Diesel, 5% POMDME and 10% POMDME - NO_x emissions @ BMEP=10.5bar

Figure 3.40 demonstrates as, even at 10.5 bar BMEP, the investigated oxygenated fuels did not lead to significant increase in NO_x emissions.

A trade-off Soot NO_x plot is shown, even for the 10.5 bar BMEP (figure 3.41), in order to clearly highlight the operating conditions providing the best results. Within the 18% O_2 at intake condition, which clearly appears to be the best compromise for a reduction in both soot and NO_x , the most retarded start of injection (-6 cad atdc) allows, for any investigated fuels, a further reduction in NO_x probably because of the decrease in combustion temperature due to a higher fraction of the combustion process taking place during the expansion stroke.

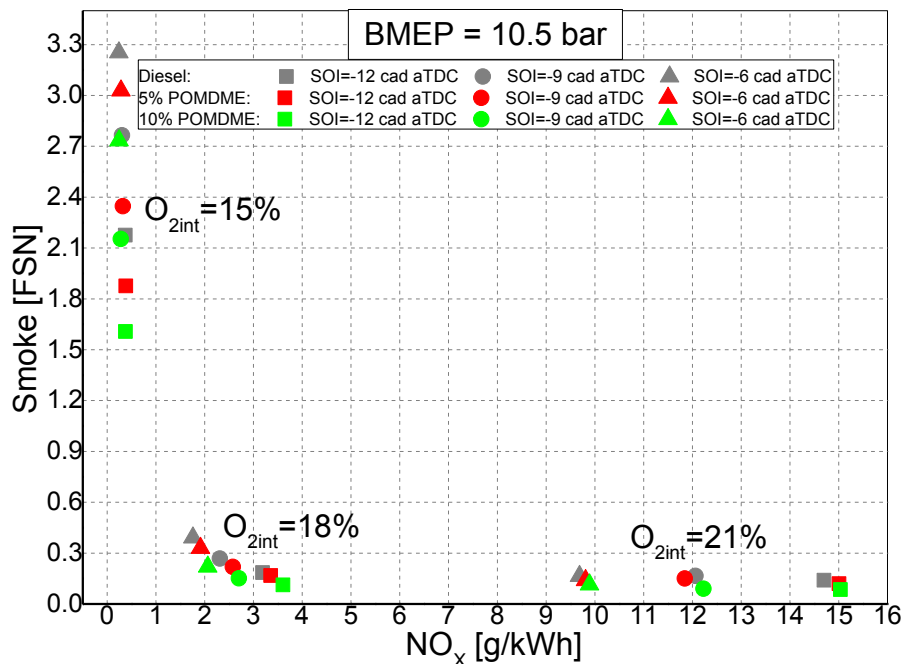


Figure 3.41: Diesel, 5% POMDME and 10% POMDME - Smoke NO_x trade-off
@BMEP=10.5bar

Finally results of break specific fuel consumption for the different investigated fuels are discussed in figure 3.42. Once more the lower energy content of the oxygenated fuels forces to increase the injected fuel amount in order to achieve a fixed power output value. An average increase of 2.3% and 4.3% has been calculated over the whole experimental investigation at 10.5 bar BMEP for the 5% POMDME and 10% POMDME blends respectively. Despite the observed increase in break specific fuel consumption, no significant variation in CO_2 at exhaust for the different fuels is found (figure 3.43), underlining, once more, as the use of the oxygenated blends is not negatively affecting combustion efficiency.

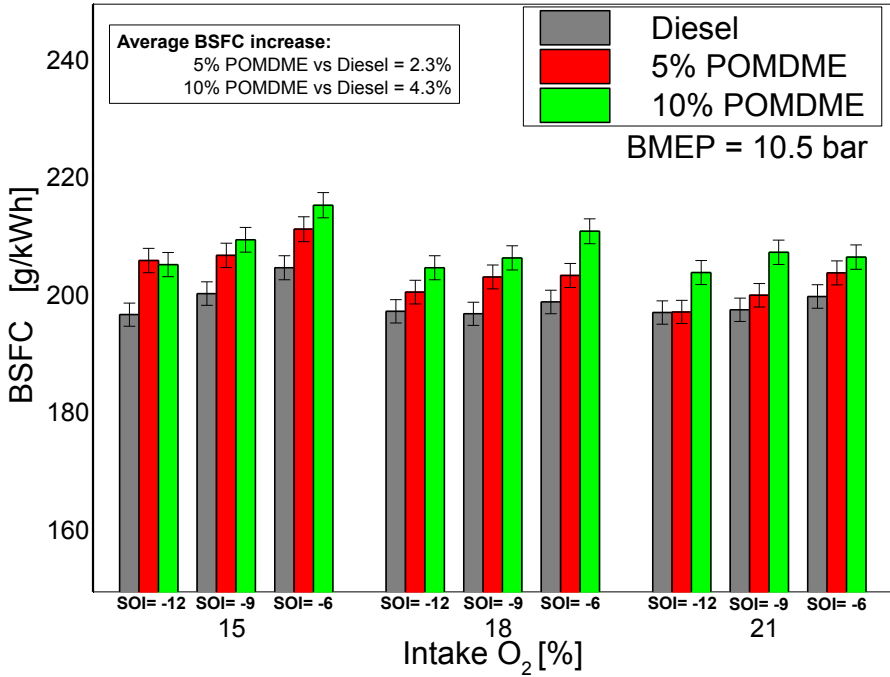


Figure 3.42: Diesel, 5% POMDME and 10% POMDME – BSFC @ BMEP=10.5bar

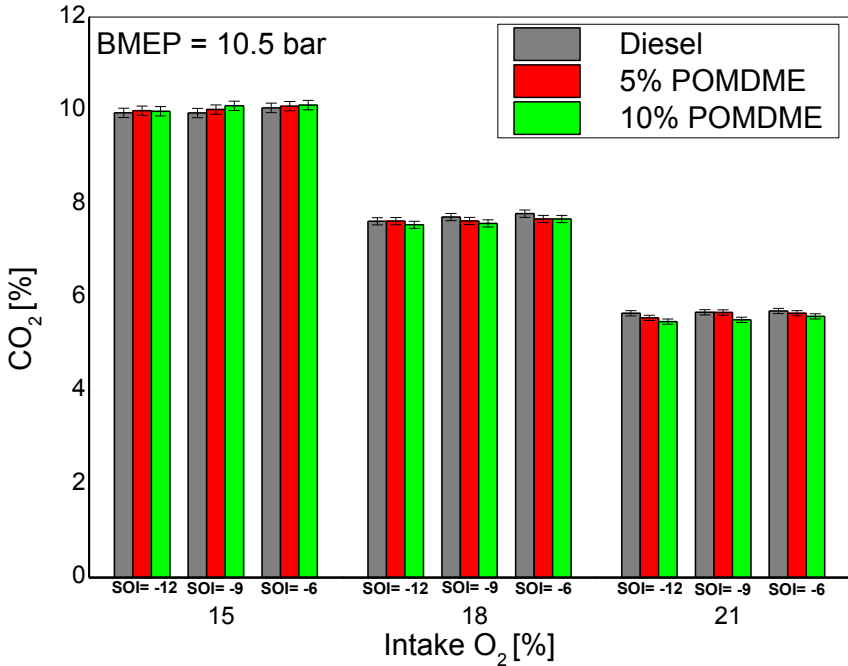


Figure 3.43: Diesel, 5% POMDME and 10% POMDME – CO₂ emissions @ BMEP=10.5bar

Chapter 4

Conclusions and Outlook

Previous research on oxygenated fuels has shown the potential of reducing soot emissions from diesel engines. In this work, an experimental investigation conducted on several fuels and different combustion modes with the aim of providing further insight into the capability of fuel composition, molecular oxygen and combustion mode to contribute reducing mainly soot emissions has been presented. In the following, the observations from the experimental work are listed and commented. Finally, an outlook on how the investigation could be further enriched is proposed.

Experimental observations

The experimental investigation has been conducted on a modern automotive direct injection Diesel engine at 2500rpm and 0.8MPa BMEP (one of the NEDC operating conditions), exploring two combustion phasings (CA50=18 and 21 cad atdc) and two percentages of oxygen at intake (17 and 19). Selecting a proper injection pressure and timing, a premixed combustion mode has been attained for any fuel and the analysis of the impact of physical and chemical properties, such as cetane number, net heat value, fuel volatility and oxygen content, on combustion evolution, engine performance and exhaust emissions has been carried on, allowing the following observations:

- Fuel properties have a strong impact on soot emissions. Blends composed of diesel-gasoline or diesel-butanol determined the maximum reduction in smoke emissions compared to the diesel fuel. This result allows to state that, under a premixed combustion mechanism with high ignition delay, because of a better air-fuel mixing, homogeneous mixture is enhanced and locally rich regions, responsible of soot formation, reduced.
- No significant difference for NO_x emissions has been found between the investigated fuels, operating at fixed O₂ percentage at intake. This behavior shows that molecular oxygen may not lead to an increase in NO_x formation under late premixed combustion.
- Retarded combustion phasing associated with reduced oxygen percentage at intake determines a strong reduction in combustion noise, for any tested fuel. This result is attributable to the development of the combustion process mainly during the expansion stroke leading to a decrease of in-cylinder pressure rise and peak.

In order to isolate the contribution of molecular oxygen with regard to soot reduction, the experimental work has been continued within a cylindrical constant volume, temperature and pressure controlled cell, analyzing several highly oxygenated fuels belonging to the poly(oxyethylene)dimethylethers family. The fuels were: Dimethoxymethane (DMM or OME1), OME2, a mixture of OME2, OME3 and OME4 and several blends of OME2 in commercial diesel. The effect of increasing oxygen content on combustion and soot formation as well as oxidation processes has been studied for different temperatures at start of combustion. The activity has been conducted focusing on in-cell optical measurements in a first phase and exhaust emission analysis in a second phase. Results have been shown for different temperatures at start of combustion and demonstrate that:

- A massive reduction of the soot formation dominated phase when increasing the oxygenated fraction in the blend is achieved.
- 2D-2-colour-pyrometry images gave the possibility of determining a specific area of soot formation showing its reduction with increasing oxygen content in the blend.
- A strong dependency of in-chamber soot concentration on temperature at SOC is observed. In fact an increase in temperature determines enhanced soot formation (higher kL peaks at end of the soot formation dominated phase) and oxidation (increased slope of the soot oxidation dominated phase) processes. Instead lower temperatures lead to an increasing premixed combustion fraction with a consequent reduction of soot formation.
- In-chamber flame luminosities of pure oxygenated fuels are extremely diminished in comparison with diesel fuel probably because of no contribution from soot radiation. Moreover a comparison between the integral of luminosity at 309 nm (OH intensity) and the rate of heat release over different temperatures at SOC showed that the correlation between start of OH signal and RoHR is dependent on temperatures @ SOC and premixed combustion fraction. This means that moving towards a premixed combustion mode, temperatures are too low to provide, in the earliest phase, a visible OH signal which is no longer directly correlated to the RoHR signal, as it instead at high temperatures @ SOC.
- Pure oxygenated fuels are characterized by a nearly smokeless combustion and an increase of O₂ content in blends is associated to a not linear soot reduction. In fact an addition of just 5% of oxygenated fuel within commercial diesel permits a reduction in soot emissions of about 30%.
- Further soot reduction could be achieved if operating towards a premixed dominated combustion mode.

- Particulate matter in oxygenated fuels is characterized by far smaller dimensions with respect to those from commercial diesel combustion probably because of an oxidation effect on nucleation cores.

With particular reference to the OME2/3/4 mixture, characterized by an oxygen content of 46.8%wt, the achieved soot reduction, with respect to commercial diesel, has been more than 95%. Since this fuel is characterized by similar physical properties to diesel thus not requiring substantial modifications to the engine infrastructure, it could be produced on industrial scale to be blended with conventional diesel. In this way the blend could take the advantages of both fuels: diesel high energy content and POMDME strong capability of reducing soot formation. Therefore, being blends of POMDME in diesel of particular interest for the market, a 5% and a 10% POMDME in diesel have been selected for a further investigation conducted on a single cylinder “heavy duty” direct injection diesel engine. The experimental work aimed to examine achievable engine performance and exhaust emissions taking into account not only particulate matter but nitrogen oxides, unburned hydrocarbons, carbon monoxide and carbon dioxide as well. The main conclusions that can be drawn from the analysis of the experimental activity are listed in the following:

- A reduction in soot emissions up to 34% has been detected with the 10% POMDME in diesel blend, investigating operating conditions with similar premixed – diffusive combustion mode ratios.
- NO_x emissions have not been significantly affected by the adoption of blends containing a percentage of oxygenated fuel up to 10%.
- No significant decay in combustion efficiency has been detected operating the engine with the 5% POMDME and 10% POMDME blends. This result is confirmed by similar values, detected for the different investigated fuels, both in unburned hydrocarbons, carbon monoxide and carbon dioxide.
- An increase in BSFC has been detected for any investigated fuel when retarding the start of injection from -12 to -6 cad atdc and with increased EGR rates because of a lower efficiency. In addition, with respect to the comparison commercial diesel – investigated blends, a 2.2% and a 4% increase in BSFC has been detected with 5% POMDME and 10% POMDME respectively. Therefore fuel economy could be the main reason for considering, in a hypothetical industrial scale production, 10% as a maximum percentage of POMDME to be blended in commercial diesel.

Outlook

The experimental activity discussed in the present dissertation aimed to bring a further scientific contribution to the knowledge on oxygenated fuels properties and their ability of reducing mainly soot emissions in diesel engine combustion. Different fuels have been investigated and their impact on exhaust emissions evaluated. Even though the presence of molecular oxygen seems to be indisputably favorable for soot reduction at the exhaust of diesel engine, it is absolutely not trivial to determine which fuels and in which percentages could be blended in commercial diesel in order to obtain the maximum benefit in soot emissions without an unacceptable increase mainly in fuel consumption. In addition, the adoption of fuels with similar physical and chemical properties with respect to commercial diesel allows their use in existing engines without modifications in the injection system. Of course fuel economy plays a major role in considering alternative fuels production on industrial scale and therefore, even though they appear to be interesting for environment protection, further investigation should be carried on in order to determine, in the whole range of the engine operative conditions, whether the use of such fuels could be concretely proposed on the market.

Appendix A

Nomenclature

Symbol	Description
<i>A/F</i>	Air to fuel ratio
<i>BaSO₄</i>	Barium sulfate
<i>BMEP</i>	Brake mean effective pressure
<i>BSFC</i>	Break specific fuel consumption
<i>C</i>	Carbon
<i>CA50</i>	Crank angle at which 50% of injected fuel is burnt
<i>CCD</i>	Charged coupled device
<i>C₂H₅OH</i>	Ethanol
<i>C₃H₇OH</i>	Propanol
<i>C₄H₉OH</i>	Butanol
<i>CH₃OH</i>	Methanol
<i>CH₄N₂O</i>	Urea
<i>CN</i>	Cetane number
<i>C-N</i>	Cyanide radicals
<i>CO</i>	Carbon oxide
<i>CRT</i>	Continuously regenerating trap
<i>DEF</i>	Diesel exhaust fluid
<i>DI</i>	Direct injection
<i>DME</i>	Dimethyl ether
<i>DMM or OME1</i>	Dimethoxymethane
<i>DOC</i>	Diesel oxidation catalyst
<i>DPF</i>	Diesel particulate filter
<i>DPNR</i>	Diesel particulate-NO _x reduction system
<i>ECU</i>	Electronic control unit
<i>EGR</i>	Exhaust gas recirculation
<i>FAME</i>	Fatty-acid methyl ester
<i>FAP</i>	Peugeot-Citroen particulate filter system
<i>FSN</i>	Filter smoke number
<i>FWHM</i>	Full width at half maximum
<i>H</i>	Hydrogen
<i>HCCI</i>	Homogeneous charge compression ignition
<i>HCN</i>	Hydrocyanic acid
<i>H₂O</i>	Water
<i>IMEP</i>	Indicated mean effective pressure
<i>INCA</i>	Integrated Calibration and Measurement System
<i>LNT</i>	Lean NO _x trap
<i>LTC</i>	Low temperature combustion

Symbol	Description
<i>N</i>	Nitrogen
<i>NDIR</i>	Non-Dispersive Infra-Red
<i>NDUV</i>	Non Dispersive Ultra Violet
<i>NEDC</i>	New European driving cycle
<i>NH₃</i>	Ammonia
<i>NMHC</i>	Non-methanic hydrocarbons
<i>NO</i>	Nitrogen monoxide
<i>NO₂</i>	Nitrogen dioxide
<i>NO_x</i>	Nitrogen oxides
<i>O₂</i>	Oxygen
<i>OLP</i>	Optical light probe
<i>OME</i>	Oxymethilethers
<i>PAH</i>	Polycyclic aromatic hydrocarbons
<i>PCCI</i>	Premixed charge compression ignition
<i>PEMS</i>	Portable emission measurement systems
<i>PM</i>	Particulate matter
<i>POMDME</i>	Poly(oxymethylene)dimethilethers
<i>5% POMDME</i>	5% Poly(oxymethylene)dimethilethers in diesel blend
<i>10% POMDME</i>	10% Poly(oxymethylene)dimethilethers in diesel blend
<i>RDE</i>	Real-driving emissions
<i>RME</i>	Rapeseed methyl ether
<i>RME50</i>	Blend of 50% in volume of rapeseed oils in diesel
<i>RoHR</i>	Rate of heat release
<i>SCR</i>	Selective catalyst reduction
<i>SME50</i>	Blend of 50% in volume of soybean oils in diesel
<i>SOC</i>	Start of combustion
<i>SOI</i>	Start of injection
<i>SOF</i>	Soluble organic fraction
<i>T_{BB}</i>	Black body temperature
<i>TDC</i>	Top dead center
<i>TE</i>	Thermal efficiency
<i>TWC</i>	Three-way catalysts
<i>ULSD</i>	Ultra-low sulfur diesel
<i>VVT</i>	Variable valve timing
<i>2D2CP</i>	Two dimensional two colour pyrometry
ε	Emissivity
λ	Relative air/fuel ratio
ϕ	Equivalence ratio
τ	Transmissivity

List of Tables

I.I	European Union emission standards for passenger car	3
I.II	Main properties of biodiesel from sunflower and cottonseed with respect to conventional diesel	28
I.III	Different molecular structures of the four butanol isomers diesel	30
I.IV	Main alcohol fuels properties with respect to conventional diesel ones diesel.....	30
I.V	Physical properties of conventional diesel (CDF), DME, DMM and POMDMEs diesel....	32
II.I	Accuracy of the acquired quantities	38
II.II	Main properties of the different fuels	39
II.III	Operating conditions	40
II.IV	Main properties of the different fuels	42
II.V	MTU – 396 single cylinder engine specifications.....	53
II.VI	Operating conditions	58

List of Figures

1.1	Diesel penetration in the EU15+EFTA as percentage of registered new cars	1
1.2	New passenger cars share in the EU over the years 2011-2014.....	2
1.3	New passenger cars (in million units) in the EU by emission classes	4
1.4	Soot formation process from gas phase to solid agglomerated particles	8
1.5	ϕ - T map for diesel combustion	10
1.6	NO _x – Soot trade-off in conventional diesel combustion.....	12
1.7	Sketch of the different injections	13
1.8	ϕ - T diagram with contours of different combustion mechanisms	15
1.9	Scheme of a complete diesel after treatment system.....	18
1.10	Catalytic Conversion of Carbon Monoxide and Hydrocarbons	19
1.11	Scheme of a Continuously Regenerating Trap.....	21
1.12	Selective Catalyst Reduction system.....	23
1.13	Diesel Particulate – NOX Reduction system	25
1.14	Raw oil or fats to Biodiesel process	26
1.15	Chemical process for methyl ester biodiesel.....	26
1.16	POMDME process chain.....	33
2.1	Automotive four cylinder diesel engine test bench.....	36
2.2	Sketch of experimental engine set-up	37
2.3	Experimental apparatus (cell, optical set-up and particle spectrometer)	41
2.4	In cell pressure and energizing signal to the injector	43

2.5	Optical set-up for 2D2CP and OH chemiluminescence.....	45
2.6	Black body radiation	46
2.7	Schematic overview of the 3 – colour – pyrometry method	50
2.8	Auto – calibration procedure for temperature and kL value	51
2.9	MTU-396 Single Cylinder Diesel Engine.....	52
2.10	Scheme of the engine plus external injection systems	54
2.11	MTU-396 Single Cylinder Diesel Engine with external injection system.....	55
2.12	Pneumatic valves, flow meter and the two three way electro-valves on the injector	56
3.1	Instantaneous rate of heat release traces for the investigated fuels at O ₂ int=19%_CA50=18	60
3.2	Instantaneous rate of heat release traces for the investigated fuels at O ₂ int=19%_CA50=21	60
3.3	Instantaneous rate of heat release traces for the investigated fuels at O ₂ int=17%_CA50=18	61
3.4	Instantaneous rate of heat release traces for the investigated fuels at O ₂ int=17%_CA50=21	61
3.5	Smoke emissions from the different investigated fuels	62
3.6	Ignition delay vs fuel blends and CN for the different test conditions	63
3.7	NO _x emissions from the different investigated fuels.....	65
3.8	Combustion temperatures for the investigated fuels at O ₂ int=17%_CA50=21.....	65
3.9	NO _x Smoke trade-off for the different fuels	66
3.10	BSFC from the different fuels.....	67
3.11	Thermal efficiency from the different fuels	68
3.12	Combustion noise from the different fuels.....	69

3.13	Combustion noise vs CAD ATDC with $dP/d\Theta_{max}$	69
3.14	RoHR and energizing signal to the piezo injector (start at time 0) for OME2-50%, OME2-30% and OME2-5% at 1150K@SOC	71
3.15	kL factor and energizing signal to piezo injector (start at time 0) for OME2-50%, OME2-30% and OME2-5% at 1150K@SOC	72
3.16	RoHR and energizing signal to piezo injector (start at time 0 for OME2-50%, OME2-30% and OME2-5% at 960K@SOC	73
3.17	kL factor and energizing signal to piezo injector (start at time 0) for OME2-50%, OME2-30% and OME2-5% at 960K@SOC	73
3.18	RoHR and energizing signal to piezo injector (start at time 0) for OME2-50%, OME2-30% and OME2-5% at 830K@SOC	74
3.19	kL factor and energizing signal to piezo injector (start at time 0) for OME2-50%, OME2-30% and OME2-5% at 830K@SOC	74
3.20	Overlapping of fuel jet for OME2-5% (contoured in red) and OME2-50% (contoured in blue) at 1150K@SOC and 1.4, 2.2 and 3.5 ms after SOI	76
3.21	Overlapping of fuel jet for OME2-5% (contoured in red) and OME2-50% (contoured in blue) at 1010K@SOC and 1.4, 2.2 and 3.5 ms after SOI	76
3.22	Luminosity at 309 ± 5 nm – 1150K@SOC	77
3.23	Luminosity at 309 ± 5 nm – 960K@SOC	78
3.24	Luminosity at 309 ± 5 nm – 830K@SOC	78
3.25	OH chemiluminescence 1150K and 1010K @ SOC for pure OME2	79
3.26	OH chemiluminescence 930K and 830K @ SOC for pure OME2	80
3.27	Normalized Soot Mass for the investigated fuels at 1010K @ SOC	81
3.28	Normalized Soot Mass: OME2/3/4, OME2 pure and OME2 in diesel blends at different temperatures @ SOC	82
3.29	OME2-5% and OME2 pure at 1150K @ SOC: particle concentration	83

3.30	Diesel, 5% POMDME and 10% POMDME - Smoke emissions @ BMEP=8bar	84
3.31	Diesel, 5% POMDME and 10% POMDME - NO _x emissions @ BMEP=8bar	85
3.32	Diesel, 5% POMDME and 10% POMDME - Smoke NO _x trade off @ BMEP=8bar	86
3.33	Diesel, 5% POMDME and 10% POMDME – Rate of heat release curves @BMEP=8bar, intake O ₂ =18% and SOI=-12 cad atdc	86
3.34	Diesel, 5% POMDME and 10% POMDME - HC emissions @ BMEP=8bar	87
3.35	Diesel, 5% POMDME and 10% POMDME - CO emissions @ BMEP=8bar	88
3.36	Diesel, 5% POMDME and 10% POMDME - BSFC @ BMEP=8bar	88
3.37	Diesel, 5% POMDME and 10% POMDME - CO ₂ emissions @ BMEP=8bar	89
3.38	Diesel, 5% POMDME and 10% POMDME - Exhaust O ₂ @ BMEP=8bar.....	90
3.39	Diesel, 5% POMDME and 10% POMDME - Smoke emissions @ BMEP=10.5bar.....	91
3.40	Diesel, 5% POMDME and 10% POMDME - NO _x emissions @ BMEP=10.5bar	91
3.41	Diesel, 5% POMDME and 10% POMDME - Smoke NO _x trade-off @BMEP=10.5bar.....	92
3.42	Diesel, 5% POMDME and 10% POMDME - BSFC @ BMEP=10.5bar.....	93
3.43	Diesel, 5% POMDME and 10% POMDME - CO ₂ emissions @ BMEP=10.5bar	93

Bibliography

- [1] ACEA Communications Department, "European Automobile Manufacturers Association: The automobile industry pocket guide 2014 and 2015-2016." 2015.
- [2] "https://www.ccohs.ca/oshanswers/chemicals/how_do.html." Accessed September 2015.
- [3] B. Giechaskiel, A. Mamakos, J. Andersson, P. Dilara, G. Martini, W. Schindler, and A. Bergmann, "Measurement of Automotive Nonvolatile Particle Number Emissions within the European Legislative Framework: A Review," *Aerosol Sci. Technol.*, Feb. 2012.
- [4] "<http://www.dieselnet.com>." Accessed September 2015.
- [5] B. Onursal and S. Gautam, *Vehicular air pollution: experiences from seven Latin American urban centers*, vol. 373. World Bank Publications, 1997.
- [6] R. C. Yu, V. W. Wong, and S. M. Shahed, "Sources of Hydrocarbon Emissions from Direct Injection Diesel Engines," 1980.
- [7] C. P. Koci, Y. Ra, R. Krieger, M. Andrie, D. E. Foster, R. M. Siewert, R. P. Durrett, I. Ekoto, and P. C. Miles, "Detailed Unburned Hydrocarbon Investigations in a Highly-Dilute Diesel Low Temperature Combustion Regime," *SAE Int. J. Engines*, vol. 2, no. 1, pp. 858–879, 2009.
- [8] R. J. Last, M. Krüger, and M. Dürnholz, "Emissions and Performance Characteristics of a 4-Stroke, Direct Injected Diesel Engine Fueled with Blends of Biodiesel and Low Sulfur Diesel Fuel," 1995.
- [9] J. B. Heywood, *Internal Combustion Engine Fundamentals*. 1988.
- [10] S. Caruso, "Diesel Injection Analysis for New Premium Fuel Research and Emission Reduction." 29-Nov-2010.
- [11] M. Piacentini, "Fundamental aspects of NO_x storage-reduction catalysts for automotive lean combustion engines." ETH, 2006.
- [12] Peter Mockl, Uwe Tietge, Vicente Franco, John German, Anup Bandivadekar, Norbert Ligterink, Udo Lambrecht, Jörg Kühlwein, and Iddo Riemersma, "From laboratory to road: A 2014 update | International Council on Clean Transportation," no. September, 2014.

- [13] L. Yang, V. Franco, A. Campestrini, J. German, and P. Mock, "NO_x control technologies for Euro 6 Diesel passenger cars Market penetration and experimental performance assessment," no. X, 2015.
- [14] "<http://yosemite.epa.gov/opa/admpress.nsf/0/F51C2FDEDA736EA285257A1E0050C45F>". Accessed January 2016.
- [15] M. Lapuerta, R. Ballesteros, and J. Rodríguez-Fernández, "Thermogravimetric analysis of diesel particulate matter," *Meas. Sci. Technol.*, vol. 18, no. 3, pp. 650–658, Mar. 2007.
- [16] H. Bockhorn, *Soot formation in combustion: mechanisms and models*. 2013.
- [17] D. R. Tree and K. I. Svensson, "Soot processes in compression ignition engines," *Prog. Energy Combust. Sci.*, vol. 33, no. 3, pp. 272–309, Jun. 2007.
- [18] W. Bartok and A. F. Sarofim, "Fossil fuel combustion: A source book," Dec. 1991.
- [19] I. Glassman, *Combustion*. San Diego: Academic Press, 1996.
- [20] K. Akihama, Y. Takatori, K. Inagaki, S. Sasaki, and A. M. Dean, "Mechanism of the Smokeless Rich Diesel Combustion by Reducing Temperature," 2001.
- [21] S. L. Plee, T. Ahmad, J. P. Myers, and G. M. Faeth, "Diesel NO_x emissions—A simple correlation technique for intake air effects," *Symp. Combust.*, vol. 19, no. 1, pp. 1495–1502, Jan. 1982.
- [22] H. Semerjian and A. Vranos, "NO_x formation in premixed turbulent flames," *Symp. Combust.*, vol. 16, no. 1, pp. 169–179, Jan. 1977.
- [23] "Non-Sooting, Low Flame Temperature Mixing-Controlled DI Diesel Combustion (2004-01-1399 Technical Paper)- SAE Digital Library." [Online]. Available: <http://digitallibrary.sae.org/content/2004-01-1399>. Accessed October 2015.
- [24] A. Bertola, "Technologies for Lowest NO_x and Particulate Emissions in DI-Diesel Engine Combustion - Influence of Injection Parameters , EGR and Fuel Composition," no. 15373, 2003.
- [25] N. Ladommatos, S. M. Abdelhalim, H. Zhao, and Z. Hu, "The Dilution , Chemical and Thermal Effects of Exhaust Gas Recirculation on Diesel Engine Emissions - Part 2 : Effects of Carbon Dioxide," *SAE Int.*, no. 412, 1996.
- [26] N. Ladommatos, S. M. Abdelhalim, H. Zhao, and Z. Hu, "The Dilution , Chemical

- , and Thermal Effects of Exhaust Gas Recirculation on Diesel Engine Emissions - Part 4 : Effects of Carbon Dioxide and Water Vapour," no. 412, 1997.
- [27] S. M. Abdelhalim, N. Ladommatos, H. Zhao, and Z. Hu, "The Dilution , Chemical , and Thermal Effects of Exhaust Gas Recirculation on Diesel Engine Emissions - Part 4 : Effects of Carbon Dioxide and Water Vapour," no. 412, 1997.
- [28] P. Kyrtatos, "the Effects of Prolonged Ignition Delay Due To Charge Air Temperature Reduction on," no. 21064, 2013.
- [29] R. Miller and H. Lieberherr, "The Miller supercharging system for diesel and gas engines operating characteristics," *Congr. Combust. Engine Conf. CIMAC*, 1957.
- [30] E. Codan and C. Mathey, "Emissions– A New Challenge for Turbochargers," *CIMAC Congr. Vienna, Pap.*, 2007.
- [31] J. Kim and D. K. Lieu, "A new electromagnetic engine valve actuator with less energy consumption for variable valve timing," *J. Mech. Sci. Technol.*, vol. 21, no. 4, pp. 602–606, Apr. 2007.
- [32] C. S. D. Katey E. Lenox, R. M. Wagner, J. B. Green Jr., J. M. Storey, "Extending Exhaust Gas Recirculation Limits in Diesel Engines," in *A&WMA 93rd Annual Conference and Exposition*, 2000.
- [33] S. Mendez and B. Thirouard, "Using Multiple Injection Strategies in Diesel Combustion: Potential to Improve Emissions, Noise and Fuel Economy Trade-Off in Low CR Engines," *SAE Int. J. Fuels Lubr.*, vol. 1, no. 1, pp. 662–674, 2008.
- [34] M. Russell, "The dependence of diesel combustion on injection rate," *SAE Pap. 984005*, 1998.
- [35] R. Ehleskog, R. L. Ochoterena, and S. Andersson, "Effects of Multiple Injections on Engine-Out Emission Levels Including Particulate Mass from an HSDI Diesel Engine," *SAE Pap. 2010-01-0612*, vol. 2007, no. 724, pp. 2007–01–0910, 2007.
- [36] M. Badami, F. Mallamo, F. Millo, and E. E. Rossi, "Experimental investigation on the effect of multiple injection strategies on emissions, noise and brake specific fuel consumption of an automotive direct injection common-rail diesel engine," *Int. J. Engine Res.*, vol. 4, no. 4, pp. 299–314, Jan. 2003.
- [37] J. Arrègle, J. V. Pastor, J. J. López, and A. García, "Insights on postinjection-associated soot emissions in direct injection diesel engines," *Combust. Flame*, vol. 154, no. 3, pp. 448–461, Aug. 2008.

- [38] M. Bobba, M. Musculus, and W. Neel, "Effect of Post Injections on In-Cylinder and Exhaust Soot for Low-Temperature Combustion in a Heavy-Duty Diesel Engine," *SAE Int. J. Engines*, vol. 3, no. 1, pp. 496–516, Apr. 2010.
- [39] B. Song and Y. Choi, "Investigation of variations of lubricating oil diluted by post-injected fuel for the regeneration of CDPF and its effects on engine wear t," vol. 22, pp. 2526–2533, 2008.
- [40] E. Alano, E., Amon, B., and Jean, "Fuel Vaporizer: Alternative Solution for DPF Regeneration," *2010-01-0561 SAE Tech. Pap.*, 2010.
- [41] A. Hein, E., Kotrba, A., Inclan, T., and Bright, "Secondary Fuel Injection Characterization of a Diesel Vaporizer for Active DPF Regeneration," *2014-01-1494 SAE Tech. Pap.*, 2014.
- [42] S. Kook, C. Bae, P. C. Miles, D. Choi, and L. M. Pickett, "The Influence of Charge Dilution and Injection Timing on Low-Temperature Diesel Combustion and Emissions," 2005.
- [43] R. Opat and Y. Ra, "Investigation of Mixing and Temperature Effects on HC/CO Emissions for Highly Dilute Low Temperature Combustion in a Light Duty Diesel Engine," *Sae Tech. Pap. Ser.*, vol. 2007, no. 724, pp. 776–0790, 2007.
- [44] A. W. (Bill) Gray and T. W. Ryan, "Homogeneous Charge Compression Ignition (HCCI) of Diesel Fuel," 1997.
- [45] P. M. Najt and D. E. Foster, "Compression-Ignited Homogeneous Charge Combustion," Feb. 1983.
- [46] M. Christensen and B. Johansson, "Supercharged Homogeneous Charge Compression Ignition (HCCI) with Exhaust Gas Recirculation and Pilot Fuel," 2000.
- [47] K. Nakagome, N. Shimazaki, K. Niimura, and S. Kobayashi, "Combustion and Emission Characteristics of Premixed Lean Diesel Combustion Engine," 1997.
- [48] R. H. Stanglmaier and C. E. Roberts, "Homogeneous Charge Compression Ignition (HCCI): Benefits, Compromises, and Future Engine Applications," 1999.
- [49] K. et al. Cracknell, R., Rickeard, D., Ariztegui, J., Rose, "Advanced Combustion for Low Emissions and High Efficiency Part 2: Impact of Fuel Properties on HCCI Combustion," *SAE Technical Paper 2008-01-2404*, 2008.
- [50] G. T. Kalghatgi, "Auto-Ignition Quality of Practical Fuels and Implications for Fuel Requirements of Future SI and HCCI Engines," 2005.

- [51] P. Duret, "Gasoline CAI and Diesel HCCI : the Way towards Zero Emission with Major Engine and Fuel Technology Challenges NEW GENERATION OF ENGINE COMBUSTION," *Fuel Cell*, vol. 20024280, pp. 1–11, 2002.
- [52] A. Helmantel, "HCCI operation of a passenger car common rail DI diesel engine with early injection of conventional diesel fuel," *Congr. 2004, SAE Pap. 2004-01-*, vol. 2004, no. 724, 2004.
- [53] A. Piperel, X. Montagne, and P. Dagaut, "SAE TECHNICAL HCCI Engine Combustion Control using EGR : Gas Composition Evolution and Consequences on Combustion Processes," 2007.
- [54] M. . Hillion, J. . Chauvin, O. . Grondin, and N. . Petit, "Active combustion control of diesel HCCI engine: Combustion timing," *SAE Tech. Pap.*, vol. 2008, no. 724, 2008.
- [55] E. Mancaruso, S. S. Merola, and B. M. Vaglieco, "Extinction and Chemiluminescence Measurements in CR DI Diesel Engine Operating in HCCI Mode," vol. 2007, no. 724, pp. 776–790, 2007.
- [56] M. Kang, J., Chang, C., Chen, J., and Chang, "Concept and Implementation of a Robust HCCI Engine Controller," *SAE Tech. Pap. 2009-01-1131*.
- [57] S. Juttu, S. S. Thipse, N. V. Marathe, and M. K. G. Babu, "Homogeneous Charge Compression Ignition (HCCI): A New Concept for Near Zero NO_x and Particulate Matter (PM) from Diesel Engine Combustion," 2007.
- [58] M. Lewander, K. Ekholm, B. Johansson, P. Tunestål, N. Milovanovic, N. Keeler, T. Harcombe, and P. Bergstrand, "Investigation of the Combustion Characteristics with Focus on Partially Premixed Combustion in a Heavy Duty Engine," *SAE Int. J. Fuels Lubr.*, vol. 1, no. 1, pp. 1063–1074, 2008.
- [59] C. M. Lewander, B. Johansson, and P. Tunestal, "Extending the Operating Region of Multi-Cylinder Partially Premixed Combustion using High Octane Number Fuel," 2011.
- [60] S. Kimura, O. Aoki, Y. Kitahara, and E. Aiyoshizawa, "Ultra-Clean Combustion Technology Combining a Low-Temperature and Premixed Combustion Concept for Meeting Future Emission Standards," 2001.
- [61] N. Weall, A. and Collings, "Investigation into Partially Premixed Combustion in a Light-Duty Multi-Cylinder Diesel Engine Fuelled with a Mixture of Gasoline and Diesel," *SAE Tech. Pap. 2007-01-4058*, 2007.

- [62] H. Yun, M. Sellnau, N. Milavanovic, and S. Zuelch, "Development of Premixed Low-Temperature Diesel Combustion in a HSDI Diesel Engine," *2008 SAE World Congr.*, vol. 2008, no. SP-2168, pp. 776–790, 2008.
- [63] V. Manente, P. Tunestal, B. Johansson, and W. J. Cannella, "Effects of Ethanol and Different Type of Gasoline Fuels on Partially Premixed Combustion from Low to High Load," 2010.
- [64] V. Manente, B. Johansson, and P. Tunestal, "Partially Premixed Combustion at High Load using Gasoline and Ethanol, a Comparison with Diesel," 2009.
- [65] N. Shimazaki, T. Tsurushima, T. Nishimura, and N. T., "Dual Mode Combustion Concept With Premixed Diesel Combustion by Direct Injection Near Top Dead Center," *SAE Int.*, vol. 2003–01–07, 2003.
- [66] G. Kalghatgi, L. Hildingsson, A. Harrison, and B. Johansson, "Low- NO_x, low-smoke operation of a diesel engine using 'premixed enough' compression ignition – Effects of fuel autoignition quality, volatility and aromatic content," in *THIESEL 2010, Thermo and fluid dynamic processes in diesel engines, Valencia*, 2010.
- [67] G. T. Kalghatgi, P. Risberg, and H.-E. Ångström, "Advantages of Fuels with High Resistance to Auto-ignition in Late-injection, Low-temperature, Compression Ignition Combustion," 2006.
- [68] V. Manente, C.-G. Zander, B. Johansson, P. Tunestal, and W. Cannella, "An Advanced Internal Combustion Engine Concept for Low Emissions and High Efficiency from Idle to Max Load Using Gasoline Partially Premixed Combustion," 2010.
- [69] D. Han, A. M. Ickes, S. V. Bohac, Z. Huang, and D. N. Assanis, "Premixed low-temperature combustion of blends of diesel and gasoline in a high speed compression ignition engine," *Proc. Combust. Inst.*, vol. 33, no. 2, pp. 3039–3046, Jan. 2011.
- [70] G. Valentino, F. Corcione, S. Iannuzzi, and S. Serra, "Effects of Premixed Low Temperature Combustion of Fuel Blends with High Resistance to Auto-ignition on Performances and Emissions in a High Speed Diesel Engine," *SAE Tech. Pap. 2011-24-0049*.
- [71] G. Valentino, F. E. Corcione, S. Iannuzzi, and U. Cagliari, "An Experimental Analysis on Diesel / n-Butanol Blends Operating in Partial Premixed Combustion in a Light Duty Diesel Engine," *Energy Fuels*, 2012.

- [72] F. Corcione, G. Valentino, C. Tornatore, S. Merola, and L. Marchitto, "Optical Investigation of Premixed Low-Temperature Combustion of Lighter Fuel Blends in Compression Ignition Engines," 2011.
- [73] G. Valentino, S. Iannuzzi, and F. E. Corcione, "Effects of Low Temperature Premixed Combustion (LTPC) on Emissions of a Modern Diesel Engine for Passenger Cars," 2010.
- [74] B. et al. Hildingsson, L., Kalghatgi, G., Tait, N., Johansson, "Fuel Octane Effects in the Partially Premixed Combustion Regime in Compression Ignition Engines," *SAE Technical Paper 2009-01-2648*, 2009.
- [75] D. CHOI, P. C. MILES, H. YUN, and R. D. REITZ, "A Parametric Study of Low-Temperature, Late-Injection Combustion in a HSDI Diesel Engine," *JSME Int. J. Ser. B*, vol. 48, no. 4, pp. 656–664, May 2005.
- [76] S. L. Kokjohn, R. M. Hanson, D. A. Splitter, and R. D. Reitz, "Experiments and Modeling of Dual-Fuel HCCI and PCCI Combustion Using In-Cylinder Fuel Blending," *SAE Int. J. Engines*, vol. 2, no. 2, pp. 24–39, Nov. 2009.
- [77] "<http://www.nettinc.com/information/emissions-faq/what-is-a-diesel-oxidation-catalyst>". Accessed November 2015.
- [78] "<http://emissiontecheurope.nl/producten-roetfiltersystemen/johnson-matthey/passieve-systemen/>". Accessed January 2016.
- [79] "https://www.dieselnet.com/tech/cat_NOx-trap.php#chem". Accessed November 2015.
- [80] "<http://www.dieselforum.org/about-clean-diesel/what-is-scr>" Accessed November 2015.
- [81] T. Maunula, "NOX Reduction with the Combinations on LNT and SCR in Diesel Applications," (No. 2013-24-0161). *SAE Tech. Pap.*, no. x, pp. 195–206, 2013.
- [82] "http://energy.gov/sites/prod/files/2014/03/f8/deer07_shoji.pdf". Accessed January 2016.
- [83] H. Fukuda, a Kondo, and H. Noda, "Biodiesel fuel production by transesterification of oils," *J. Biosci. Bioeng.*, vol. 92, no. 5, pp. 405–16, 2001.
- [84] "http://www.hielscher.com/biodiesel_processing_efficiency.htm". Accessed January 2016.
- [85] "<http://www.biodiesel.com/biodiesel/benefits/>". Accessed January 2016.

- [86] C. D. Rakopoulos, A. M. Dimaratos, E. G. Giakoumis, and D. C. Rakopoulos, "Investigating the emissions during acceleration of a turbocharged diesel engine operating with bio-diesel or n-butanol diesel fuel blends," *Energy*, vol. 35, no. 12, pp. 5173–5184, Dec. 2010.
- [87] C. Choi, G. Bower, and R. Reitz, "Effects of Biodiesel Blended Fuels and Multiple Injections on D. I. Diesel Engines (970218 Technical Paper)- SAE Digital Library," *SAE Pap. 970218*, 1997.
- [88] M. Cardone, M. Mazzoncini, S. Menini, V. Rocco, A. Senatore, M. Seggiani, and S. Vitolo, "Brassica carinata as an alternative oil crop for the production of biodiesel in Italy: agronomic evaluation, fuel production by transesterification and characterization," *Biomass and Bioenergy*, vol. 25, no. 6, pp. 623–636, Dec. 2003.
- [89] G. Valentino, L. Allocca, S. Iannuzzi, and A. Montanaro, "Biodiesel/mineral diesel fuel mixtures: Spray evolution and engine performance and emissions characterization," *Energy*, vol. 36, no. 6, pp. 3924–3932, Jun. 2011.
- [90] D. Kawano, H. Ishii, and Y. Goto, "Effect of Biodiesel Blending on Emission Characteristics of Modern Diesel Engine," *SAE Tech. Pap.*, no. 2008–01–2384, 2008.
- [91] D. Kawano, N. Mizushima, H. Ishii, Y. Goto, and K. Iwasa, "Exhaust Emission Characteristics of Commercial Vehicles Fuelled with Biodiesel," *SAE Tech. Pap.*, 2010.
- [92] S. Szwaja and J. D. Naber, "Combustion of n-butanol in a spark-ignition IC engine," *Fuel*, vol. 89, no. 7, pp. 1573–1582, 2010.
- [93] M. Yao, H. Wang, Z. Zheng, and Y. Yue, "Experimental study of n-butanol additive and multi-injection on HD diesel engine performance and emissions," *Fuel*, vol. 89, no. 9, pp. 2191–2201, Sep. 2010.
- [94] D. C. Rakopoulos, C. D. Rakopoulos, E. G. Giakoumis, A. M. Dimaratos, and D. C. Kyritsis, "Effects of butanol–diesel fuel blends on the performance and emissions of a high-speed DI diesel engine," *Energy Convers. Manag.*, vol. 51, no. 10, pp. 1989–1997, Oct. 2010.
- [95] D. C. Rakopoulos, C. D. Rakopoulos, D. T. Hountalas, E. C. Kakaras, E. G. Giakoumis, and R. G. Papagiannakis, "Investigation of the performance and emissions of bus engine operating on butanol/diesel fuel blends," *Fuel*, vol. 89, no. 10, pp. 2781–2790, Oct. 2010.

- [96] O. Doğan, “The influence of n-butanol/diesel fuel blends utilization on a small diesel engine performance and emissions”, *Fuel*, vol. 90, no. 7, pp. 2467–2472, Jul. 2011.
- [97] A. S.-T. Cheng, “Effects of oxygenates blended with diesel fuel on particulate matter emissions from a compression-ignition engine (Doctoral dissertation, University of Berkeley)”, 2002.
- [98] S. C. Sorenson and S.-E. Mikkelsen, “Performance and Emissions of a 0.273 Liter Direct Injection Diesel Engine Fuelled with Neat Dimethyl Ether,” *SAE Technical Paper 950064*, 1995.
- [99] S. Kajitani, Z. Chen, M. Konno, and K. Rhee, “Engine Performance and Exhaust Characteristics of Direct-injection Diesel Engine Operated with DME (972973 Technical Paper)- SAE Digital Library,” *SAE Technical Paper 972973*, 1997. [Online].
- [100] M. Konno, S. Kajitani, M. Oguma, T. Iwase, and K. Shima, “NO Emission Characteristics of a CI Engine Fueled with Neat Dimethyl Ether,” *SAE Tech. Pap. 1999-03-01*, 1999.
- [101] T. Fleisch, C. McCarthy, A. Basu, C. Udovich, P. Charbonneau, W. Slodowske, S.-E. Mikkelsen, and J. McCandless, “A New Clean Diesel Technology: Demonstration of ULEV Emissions on a Navistar Diesel Engine Fueled with Dimethyl Ether,” *SAE Tech. Pap. 1995-02-01*, 1995.
- [102] G. Wong, B. L. Edgar, T. J. Landheim, L. P. Amlie, and R. W. Dibble, “‘Low Soot Emission from a Diesel Engine Fueled with Dimethyl and Diethyl Ether,’ WSS/CI Paper 95F-162, October”, 1995.
- [103] S. E. Mikkelsen, J. B. Hansen, and S. C. Sorenson, “Progress with Dimethyl Ether,” in *International Alternative Fuels Conference*, 1996.
- [104] J. Burger, M. Siegert, E. Ströfer, and H. Hasse, “Poly(oxymethylene) dimethyl ethers as components of tailored diesel fuel: Properties, synthesis and purification concepts,” *Fuel*, vol. 89, no. 11, pp. 3315–3319, Nov. 2010.
- [105] J. Burger and H. Hasse, “Multi-objective optimization using reduced models in conceptual design of a fuel additive production process,” *Chem. Eng. Sci.*, vol. 99, pp. 118–126, Aug. 2013.
- [106] J. Burger, E. Ströfer, and H. Hasse, “Production process for diesel fuel components poly(oxymethylene) dimethyl ethers from methane-based products by hierarchical optimization with varying model depth,” *Chem. Eng.*

Res. Des., vol. 91, no. 12, pp. 2648–2662, Dec. 2013.

- [107] J. Burger, E. Ströfer, and H. Hasse, “Chemical equilibrium and reaction kinetics of the heterogeneously catalyzed formation of poly(oxymethylene) dimethyl ethers from methylal and trioxane,” *Ind. Eng. Chem. Res.*, vol. 51, no. 39, pp. 12751–12761, 2012.
- [108] M. B. Sirman, E. C. Owens, and K. A. Whitney, “Emissions Comparison of Alternative Fuels in an Advanced Automotive Diesel Engine”, SAE International , 2000.
- [109] T. E. Kenney, T. P. Gardner, S. S. Low, J. C. Eckstrom, L. R. Wolf, S. J. Korn, and P. G. Szymkowicz, “Overall Results: Phase I Ad Hoc Diesel Fuel Test Program”, SAE International, 2001.
- [110] H. Ogawa, N. Nabi, M. Minami, N. Miyamoto, and K. Bong-Seock, “Ultra Low Emissions and High Performance Diesel Combustion with a Combination of High EGR, Three-Way Catalyst, and a Highly Oxygenated Fuel, Dimethoxy Methane (DMM)”, SAE International, 2000.
- [111] M. Härtl, P. Seidenspinner, E. Jacob, and G. Wachtmeister, “Oxygenate screening on a heavy-duty diesel engine and emission characteristics of highly oxygenated oxymethylene ether fuel OME1”, *Fuel*, vol. 153, pp. 328–335, Aug. 2015.
- [112] M. Marchionna and D. Sanlilippo, “Quality components”, *Hydrocarb. Eng.* 7.7, 2002.
- [113] L. Pellegrini, M. Marchionna, R. Patrini, C. Beatrice, N. Del Giacomo, and C. Guido, “Combustion Behaviour and Emission Performance of Neat and Blended Polyoxymethylene Dimethyl Ethers in a Light-Duty Diesel Engine”, SAE International, 2012.
- [114] L. Pellegrini, M. Marchionna, R. Patrini, and S. Florio, “Emission Performance of Neat and Blended Polyoxymethylene Dimethyl Ethers in an Old Light-Duty Diesel Car”, SAE International, 2013.
- [115] L. Pellegrini, R. Patrini, and M. Marchionna, “Effect of POMDME Blend on PAH Emissions and Particulate Size Distribution from an In-Use Light-Duty Diesel Engine”, SAE International, 2014.
- [116] B. Lumpp, D. Rothe, C. Pastötter, R. Lämmermann, and E. Jacob, “OXYMETHYLENE ETHERS AS DIESEL FUEL ADDITIVES OF THE FUTURE”, *MTZ Worldw.*, vol. 72, no. 3, pp. 34–38, Feb. 2011.

- [117] C. Barro, P. Meyer, and K. Boulouchos, "Optical Investigations of Soot Reduction Mechanisms using Post-Injections in a Cylindrical Constant Volume Chamber (CCVC)", vol. C, no. Ccvc, 2015.
- [118] R. H. Boyd, "Some physical properties of polyoxymethylene dimethyl ethers", *J. Polym. Sci.*, vol. 50, no. 153, pp. 133–141, 1961.
- [119] T. H. Fleisch and R. A. Sills, "Large-scale gas conversion through oxygenates: beyond GTL-FT", *Stud. Surf. Sci. Catal.*, vol. 147, pp. 31–36, 2004.
- [120] L. P. Lautenschütz, "Neue Erkenntnisse in der Syntheseoptimierung oligomerer Oxymethyldimethylether aus Dimethoxymethan und Trioxan", 2015.
- [121] R. Schubiger, "Untersuchung zur Russbildung und -oxidation in der dieselmotorischen Verbrennung: Thermodynamische Kenngrößen, Verbrennungsanalyse und Mehrfarbenendoskopie", no. 14445, 2001.
- [122] S. Kunte, A. Bertola, P. Obrecht, and K. Boulouchos, "No Time Temporal soot evolution and diesel engine combustion: Influence of fuel composition, injection parameters, and exhaust gas recirculation", *International Journal of Engine Research*, vol. 7, pp. 459–470, 2006.
- [123] C. Barro, "Development and Validation of a Virtual Soot Sensor Christophe Barro 2012", *Dissertation ETH No. 20788*, 2012.
- [124] "<http://motls.blogspot.ch/2010/04/on-importance-of-black-bodies.html>" Accessed January 2016.
- [125] H. C. Hottel and F. P. Broughton, "Determination of True Temperature and Total Radiation from Luminous Gas Flames," *Ind. Eng. Chem. Anal. Ed.*, vol. 4, no. 2, pp. 166–175, Apr. 1932.
- [126] T. Kamimoto and Y. Murayama, "Re-examination of the emissivity of diesel flames", *Int. J. Engine Res.*, vol. 12, no. 6, pp. 580–600, 2011.
- [127] S. Kunte, A. Bertola, and K. Boulouchos, "Potenzial moderner Verbrennungsmotoren zur Partikelminderung", in *Proceedings of the HdT-Seminar*, 2005.
- [128] C. Barro, P. Vogelín, P. Wilhelm, P. Obrecht, and K. Boulouchos, "Comparison of soot measurement instruments during transient and steady state operation", in *14th ETH conference on combustion generated nanoparticles*, 2010.
- [129] P. Kirchen, P. Obrecht, K. Boulouchos, and A. Bertola, "Exhaust-Stream and In-

Cylinder Measurements and Analysis of the Soot Emissions From a Common Rail Diesel Engine Using Two Fuels”, *J. Eng. Gas Turbines Power*, vol. 132, no. 11, p. 112804, 2010.

- [130] L. Zhu, W. Zhang, W. Liu, and Z. Huang, “Experimental study on particulate and NO_x emissions of a diesel engine fueled with ultra low sulfur diesel, RME-diesel blends and PME-diesel blends”, *Sci. Total Environ.*, vol. 408, no. 5, pp. 1050–1058, 2010.
- [131] D. H. Qi, L. M. Geng, H. Chen, Y. Z. H. Bian, J. Liu, and X. C. H. Ren, “Combustion and performance evaluation of a diesel engine fueled with biodiesel produced from soybean crude oil”, *Renew. Energy*, vol. 34, no. 12, pp. 2706–2713, 2009.
- [132] J. T. Song and C. H. Zhang, “An experimental study on the performance and exhaust emissions of a diesel engine fuelled with soybean oil methyl ester”, *Proc. Inst. Mech. Eng. Part D J. Automob. Eng.*, vol. 222, no. 12, pp. 2487–2496, 2008.
- [133] A. Tsolakis, A. Megaritis, M. L. Wyszynski, and K. Theinnoi, “Engine performance and emissions of a diesel engine operating on diesel-RME (rapeseed methyl ester) blends with EGR (exhaust gas recirculation)”, *Energy*, vol. 32, no. 11, pp. 2072–2080, 2007.
- [134] D. Agarwal, S. Sinha, and A. K. Agarwal, “Experimental investigation of control of NO_x emissions in biodiesel-fueled compression ignition engine”, *Renew. energy*, vol. 31, no. 14, pp. 2356–2369, 2006.
- [135] B. Delfort, I. Durand, A. Jaecker-Voirol, T. Lacôme, F. Paillé, and X. Montagne, “Oxygenated compounds and diesel engine pollutant emissions performances of new generation of products”, SAE Technical Paper, 2002.
- [136] D. B. Kittelson, “Engines and nanoparticles: a review”, *J. Aerosol Sci.*, vol. 29, no. 5, pp. 575–588, 1998.

Curriculum Vitae

Personal Data

Name	Stefano Emanuele Iannuzzi
Date of birth	August 12, 1981
Place of birth	Naples, Italy
Citizen of	Italy
Nationality	Italian
Address	Hofwiesenstrasse 239, 8057 Zürich, Switzerland

Education

November 2014 – April 2016	Doctoral student at the Aerothermochemistry and Combustion System Laboratory, D-MAVT, ETH Zürich.
March 2013 – October 2014	Doctoral student at University of Naples “Federico II.
September 2000 – February 2008	Master Degree in Mechanical Engineering (110/110) at University of Naples “Federico II.
September 1995 – June 2000	High School - Istituto Pontano, Naples, Italy.

Work Experience

November 2014 – Present	Research and Teaching Assistant at the Aerothermochemistry and Combustion Systems Laboratory, D-MAVT, ETH Zurich.
April 2008 – October 2014	Associate Researcher at Istituto Motori, National Research Council (C.N.R.), Naples, Italy.
March 2010 – May 2010	Associate Researcher at Friedrich - Alexander Universität, Erlangen - Nürnberg, Germany.

Publications

Isi Journals Publications

- Valentino G., Allocca L., Iannuzzi S., Montanaro A. (2011) Biodiesel/mineral Diesel fuel mixtures: spray evolution and engine performance and emissions characterization. *Energy*, 36 (6), pp. 3924-3932
- Valentino G., Esposito Corcione F., Iannuzzi S.E., Serra S. (2012) Experimental study on performance and emissions of a high speed diesel engine fuelled with n-butanol diesel blends under premixed low temperature combustion. *Fuel*, 92 (1), pp. 295-307. ISSN: 0016-2361
- Valentino G., Esposito Corcione F., Iannuzzi S.E. (2012). Effects of Gasoline-Diesel and n-Butanol-Diesel Blends on Performance and Emissions of an Automotive Direct Injection Diesel Engine. *International Journal of Engine Research*, first published on April 30, 2012 as doi:10.1177/1468087412441879
- Merola S.S., Tornatore C., Iannuzzi S.E., Marchitto L., Valentino G. (2014) Combustion process investigations in a high speed diesel engine fuelled with n-butanol diesel blend by conventional methods and optical diagnostics. *Renewable Energy*, 64, pp. 225-237. ISSN: 0960-1481
- Iannuzzi S., Barro C., Boulouchos K., Burger J. (2015) Combustion behavior and soot formation/oxidation of oxygenated fuels in a cylindrical constant volume chamber. *Fuel*, Volume 167, 1 March 2016, Pages 49–59, doi:10.1016/j.fuel.2015.11.060

Other Journals Publications

- Valentino G., Iannuzzi S., Esposito Corcione F. (2010) Effects of low temperature premixed combustion (LTPC) on emissions of a modern Diesel engine for passenger cars. *Proceedings SAE 2010 World Congress & Exhibition, Detroit (USA) 2010*, SAE Technical Paper 2010-01-0333
- Valentino G., Esposito Corcione F., Iannuzzi S., Serra S. (2011) Effects of premixed low temperature combustion of fuel blends with high resistance to auto-ignition on performances and emissions in a high speed Diesel engine. *Proceedings 10th International Conference on Engines & Vehicles – ICE 2011, Napoli (Italy) 2011*, SAE Technical Paper 2011-24-0049
- Valentino G., Esposito Corcione F., Iannuzzi S., Serra S. (2012) An Experimental Analysis on Diesel/n-Butanol Blends Operating in Partial Premixed Combustion in a Light Duty Diesel Engine. *Proceedings SAE 2012*

- World Congress & Exhibition, Detroit (USA) 2012, SAE Technical Paper 2012-01-1127
- Vogel, T., Wensing, M., Leipertz, A., Iannuzzi, S., Lutz M. (2011) Influence of the fuel quantity on the spray formation and ignition under current engine relevant conditions. SAE Technical Paper 2011-01-1928, 2011, doi:10.4271/2011-01-1928
 - Auriemma M., Iannuzzi S., Serra S., Valentino G. (2012) Injection system assessment to optimize performance and emissions of a non-road heavy duty diesel engine: Experiments and CFD Modeling. Journal of KONES Powertrain and Transport 19 (3), pp. 19-30. 2012 P 2265 ISSN 1231-4005
 - Mattarelli E., Fontanesi S., Rinaldini C., Valentino G., Iannuzzi S., Severi E., Golovitchev V. (2013) Combustion optimization of a marine diesel engine. Proceedings 11th International Conference on Engines & Vehicles – ICE 2013, Capri-Napoli (Italy) 2013, SAE Technical Paper 2013-24-0020 ISSN 0148-7191
 - Calik A.T., Sorusbay C., Ergeneman M., Cevirgen S., Valentino G., Allocca L., Iannuzzi S., Diler A., Ozen H. (2013) Investigation of the effect of boost pressure and exhaust gas recirculation rate on nitrogen oxide and particulate matter emissions in diesel engines. Proceedings 11th International Conference on Engines & Vehicles – ICE 2013, Capri-Napoli (Italy) 2013, SAE Technical Paper 2013-24-0017 ISSN 0148-7191
 - Merola S.S., De Filippo A., Valentino G., Tornatore C., Marchitto L., Iannuzzi S. (2013) Optical investigation of post-injection strategy impact on the fuel vapor with the exhaust line of a light duty diesel engine supplied with biodiesel blends. Proceedings SAE 2013 World Congress & Exhibition, Detroit (USA) 2013, SAE Technical Paper 2013-01-1127 ISSN 0148-7191
 - Valentino G., Iannuzzi S.E., Esposito Corcione F. (2013), Experimental investigation on the combustion and emissions of a light duty diesel engine fuelled with butanol-diesel blend. SAE Technical Paper 2013-01-0915 ISSN 0148-7191
 - Tornatore C., Marchitto L., Valentino G., Iannuzzi S., Merola S.S. (2013) Spectroscopic investigation of post-injection strategy impact on fuel vapor with the exhaust line of a light duty diesel engine supplied with diesel/butanol and gasoline blends. Proceedings 11th International Conference on Engines & Vehicles – ICE 2013, Capri-Napoli (Italy) 2013, SAE Technical Paper 2013-24-0066 ISSN 0148-7191
 - Merola S.S., Marchitto L., Iannuzzi S., Tornatore C., Valentino G. (2013) Multi-wavelength spectroscopic investigation of the post-injection strategy effect on the fuel vapour within the exhaust line of a light duty diesel engine fuelled with B5 and B3.0 SAE/KSAE 2013 International Powertrains, Fuels &

Lubricants Meeting. Seoul (South Korea) 2013 – SAE Paper 2013-01-2519 (ISSN 0148-7191)

- Valentino G., Iannuzzi S., "Effect of Different Fuels Properties on Emissions and Performance of a Light Duty Four-Cylinder Diesel Engine Under Premixed Combustion," SAE Technical Paper 2014-01-2674, 2014, doi:10.4271/2014-01-2674

Conference Publications

- Valentino G., Iannuzzi S., Esposito Corcione F., Minagawa T., Kamimoto T. (2009) A study on the effects of engine parameters on in-cylinder soot processes in a simulated direct injection Diesel engine via the two-color method. Proceedings 9th Congress on Engine Combustion Processes, München (Germany), 2009, pp. 33-44
- Valentino G., Allocca L., Iannuzzi S., Montanaro A. (2009) Biodiesel/mineral Diesel fuel mixtures: spray evolution and engine performances and emissions characterization. Proceedings 22nd Int. Conference on Efficiency, Cost, Optimization, Simulation and Environmental Impact of Energy Systems – ECOS 2009, Foz do Iguaçu, Paraná (Brazil) 2009, pp. 2019-2028 (ISSN 2175-5426)
- Esposito Corcione F., Iannuzzi S., Marchitto L., Merola S.S., Valentino G. (2011) Evaluation of soot and flame lift-off length in a high swirl optically accessed Diesel engine. Proceedings 10th Engine Combustion Processes Congress: Current Problems and Modern Techniques, München (Germany) 2011, pp. 437-448
- Vogel T., Wensing M., Leipertz A., Iannuzzi S., Lutz M. (2011) Effect of injected fuel quantity on spray and ignition behavior in diesel process Proceedings 10th Engine Combustion Processes Congress: Current Problems and Modern Techniques, München (Germany) 2011. ISBN 3-931901-72-6
- Valentino G., Merola S.S., Tornatore C., Iannuzzi S.E., Marchitto L. (2012) Combustion process investigations in a high speed diesel engine fuelled with nbutanol diesel blend by conventional methods and optical diagnostics. 3rd international conference on contemporary problems of thermal engineering (CPOTE 2012). Gliwice (Poland). 2012 P 2261 ISBN 978-83-61506-13-3

Other Publications

- Valentino G., Mazzei A., Iannuzzi S. (2007) Use of a vegetable based oil lubricant for the lubrication of an internal combustion engine. – Technical Note 2008NT357
- Kamimoto T., Iannuzzi S., Valentino G. (2008). Soot flame temperature evaluation through the two colours pyrometry technique. Internal report n° 2008 RR 1844
- Iannuzzi S.E., Mazzei A, Valentino G. (2009) Test bench preparation for the mounting of a single cylinder heavy duty diesel engine for marine applications. Internal report n° 2009 RR 1970